Hamburg University of Applied Sciences

Faculty of Life Sciences

Master - Thesis

A study on the technical and economic feasibility of green hydrogen production in a sanitary and heating technology company

Laurens Butin

Master course: Renewable Energy Systems (M.Sc.)

Matriculation number: [redacted]

Date of submission: June 18, 2024

First supervisor: Prof. Dr. Timon Kampschulte (HAW Hamburg)

Second supervisor: Dr. rer. nat. Henrik Zahn (8.2 Obst & Hamm GmbH)

This work was prepared in cooperation with the company 8.2 Obst & Hamm GmbH.

Abstract

The industry needs to play a vital role in the energy transition and hydrogen can provide a key element on the road to a sustainable future. By integrating green hydrogen, energy-intensive processes can be converted in a climate-friendly way. The topic of hybrid renewable energy generation in combination with green hydrogen production with simultaneous consumption of electricity and hydrogen on a large scale has not yet been sufficiently investigated. This study aims to help to narrow this gap in the literature by investigating how an industrial company can convert its complex, energy-intensive system to an autarkic model utilizing renewable energies and green hydrogen to cover the dark doldrums. The research focuses on optimizing the system, consisting of an electrolyzer with hydrogen storage and a fuel cell, in interaction with wind turbines and photovoltaic systems. The intention is to optimize the system in such a way that self-consumption of electricity and hydrogen is covered as far as possible, while producing additional green hydrogen with the surplus electricity for potential business opportunities. The modelling and optimization were carried out using the HOMER software and a custom-developed time-discrete simulation that was precisely tailored to the restrictions of the system. The results indicate that the company can achieve a degree of autarky of around 90% while producing a surplus of hydrogen that accounts for around 30% of the total hydrogen produced. The study demonstrates the promising potential of hybrid solutions with green hydrogen to shape the transition to a sustainable future.

Table of Contents

List of Figures

List of Tables

List of Formulas

Abbreviations

AEM	-	Anion exchange membrane
AFC	-	Alkaline fuel cell
AWE	-	Alkaline water electrolyzer
BImSchV	-	Verordnung zur Durchführung des Bundes-Immissionsschutzgesetzes (Ordinance on the implementation of the Federal Immission Control Act)
BESS	-	Battery energy storage system
CAPEX	-	Capital expenditures
CcH_2	-	Cryocompressed hydrogen
CHP	-	Combined heat and power
DMFC	-	Direct methanol fuel cell
DWD	-	Deutscher Wetterdienst (weather service)
EEG	-	Erneuerbare-Energien-Gesetz (Renewable energy sources act)
EL	-	Electrolyzer
FC	-	Fuel cell
HRES	-	Hydrogen renewable energy system
LCOE	-	Levelized cost of energy
LCOH	-	Levelized cost of hydrogen
LH_2	-	Liquid hydrogen
NPC	-	Net present cost
NPV	-	Net present value
NWS	-	Nationale Wasserstoffstrategie (National hydrogen strategy)
MCFC	-	Molten carbonate fuel cell
OPEX	-	Operational expenditures
PEM	-	Proton exchange membrane
PEMFC	-	Proton exchange membrane fuel cell
PPA	-	Power Purchase Agreement
PV	-	Photovoltaics
RE	-	Renewable energy
SOEC	-	Solid oxide electrolyzer cell
SOFC	-	Solid oxide fuel cell
PAFC	-	Phosphoric acid fuel cells

1 Introduction

As part of the solution for a sustainable future, the integration of hydrogen as a renewable energy source promises to reform the industrial sector and drive the energy transition towards greater climate responsibility and energy security.

In order to become climate-neutral, the Paris Agreement (2015) and the German government's climate protection policy (2021/2022) aim for a 65% decrease in greenhouse gas emissions by 2030 and an 100% reduction by 2045. To meet the emissions targets, processes that are currently powered by fossil fuels must be replaced with alternative energy sources with lower or no CO_2 emissions. Electrification is often cost- and resource-efficient due to its high efficiency, but it is not always possible. Consequently, hydrogen becomes crucial, especially for energy demands where direct electricity usage is not possible such as in certain industrial applications like the steel sector (Fraunhofer ISI & ISE 2019, pp. 6-7). A study by Agora Energiewende shows a possible path for achieving 80% renewable electricity by 2030 and a climate-neutral electricity system by 2035. The integration of industry and sector coupling plays a decisive role in this process, surplus electricity must be used for hydrogen electrolysis among others (Prognos and Consentec 2022, pp. 7-19).

This underlines the goal of the German National Hydrogen Strategy (2020), which aims to accelerate the market ramp-up of hydrogen technologies, especially in the industrial sector, and at the same time the switch to green hydrogen applications in order to decarbonize emission-intensive industrial processes (BMWi 2020, pp. 5-12).

There is a controversial discussion regarding the areas of application and the extent to which hydrogen should be used in direct comparison with other options such as direct electrification. It is determined that the so-called no-regret applications, i.e. applications for which there are currently hardly any economically attractive alternative technology options (e.g. in certain industrial applications such as the steel sector and basic chemicals), are the driver of hydrogen demand (Wietschel et al. 2023, pp. 25-26).

Moreover, hydrogen is characterized by low self-discharge and high energy density, which makes it attractive for storage, but high initial costs and infrastructure deficits hinder its growth (Arsad et al. 2022, pp. 3, 21). This relevance is shown in the substantial research into hybrid renewable energy systems (HRES) and hydrogen technologies (Bahramara et al. 2016; Kalinci et al. 2017).

According to studies, storage systems with only one storage type frequently overestimate storage or generation capacity (Bhandari and Shah 2021, p. 2). Studies of smaller setups using HOMER software have demonstrated that off-grid PV/BESS/FC/EL/storage systems are less expensive than diesel-powered options (Das et al. 2017, pp. 14-15). Similarly, systems combining PV/EL/FC/storage can have a lower levelized cost of energy (LCOE) than other

models (Hussin et al. 2019). Optimizing PV, electrolyzer, compressor, and storage systems can significantly affect hydrogen production costs (Muñoz Díaz et al. 2023, p. 1). Research that looked at numerous electrolysis scenarios using different electricity sources found that producing hydrogen only from surplus wind power is not cost effective. The ideal capacity ratio between renewables and electrolyzer in a grid-connected system was discovered to be 4:1 for the lowest carbon emissions and the highest Net Present Value (NPV), while a ratio of 1:1 was best for LCOE and LCOH. The combination of wind and photovoltaics lowered grid demand by 80% (Sorrenti et al. 2023, pp. 10-11).

Gutiérrez-Martín et al. provide a techno-economic analysis tool that optimizes efficiency, scalability, and cost for battery-assisted electrolysis, reducing hydrogen production costs (Gutiérrez-Martín et al. 2023). Although HOMER is extensively utilized, other algorithms and tools are also utilized globally (Khan et al. 2022; Fabianek and Madlener 2023). HOMER is a popular simulation software for optimizing hybrid energy systems, both off-grid and grid-connected, through detailed analysis of various energy components. However, HOMER has drawbacks, including a lack of support for multi-target issues and hourly fluctuations (Khan and Javaid 2020, p. 2).

Despite the broad literature, Khan et al. highlighted a research gap in the optimization of HRES using hydrogen technologies and emphasized the necessity for more research (Khan et al. 2022, pp. 1-7). Since then, this has not changed significantly and shall be specified further for this study. At the present there are barely any extensive investigations that deal with the industrial production and use of green hydrogen and with hourly consumption. This complexity has not been considered in its entirety and deserves more in-depth study due to the emerging urgency.

The thesis aims to answer the following question: How can companies use solar and wind energy efficiently to cover the load profile and generate green hydrogen while ensuring economic performance, with a focus on a high degree of self-sufficiency and co-location strategies?

The aim of this work is to gain new insights into the needed size of the electrolyzer, hydrogen storage and fuel cell components in question in order to achieve a high degree of autarky. This raises the question of whether there is a tipping point at which increasing size of the components only has a minor effect in terms of autarky. Another relevant consideration in this setup is the possibility of hydrogen overproduction and to what extent it could support a business case such as a hydrogen filling station. Overall, the aim is to be able to give an order of magnitude for the components mentioned so that both a technically optimal design and an economically viable solution emerge in the end.

The topic of climate-neutral production is currently of particular interest to the company considered, as it has set itself the goal of being CO_2-neutral by 2035. Therefore, the question of

how to transition the company as effectively and cost-efficiently as possible is of great importance.

A system that reflects the structure of one of the company's production sites was examined. The project is to create a model for the year 2035 in order to investigate what an optimal design of the overall system could look like and what values could be achieved in terms of self-sufficiency and hydrogen production volumes. In this case study electricity is generated using wind and PV systems that are co-located with the facility. The factory has a high electricity consumption as well as an hourly hydrogen consumption for production purposes. The load profiles of electricity and hydrogen from 2023 were extrapolated according to the company's forecasts for 2035. In addition to covering the load profile, the surplus electricity is used to operate an electrolyzer. The green hydrogen produced is used to cover the hourly hydrogen consumption and as intermediate storage. In the event of a dark doldrums, the stored hydrogen is converted back into electricity via a fuel cell in order to draw as little electricity as possible from the grid and thus achieve a high degree of autarky.

The analyzed company to which this setup with the specific conditions and characteristics applies should remain unknown. Therefore, no further specific information on names, locations, or other details will be provided.

In order to carry out an analysis, assumptions were made about the various aspects such as generation capacity and consumption data. These were discussed and agreed on with the parties involved in spring 2024. The following analysis is based on these assumptions. The values determined represent a possible scenario from the time when the analysis was prepared, and they form the basis for all further results and follow-up questions and conclusions. A customized MATLAB code was used to model the system and the broadly used software HOMER - Hybrid Optimization Model for Electric Renewable - (HOMER Pro 2024) was used for comparison and a better classification. A simulation with the PVsyst software (PVsyst SA 2024) creates the basis for the generation data of the PV system and HOMER was used to model the wind part. Moreover, a brief comparison will be made between a hydrogen system and a system with battery storage when discussing the storage options.

Due to the limited scope of this study, the topic of load management cannot be addressed. In industry, it can be a relevant lever to align the consumption of electricity and the production of hydrogen with the available resources such as wind and solar. However, integrating this complexity exceeds the scope of this work and should be considered separately.

The work is divided into six sections. After the introduction to the topic and the description of the project, the second chapter presents the most important theoretical and technical principles of the key components and mechanisms. Chapter three describes the methodology of the study and explains the approach which was used. The results are presented in chapter four and discussed in chapter five. Finally, the most important findings are summarized in chapter six and an outlook on future research perspectives is provided.

2 Theoretical and technical basics

The theoretical and technical foundations are presented on which this study and the system to be analyzed are based. The system consists of wind and PV systems on the generation side. These two areas have already been thoroughly researched and are well established on the market and are not described in detail below. The main elements under consideration are the hydrogen electrolyzer, the associated storage system and the fuel cell. The associated components such as compressors, converters, water purification units, coolers, heat exchangers, rectifier and inverters form only a smaller part and are not the focus of the work. Thus, they are only mentioned in context.

2.1 Functional principle of hydrogen production and use

The idea behind water electrolysis has been around for a long time. The first experiments on water electrolysis were carried out as early as 1789. More than 400 electrolysis units were already in operation by 1902 (Grigoriev et al. 2020, pp. 1-2).

The basic scheme of hydrogen electrolysis is based on the same reactions, regardless of the type of electrolyzer or fuel cell. This scheme is briefly described at the beginning. More detailed and specific mechanisms and characteristics will be worked out later for the individual types of electrolyzers and fuel cells.

The interaction of electrolyzers and fuel cells can be understood as a sustainable energy cycle that utilizes the potential of renewable energies. The energy is stored in a tank in the form of hydrogen. This cycle uses basic chemical reactions to split water into its components and thereby storing energy. Later, recombination of the components releases energy, which can be used.

During the process of electrolysis, water (H_2O) is split into hydrogen (H_2) and oxygen (O_2) in an electrolyzer, which requires electrical energy. Due to the laws of thermodynamics, this reaction is more energy-intensive than the electric energy released during recombination in the fuel cell. Renewable energy sources such as wind and solar energy can be used for electrolysis so that green hydrogen can be produced in an environmentally friendly way. This enables the storage and transportation of renewable energy and compensates for its volatility.

The second process takes place in a fuel cell where the produced hydrogen reacts with oxygen, a process known as the "oxyhydrogen reaction". This reaction, which can be explosive if not controlled, generates energy. Hydrogen and oxygen recombine to form water, releasing energy in this process. This energy can be converted into electrical energy, e.g. to power electric vehicles or supply electricity and heat to buildings.

The cycle of electrolysis and fuel cell technology generates a sustainable energy concept. Surplus renewable energy is used to produce hydrogen that can be stored and transported.

When needed, this hydrogen can then be used in fuel cells to provide clean energy in the form of electricity and heat. This process makes it possible to use renewable energy over longer periods of time and longer distances, contributes to decarbonization and supports the creation of a flexible and sustainable energy system. The potential of hydrogen as an energy carrier and storage medium can be exploited if a combination of water electrolysis and hydrogen fuel cells is used (Zhang and Zeng 2015, pp. 1-3).

The following sections 2.2 to 2.4 provide a more comprehensive insight into the functioning of fuel cells and electrolyzers and allow a detailed look at how they work. Beforehand, the difference between the various types of hydrogen and how it is produced will be described.

The production of hydrogen can be categorized in different colors according to the "hydrogen color theory" (IKEM 2020, pp. 8-12), depending on the raw material, production and storage process.

White hydrogen: is the naturally occurring hydrogen that can mainly be obtained through fracking. **Black hydrogen**: is obtained from hard coal using thermal energy. **Brown hydrogen**: is obtained from brown coal using thermal energy. The major difference between brown coal and hard coal is that the former is younger and less energy-rich, contains more carbon and is older. **Grey hydrogen**: is produced from natural gas using thermal energy. The hydrogen produced from the last three types are classified as fossil hydrogen. In addition to hydrogen, this process produces simultaneous CO_2, which escapes into the atmosphere. If this CO_2 is now captured and stored (Carbon Capture and Storage - CCS), it is classified as **blue hydrogen**. With this method, great efforts are made to reduce the carbon footprint (Martinez Lopez et al. 2023, p. 1). However, this means that only a small amount of CO_2 is released into the atmosphere rather than the entire amount. Another color classification is **turquoise hydrogen**. This is produced from fossil methane (CH_4) using thermal energy. **Red hydrogen** is produced from water using nuclear energy. This is also sometimes referred to as **pink hydrogen** (Lazard 2023, p. 31). **Orange hydrogen**: is produced with the help of energy from biomass and from organic substances and possibly water. This hydrogen can also be described as CO_2-neutral, as the CO_2 escaping into the atmosphere was previously removed from the atmosphere through the biomass. Another classification is **yellow hydrog**en. Here the electrolysis is carried out with grid electricity (Lazard 2023, p. 31). The final category is **green hydrogen**. This is produced from water and with the help of renewable energies. Only green hydrogen is truly considered CO_2-neutral alongside orange hydrogen; red/pink hydrogen, which is produced using nuclear energy, is excluded at this point, partly because of the risks posed by nuclear waste and possible catastrophic accidents (Düsterlho et al. 2023, pp. 7-8).

Hydrogen types can also be classified according to the energy used for production, the technology and the process. The focus of this study and its further consideration is on green hydrogen. In addition to renewable energy sources such as wind and PV, there is also biomass gasification and geothermal energy (Bhandari and Shah 2021, pp. 3-4). However, studies have

shown that the production of green hydrogen is not yet cost-effective if only renewable energies are used (Sorrenti et al. 2023, p. 1). In contrast, the costs of hydrogen production with a grid-connected PV system are competitive in relation to those of hydrogen from fossil fuels. Furthermore, there are economies of scale and learning effects for electrolyzers, which offer potential for price reductions (Bhandari and Shah 2021, pp. 14-15).

It is becoming increasingly clear that hydrogen and its other synthesis products are important in achieving CO_2 neutrality. This includes all energy-consuming sectors such as transportation, industry and buildings. Hydrogen electrolysis will become an important industrial policy element in becoming a flexibility option in the German power grid and gaining a share of hydrogen production. Green hydrogen can make an important contribution to the CO_2 neutrality of the sectors, however currently hydrogen is produced almost exclusively from fossil sources such as natural gas and coal, with methane steam reforming (SMR) being the most commonly used.

In principle, the future demand for electrolyzers is derived from the projected demand for hydrogen. Several processes are available for hydrogen electrolysis. In addition to alkaline water electrolysis (AWE) and PEM electrolysis (PEM: Proton Exchange Membrane), high-temperature electrolysis, which uses a solid oxide electrolyte made of ceramic materials (SOEC: Solid Oxide Electrolyzer Cell), can also be used. These three technologies have the highest technology readiness level. In addition to these technologies, other processes offer potential, but they are not yet as advanced and are currently only being researched to a limited extent or are hardly being promoted in an industrial context. These include alkaline membrane electrolysis (AEM: anion exchange membrane).

The interest in green hydrogen for industry has increased, and with it the interest in electrolysis technology, not only because of its potential linked to sector coupling. This essentially refers to the energy technology and energy economy linking of electricity, heat and mobility, industrial processes and their infrastructures. Nevertheless, the production of electrolyzers has so far been limited to a small number of players, limited personnel and, in particular, small-scale production facilities. With around 20% of greenhouse gas emissions in Germany, the industrial sector has an important role to play in achieving the Paris climate targets (Fraunhofer ISI & ISE 2019, pp. 6-12, 23).

2.2 Various types of electrolyzers

The market offers various electrolyzer technologies as explained above. The following section examines these different technologies and highlights their differences. In addition, the suitability of these different types for different applications will be discussed as well.

There are currently four technologies on the marked, which are used most commonly. AWE is the most mature one, PEM technology also promises to be successful for large-scale applications in the future. This technology is expected to have the lowest capital cost (Tuinema

et al. 2020). Nevertheless, both technologies can already produce hydrogen on a larger scale at this point of time. Another technology is AEM, however, it is still in the research and development phase. These three types belong to the low-temperature technologies (Martinez Lopez et al. 2023, pp. 3-4). The fourth technology is SOEC electrolyzers which is classified to the high-temperature range. This technology is still in the early stages, but the first products are already on the market. The names of the technologies sometimes differ in the literature. In the following, the abbreviation AWE is used for alkaline electrolysis. It can also sometimes be found under AEL (alkaline electrolyzers) (Reksten et al. 2022).

The basic idea of the different types of electrolyzer is based on the same principle. The typologies differ in the materials used, the chemical components involved in the reactions and their mode of operation, i.e. the temperature. Thus, they have different conditions under which they perform. Accordingly, they can be used in different ways. However, the basic principle of the electrolyzers is the same, which is a chemical reduction-oxidation reaction (redox). Electrons are generated on one side, the anode (oxidation), on the other side, the cathode, these are consumed (reduction). The reactions at the electrodes differ depending on whether the electrolyte is acidic or alkaline. The reaction requires additional energy in the form of electricity and heat in order to take place. The enthalpy of reaction is the change in enthalpy between reactants and products (Martinez Lopez et al. 2023, p. 2). The overall reaction can be summarized as follows:

$$2\,H_2O(l) \rightarrow 2\,H_2(g) + O_2(g) \qquad (1)$$

In the following the four technologies are described and finally, the results and characteristics are summarized in a table.

AWE/Alkaline electrolysis: In general, the electrodes are made of nickel or are coated with Raney nickel as a catalyst on the cathode. The electrodes are immersed in an alkaline solution (potassium or sodium hydroxide; KOH/NaOH). A porous separator (diaphragm) forms a barrier between the electrodes. The separator consists of a mixture of zirconium dioxide and polysulfide with the trade name Zirfon. This separator ensures that the hydrogen and oxygen gases remain separate and do not blend, which could be dangerous. However, the diaphragm allows the transport of hydroxyl ions (OH^-) so that the desired reaction can take place at all.

The production of 1 kg of hydrogen consumes between 47 kWh and 66 kWh of electricity. Other features of AWE are the low operating temperature, low-cost stacks compared to other technologies, and they are already well represented on the market on a multi-megawatt scale. There are currently a large number of manufacturers worldwide that are successfully operating in industrial applications (Shiva Kumar and Lim 2022, pp. 4-6). Although the ramp-up time is not as fast as PEM and takes a few minutes to start up (Martinez Lopez et al. 2023, pp. 10-11).

PEM: gets its name from the thin polymer membrane used, a solid electrolyte for conducting the ions: Polymer-Electrolyte-Membrane. The membrane is usually made of the material Nafion and is very acidic, as it contains H^+ ions. As a result, materials in contact with it, such as the electrodes and catalyst layers, can corrode. To avoid this, more robust but rarer elements such as platinum and ruthenium are used, resulting in higher costs (Martinez Lopez et al. 2023, p. 4). The ionic charge carriers H^+ can penetrate the proton-conducting membrane. This is how the cell works and the reason behind the possibility of the reaction in general. The highly active area of the metal surface of the Pt-electrodes and the lower pH value of the electrolyte ensure faster operation than it is the case with AWE. Additionally, PEM is safer due to the fact that no corrosive electrolytes are used. PEM also works, similar to AWE, at low temperatures. The technology is currently being used for industrial and transportation applications. Electricity consumption in the production of hydrogen is in the same range as AWE (Shiva Kumar and Lim 2022, pp. 10-13).

PEM offers several advantages over the other described technologies. It has high load flexibility and the ability to provide grid balancing services. The minimum operating limit can go down to 5% of the rated capacity. In comparison, the other technologies are normally around 20% with simple interconnection (Grigoriev et al. 2020, pp. 7, 17).

AEM: This is a comparatively new technology that combines the properties of PEM and AWE. It utilizes the advantages of PEM, but operates under alkaline conditions; however, no rare materials such as iridium or platinum are required. Inexpensive transition metal catalysts are used instead of precious metal catalysts. A slightly concentrated alkaline solution (1M KOH)/distilled water is used as electrolyte. The main difference to AWE is that the diaphragm (asbestos/zirconium) is replaced by an anion exchange membrane.

AEM technology is still in the development phase. Chemical, mechanical and thermal stability is still a challenge, so longevity is not yet guaranteed at this stage. Nevertheless, the first commercial products are already available. The advantage of this technology lies in its high performance and low cost compared to other technologies (Shiva Kumar and Lim 2022, pp. 7-10; Martinez Lopez et al. 2023, p. 4).

SOEC: They are classified as high-temperature electrolyzers. A solid ion-conducting ceramic is used as electrolyte, which allows the operation at around 700°C to 900°C. Due to these high temperatures and the resulting improved reaction kinetics, higher efficiencies (up to 90%) can be achieved compared to other technologies. However, the high temperature is one disadvantage and the material degradation is higher as well (Bhandari and Shah 2021, p. 7).

In addition, water is used in the aggregate state steam during operation. This significantly reduces the energy consumption required to split the water into its individual components, which is one of the reasons for the higher efficiency. The process can also be easily integrated into a downstream chemical synthesis or the excess heat can be reused in other processes. SOEC does not require precious metal electrocatalysts, although one disadvantage is the low

long-term stability. Oxygen ion-conducting ceramics are used as solid membranes, enabling them to conduct the oxide ions ($O2^-$). This electrolyte most frequently consists of yttrium-stabilized zirconium dioxide (YSZ).

Solid oxide water electrolysis is still in the development and commercialization phase, but products such as the Sunfire-HyLink SOEC are already on the market (Grigoriev et al. 2020, pp. 10-13; Shiva Kumar and Lim 2022, pp. 13-16).

The degradation of the cells respectively stacks for all technologies is a decisive factor. It influences how long a stack can be operated before it needs to be replaced. There is little information in the literature about the extent of possible degradation. Some of them are in a wide range, for example values from <1% to 4% per year are given (Grigoriev et al. 2020, p. 18).

The structure of a unit is similar for all technologies: It consists of the components described above, such as electrodes and membranes, these individual cells are then connected to form so-called stacks. Several of these stacks are interconnected and create a module, which in turn is installed in a container, for example, and is an essential part of an electrolyzer. The structure of a cell for AWE, PEM and SOEC can be seen in Figure 1.

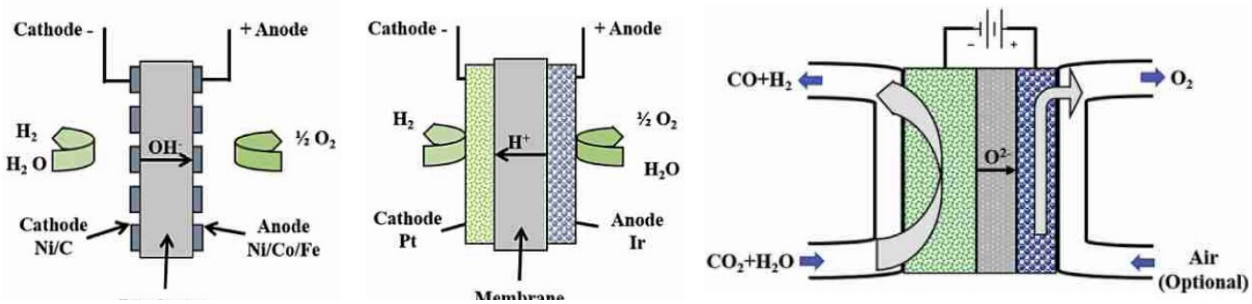

Figure 1: Schematic cell structure of AWE (left), PEM (center) and SOEC (right), (Khatib et al. 2019, pp. 2-3)

The lower limit of the operating mode can also be brought down to around 5% by interconnecting the individual stacks in a smart way. However, this advantage can have an impact on the financial side as well (Martinez Lopez et al. 2023, pp. 10-11).

The cost trend in recent decades has shown a significant reduction (Saba et al. 2018, pp. 12-13). PEM is still more costly than AWE, but the gap will decrease, if not even close, in the upcoming years. Further technological development and the effect of scale will ensure further significant cost reductions (Reksten et al. 2022).

A study was conducted on the environmental impact of expanding the electrolyzer market (for AWE and PEM) into the GW range. A potential reduction in the environmental impact of advanced stacks was identified. In addition to the stacks as the primary contributors to the impact categories, the power source is identified as primarily responsible as well. Overall, AWE and PEM perform comparably and have similar effects (Krishnan et al. 2024, p. 15).

The following Table 1 provides an overview of the electrolyzer technologies and their features.

Table 1: Technical characteristics of typical water electrolysis technologies

	AWE	PEM	AEM	SOEC
Anode reaction	$2\ OH^- \rightarrow H_2O + ½\ O_2 + 2e^-$	$H_2O \rightarrow 2\ H^+ + ½\ O_2 + 2e^-$	$2\ OH^- \rightarrow H_2O + ½\ O_2 + 2e^-$	$O_2^- \rightarrow ½\ O_2 + 2e^-$
Cathode reaction	$2\ H_2O + 2e^- \rightarrow H_2 + 2\ OH^-$	$2\ H^+ + 2e^- \rightarrow H_2$	$2\ H_2O + 2e^- \rightarrow H_2^+ 2\ OH^-$	$H_2O + 2e^- \rightarrow H_2 + O_2$
Overall reaction	$H_2O \rightarrow H_2 + ½\ O_2$	$H_2O \rightarrow H_2 + ½\ O_2$	$H_2O \rightarrow H_2 + ½\ O_2$	$H_2O \rightarrow H_2 + ½\ O_2$
Electrolyte	KOH/NaOH (5M)	Solid polymer electrolyte (PFSA)	DVB polymer support with 1 M KOH/NaOH	Yttria stabilized Zirconia (YSZ)
Separator	Asbestos/Zirfon/Ni	Nafion	Fumatech	Solid electrolyte (YSZ)
Nominal current density	0.2 – 0.8 A/cm2	1 – 2 A/cm^2	0.2 – 2 A/cm^2	0.3 – 1 A/cm^2
Voltage range	1.4 – 3 V	1.4 – 2.5 V	1.4 – 2.0 V	1.0 – 1.5 V
Operating Temperature	70 – 90 ◦C	50 – 80 ◦C	40 – 60 ◦C	650 – 900 ◦C
H_2 purity	99.5 – 99.9998%	99.9 – 99.9999%	99.9 – 99.9999%	99.9%
Efficiency	50% – 80%	57% – 80%	50% – 83%	74% - 81%
Lifetime (stack)	60,000-90,000 h	20,000-60,000 h	50,000–80,000 h	20,000 h
Development status	Mature	Commercialized	Commercialized	R & D
Ramp-up to full power*	10 min	3 min	25 min	N/A
Ramp-up from min to full load	10 min	10 sec.	N/A	N/A

* Cold start sequence

Adapted from (Khatib et al. 2019, p. 4; Grigoriev et al. 2020, pp. 2, 18; Bhandari and Shah 2021, p. 6; Shiva Kumar and Lim 2022, p. 5; Martinez Lopez et al. 2023, p. 8)

The advantages and disadvantages of the individual electrolyzer technologies are shown in Table 2.

Table 2: Advantages and disadvantages of typical water electrolysis technologies

Electrolysis technology	Advantages	Disadvantages
AWE	★ Well established Technology ★ Commercialized for industrial applications ★ Noble metal-free electrocatalysts ★ Relatively low cost ★ Long-term stability ★ Cost effective	★ Limited current densities ★ Crossover of the gasses ★ High concentrated (5M KOH) liquid electrolyte
PEM	★ Commercialized technology ★ Operates higher current densities ★ High purity of the gases ★ Compact system design ★ Quick response ★ Good partial load ★ Dynamic operation	★ Cost of the cell components ★ Noble metal electrocatalysts ★ Acidic electrolyte ★ Reduction of current efficiency ★ Reduction of stack component lifetime
AEM	★ Noble metal-free electrocatalysts ★ Low concentrated (1M KOH) liquid electrolyte ★ Low cost ★ Compact cell design	★ Limited stability ★ Under development ★ Low current densities ★ Membrane degradation ★ Excessive catalyst loading
SOEC	★ High working temperature ★ High efficiency ★ Noble free catalyst	★ Limited stability ★ Under development ★ Bulky system design

Adapted from (Grigoriev et al. 2020, p. 2; Salehmin et al. 2022, p. 2; Shiva Kumar and Lim 2022, p. 5; Malek et al. 2023, p. 6)

In conclusion, it can be stated that the two technologies AWE and PEM are the most advanced and have the necessary maturity for project implementation. PEM stands out with its fast and dynamic operation, but comes with higher costs due to the use of noble metals as well. The two technologies AEM and SOEC are still under development or have only just entered the market. The low durability is another disadvantage.

2.3 Hydrogen storage systems

Storing hydrogen provides the possibility to use the energy produced in the form of hydrogen at a later point in time when it is needed. Hydrogen energy storage systems close the power-to-power conversion cycle. This allows fluctuations on the generation and consumer side to be absorbed, load balancing to reduce peak loads and any frequency regulation to be carried

out (Bhandari and Shah 2021, pp. 1-2; Arsad et al. 2022, pp. 3-4). Due to their low self-discharge and high energy density, hydrogen storage systems have good arguments for serving as an alternative to electricity storage. They can be used for both short-term and long-term energy storage. In contrast to battery storage systems, even large-scale applications are not hindered by poor properties such as a high self-discharge rate and capacity losses (Arsad et al. 2022, p. 3; Yang et al. 2024, p. 22).

Hydrogen can be stored in various ways, mainly divided into physical and material methods. The former includes compressed gases, liquids and the cryocompressed form, while the latter uses absorption or adsorption processes (Hassan et al. 2021, pp. 6-7). The most common method is storage under pressure, but due to the low relative density, energy is required for compression. Another option is to liquefy hydrogen at -253°C. However, this process is very energy-intensive and around 40% of the energy is lost. Another option is storage in metal hydrides (material based) where the hydrogen can be absorbed and desorbed again when heated. When using a liquid organic hydrogen carrier, the hydrogen can be absorbed (hydrogenated) by the organic compounds at high pressure and high temperature and recovered again (dehydrogenated) (Bhandari and Shah 2021, p. 7). Compared to pressure storage, the material-based variant has the disadvantage that energy is required for discharging which influences the costs further (Lange et al. 2024, p. 12). Although this variant has the greatest potential since this type of storage is very safe, practical and advantageous. However, further research and improvement is still required in this domain (Arsad et al. 2022, p. 21).

There are two options for storing hydrogen on a large scale: either in specific hydrogen storage facilities or in the existing natural gas infrastructure. For the second option, the financial framework for the hydrogen core network in Germany was approved by the Federal Council in April 2024. The existing gas network is to be converted and expanded so that it can also be used for hydrogen. The Germany-wide hydrogen network is to be realized by 2032 and will cover around 9,700 km across all federal states and even become part of a European network. However, the route of the network has not yet been decided making it possible to rule out this option for this project at the present time. It is unclear whether it will be realized within reach of the production site and whether a connection is possible (E-Bridge 2024). But for the future this appears to be the most economical way of storing and transporting hydrogen in large quantities if the corresponding infrastructure is available and usable (Yang et al. 2023, p. 23).

Pressure vessel/tanks: This is currently the most sophisticated form of hydrogen storage; the storage tanks can be divided into four categories. The typical operating pressure for type I is between 150 bar and 300 bar with an energy of 0.396 kWh/l (at 150 bar) and 0.792 kWh/l (at 350 bar). Due to its low gravimetric density, this type is only used for stationary applications, often for on-site storage as an industrial gas. With type II, pressures of up to 1,000 bar are possible. These storage tanks are often used for stationary high-pressure gas storage, for

example at hydrogen filling stations. The energy required to compress hydrogen to 700 bar is around 10% of its energy content. With this compression, the hydrogen density increases from 0.1 kg/m³ to 40 kg/m³ or from 0.0033 kWh/l to 1.32 kWh/l. However, this increase in pressure also increases the safety issue. Type III and IV pressure vessels, designed for 300 to 700 bar, have a metallic or polymeric inner container coated with fibers. As a result, they are lighter and offer better transportation conditions and thus are often used in aerospace, military, marine and vehicle applications, but they are comparatively expensive.

One other type of hydrogen storage is in **liquid form**. This achieves a much higher gravimetric and volumetric density than compressed storage. However, this type of storage is much more difficult and consumes more energy. The storage of liquid hydrogen (LH_2) requires a temperature of 20 K, which achieves the high storage density of 70.9 kg/m³ (2,343 kWh/l). This type of storage poses a lower safety risk due to the low storage pressure of 4 bar. One disadvantage of this variant, however, is that the total energy consumption for liquid storage accounts for around 35% of the energy content of the stored hydrogen. This type is limited to aerospace applications. Here, high volumetric and gravimetric energy storage densities are required and the high-power consumption is accepted.

The last type to be mentioned is the storage of **cryocompressed hydrogen** (CcH2). Although liquid hydrogen has a higher density, the evaporation losses are significant. Cryocompression is usually a combination of compression and cooling/liquefaction with conditions of temperatures between 35 and 110 K and a pressure of 50 to 700 bar. The result is a density of 60 to 71.5 kg/m³. The disadvantage of this type of storage is that CcH2 is more affected by heat leakage, and it has a higher energy consumption than compressed gaseous hydrogen. This type of storage is moreover associated with high costs (Preuster et al. 2017, pp. 4-10; Hassan et al. 2021, pp. 6-7; Yang et al. 2023, pp. 3-8; Yang et al. 2024, pp. 9-16).

One of the main challenges with hydrogen storage are the relatively high cost. In order to keep up with other technologies and to support the dynamics on the market, a reduction in costs is necessary (Arsad et al. 2022, p. 21; Yang et al. 2024, p. 22). The option of using natural vessels like salt caverns as storage was not included in the analysis at this point. This study is not intended to cover all storage options and their detailed processing, as this is beyond the scope of possibilities in this context.

2.4 Fuel cell technologies

In principle, the fuel cell uses the same process as an electrolyzer, only it operates in the opposite direction. The different types of fuel cells find their complementary process in electrolyzers according to their names. In water electrolysis, electricity is used to separate water into hydrogen and oxygen. In the fuel cell process, the hydrogen is combined with oxygen to generate electricity. The by-products of this process are water and heat:

$$\frac{1}{2}O_2 + H_2 \rightarrow H_2O + Electricity + Heat \quad (2)$$

For example, the fuel cell can use the stored hydrogen to generate electricity if not enough electricity is generated by renewable energies, or if the load cannot be fully covered due to high consumer demand (Okundamiya 2021).

The different types of fuel cells all work according to this principle and can be classified based in their operating temperature (Figure 2). Low-temperature fuel cells (50°C to 250°C) include alkaline fuel cells (AFC), direct methanol fuel cells (DMFC), proton exchange membrane fuel cells (PEMFC) and phosphoric acid fuel cells (PAFC). High-temperature fuel cells (600°C to 1000°C) include molten carbonate fuel cells (MCFC) and solid oxide fuel cells (SOFC) (Harrabi et al. 2018).

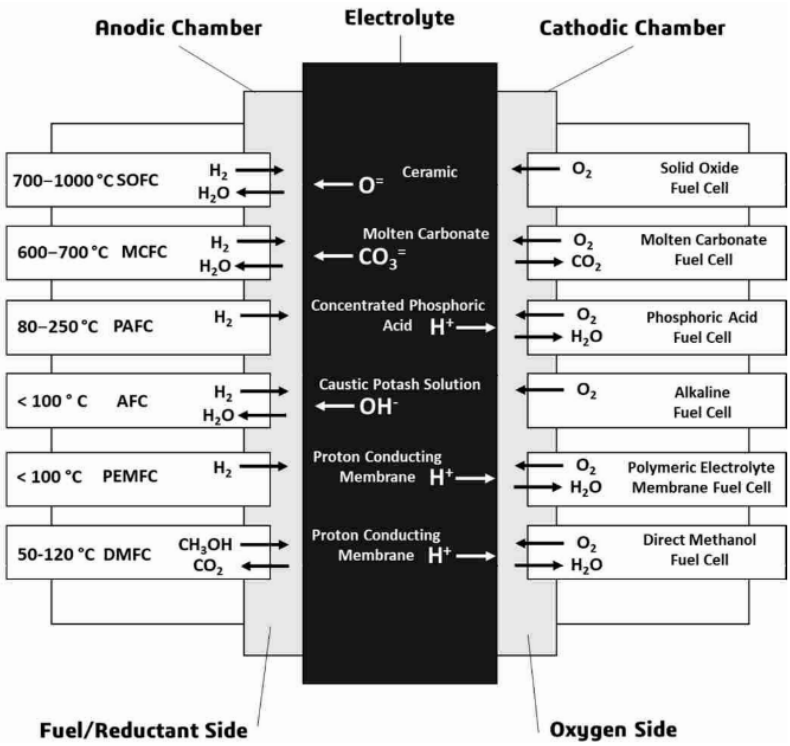

Figure 2: Overview of fuel cell technology with classification of temperature ranges (Cigolotti et al. 2021, p. 4)

An important aspect of hydrogen systems is their purity, both when the hydrogen is used by fuel cells and when it is produced by electrolyzers. For example, AWEs can supply high-purity hydrogen without any contaminations (Zhang and Zeng 2015, p. 3).

The schematic process is that hydrogen and an oxidizing gas, for example oxygen from the air, are electrochemically connected via the electrodes. The ions can be transported either through a membrane or a conductive electrolyte. At the anode, where the hydrogen is supplied, it is split into positive and negative ions, H^+ and H^-. The H^+ ions now migrate through the membrane/electrolyte to the cathode where the membrane/electrolyte serves as a separator for the H^- ions. This converts chemical energy into electrical energy. The efficiency here is significantly higher than with other common thermomechanical processes (Sazali et al. 2020,

pp. 1-5; Nanadegani and Sunden 2023, pp. 3-5). Today, between 40 and 70% electrical efficiency and over 85% with additional heat utilization are achieved. Fuel cells do not cause any environmental pollution, as no combustion process takes place, and operate quietly without any significant noise emissions. This is an advantage for on-site applications and in mobility. However, a major disadvantage is the high investment costs, which cannot yet compete with other energy generation technologies (Cigolotti et al. 2021, pp. 2-4; Nanadegani and Sunden 2023, pp. 3-5, 8).

DMFC: the oxidation of liquid methanol takes place at the anode; the resulting hydrogen ions diffuse through the electrolyte and reach the cathode. The electrons travel through an external circuit from the anode to the cathode. This technology could replace Li-ion batteries in the future and is already being used in portable devices, transportation and the military. Advantages are the compact size, high energy density and simple design, whereas disadvantages are the low cell voltage, low efficiency, low power density, high toxicity of the fuel and high costs.

PEMFC: With this technology, a hydrogen molecule is split at the anode, the hydrogen ion (H^+) diffuses through the electrolyte and reaches the cathode. The electrons on the cathode side can react with oxygen to form water via an external circuit from the anode to the cathode (Nanadegani and Sunden 2023, pp. 3-5). The PEMFC is seen as a promising option for energy supply and has a wide range of applications. For example, it can be used in stationary and mobile applications. It is characterized by its long service life, high conversion rate, fast start-up times, simple and safe handling, compact design, dynamic reactions and moderate temperatures. In addition, it is not as cost-intensive compared to other fuel cell technologies, but cannot yet keep up with other commercial products and is not yet competitive (Sharaf and Orhan 2014, p. 6; Sufaid Khan et al. 2024, p. 6).

AFC: Alkaline fuel cells use an alkaline medium whose concentration changes with temperature. The advantages of this technology lie in its fast kinetics and high performance when operated with pure hydrogen and oxygen. The main area of application to date has been space technology. However, they are very sensitive to impurities. Other features are the wide temperature and pressure range and the low costs (Sharaf and Orhan 2014; Sufaid Khan et al. 2024).

PAFC: This technology is one of the more mature and already well developed commercially. It generally operates at medium temperatures between 150°C and 220°C and is therefore suitable for combined heat and power (CHP) generation. Phosphoric acid, an inorganic substance, is used as the electrolyte (Sharaf and Orhan 2014, pp. 6-11; Sufaid Khan et al. 2024, p. 7). PAFC stands out due to its good properties such as low vapor pressure, stability and increased tolerance to CO. However, some precautions must be taken to maintain these good conditions. Nevertheless, PAFC has disadvantages such as slow start-up time, relatively low efficiency and large system size, expensive catalyst and high costs (Jamal et al. 2023, pp. 4-6).

MCFC: This type is a high-temperature fuel cell that is also suitable for combined heat and power generation and can therefore achieve very good overall efficiencies. Molten carbonate is used as the electrolyte (Sharaf and Orhan 2014, pp. 7-11). This molten carbonate, mostly potassium and lithium carbonates (Li_2CO_3 and K_2CO_3), melts due to the high temperatures and produces carbonate ions (Sufaid Khan et al. 2024, p. 7). These CO_3^{2-} ions diffuse from the cathode to the anode, where they combine with hydrogen ions and produce carbon dioxide, water and electrons. These ions are formed from atmospheric oxygen and carbon dioxide. MCFCs are efficient, tolerant of contamination and use inexpensive catalysts, but have longer start-up times and are susceptible to corrosion (Nanadegani and Sunden 2023, pp. 4-5).

SOFC: The other high-temperature fuel cell is the SOFC. This solid oxide fuel cell uses zirconium dioxide (ZrO_2) as the electrolyte which is stabilized by the use of yttrium oxide (Y_2O_3). The high temperature melts the electrolyte, which gives it its conductivity. The use of solids reduces leakage problems compared to MCFCs (Sufaid Khan et al. 2024, pp. 7-8). This technology has a high theoretical efficiency due to the high temperatures which are necessary to achieve the activation energy for the conductivity of the ceramic solid-state electrolytes (Jamal et al. 2023, p. 6). SOFC technology offers advantages such as good efficiency, high tolerance to impurities, the elimination of electrolyte problems and low costs for the catalyst. Disadvantages include slow start-up times, high thermal load, sealing problems, durability issues and high generation costs (Nanadegani and Sunden 2023, pp. 4-5).

The basic structure of a cell with the operating principle is shown again in Figure 3.

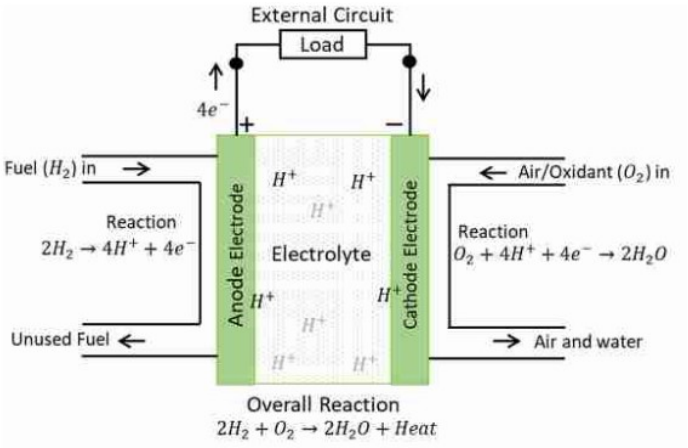

Figure 3: Schematic structure and process of a hydrogen fuel cell (Jamal et al. 2023, p. 12)

The various technologies with their special cell structure, characteristics and properties have already been presented. These cells with a voltage of less than 1 V are connected in series and parallel, which increases the voltage and current. This interconnection of the unit cells is supplemented by other components such as bipolar plates, current and electrical connections. Together they form a fuel cell stack. With other components such as a fuel processing system (i.e. fuel reformer and hydrogen storage) and a thermal management system, they form a complete fuel cell system (Nanadegani and Sunden 2023, pp. 5-6).

The properties of the different technologies are summarized briefly in Table 3.

Table 3: Technical characteristics of different fuel cells

	DMFC	PEMFC	AFC	PAFC	MCFC	SOFC
Electrolyte	Solid Nafions	Polymer membrane/ solid Nafions	Liquid KOH	Liquid H_3PO_4 (immobilized)	Molten carbonate/ liquid alkali carbonate	Ceramic/ solid yttria-stabilized zirconia (YSZ)
Charge carrier		H^+	OH^-	H^+	CO_3^{2-}	O^{2-}
Operating temperature	50-120°C	50-80°C	60-100°C	80-250°C	600-700°C	700-1000°C
Catalyst	N/A	Platinum	Platinum	Platinum	Nickel	Perovskites (ceramic)
Fuel compatibility	Liquid methanol water solution	H_2, methanol	H_2	H_2	H_2, CH_4, natural gas	H_2, CH_4, CO
Electric efficiency	35-60%	40-60%	60-70%	36-45%	55-65%	55-65%
Thermal efficiency	N/A	55%	N/A	N/A	43%	30-45%
Power range	1 W - 100 kW	10 W – 1 MW	100 W – 100 kW	100 kW – 100 MW	100 kW – 100 MW	1 kW – 100 MW
Current maximum lifetime	10,000-15,000 h	60,000-80,000 h	5,000-6,000 h	30,000-130,000 h	15,000-30,000 h	20,000-90,000 h
Start-up time	N/A	< 1 min	< 1 min	N/A	10 min	60 min

Adapted from (O'Hayre et al. 2016, p. 13; Sharaf and Orhan 2014, pp. 7-8; Sazali et al. 2020, pp. 4-11; Cigolotti et al. 2021, pp. 6, 15; Jamal et al. 2023, pp. 4-5, 13; Nanadegani and Sunden 2023, pp. 4-5)

No information is given in the literature on the operating range of a fuel cell. Only the individual manufacturers provide information on this aspect (see appendices).

The power range specified in the literature is not directly reflected in the manufacturers' information on their systems. An entire fuel cell system is made up of several interconnected systems. The information in the specification sheet usually refers to the individual stacks. The power range specified in Table 3 refers to possible power ranges for entire systems.

2.5 Interaction of renewable energy generation and hydrogen

In order to obtain a good and reliable power supply with renewable energies, a mix of different technologies can generate a better distribution of energy. Various studies have shown that there is complementarity in energy generation at different locations and times, both hourly and annually. Due to the fluctuations and uncertainties of solar radiation and wind, for example, the supply from renewables faces challenges. These can be overcome if the distribution of energy is balanced (Couto and Estanqueiro 2020, pp. 1-4). Load fluctuations and peaks can be absorbed and smoothed out by storing surplus energy which can result in greater reliability and improved power quality (Ferraz de Andrade Santos et al. 2020, pp. 1-3).

The first approach to achieve well-distributed energy generation is to start with the orientation of a PV system. A distinction can be made here between a system that is relatively south-facing respectively oriented towards the equator and a system with an east-west orientation.

An east and west-facing system offers a few advantages, including a more even generation curve throughout the day. There are no longer such high peaks at midday and the seasonal distribution is also slightly better distributed. In addition, the weather-related fluctuation is not quite so extreme and remains within a smaller range. However, the total annual yield is not as high as with a south-facing orientation (Velik 2014; Mubarak et al. 2019, pp. 1-2). The slightly better distribution of generation over a day can also correspond better with some load profiles (Lahnaoui et al. 2017). This can be explained by the Air Mass (AM). The path of light through the atmosphere becomes shorter the higher the sun is and a shorter path means that less of the light is absorbed. In other words, PV systems in the northern hemisphere with a southern orientation have a higher annual yield. Other aspects to consider when looking at the orientation options are the degree of self-sufficiency and self-consumption. Self-consumption is slightly higher with an east-west orientation. However, the degree of self-sufficiency only increases with oversized systems. Another aspect is that PV production is low in the northern hemisphere in winter anyway when the days are shorter. The sun only moves over a small area and does not rise in the east and set in the west as it does in summer, so a south orientation is suitable for achieving better generation at this time of year.

Basically, there are various arguments in favor of a south or east-west orientation. The application, the specific conditions and requirements are decisive (Azaioud et al. 2020, pp. 1-3, 21-22). The extent to which the phenomena and differences between south and east-west orientations have an effect cannot be described in general terms. These depend too much on the exact configuration and the locations.

Hybrid systems with wind and PV generation can make use of the complementarity of solar and wind energy. A temporal correlation often exists in this regard; wind and sun usually do not occur with the same intensity at the same time. A spatial correlation plays a role as well (Lindberg et al. 2021, p. 9; Hassan et al. 2023, p. 3).

The following energy chart illustrates this phenomenon (Figure 4) which shows a week in May (8.5. to 14.5.) of 2023 with net wind and PV generation in Germany. A figure for the entire year can be found in the appendix. However, the contrasts between wind and solar cannot be assumed across the board, a site-specific analysis is required (Lindberg et al. 2021, p. 19).

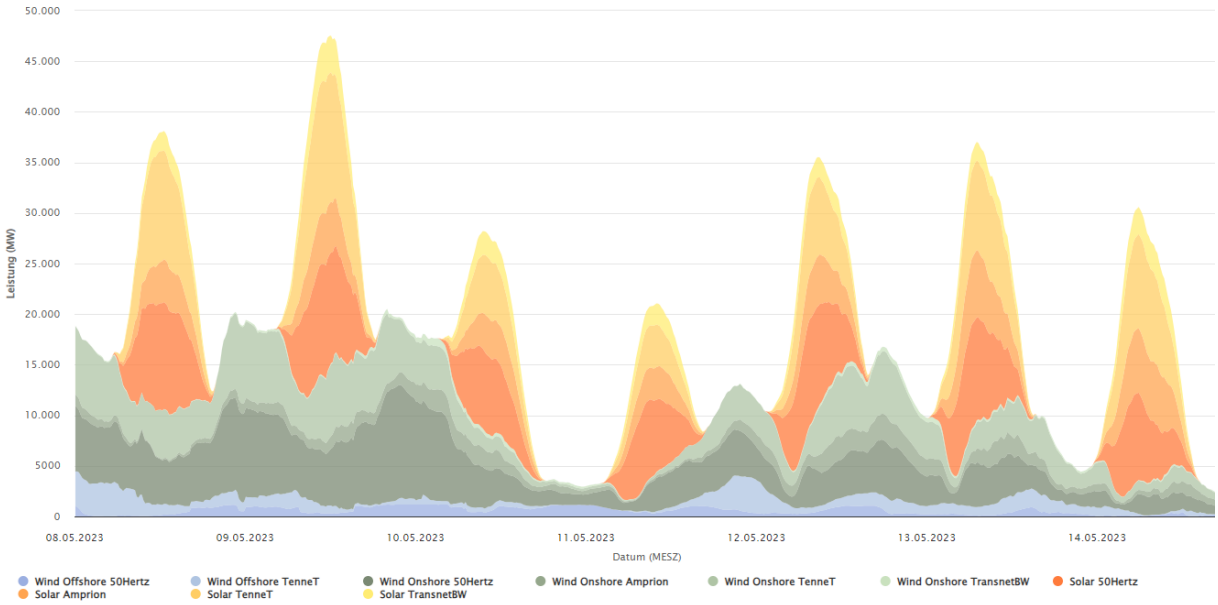

Figure 4: Public Wind and PV net electricity generation in Germany in week 19 of 2023 (Fraunhofer ISE 2024)

Wind production is shown in green (onshore) and blue (offshore), PV in yellow/orange. PV production is visible during the day, whereas wind production is more spread out and is more visible at night. However, this refers to the entire German region; a different picture will emerge if production only takes place in one location.

The joint use of wind and PV systems offers further advantages such as synergy effects in terms of infrastructure, land use and resources (Lindberg et al. 2021, p. 2).

It also plays a role how well renewables and electrolyzers can work together and whether there are effects and what their impact is. In principle, PEM and AWE electrolyzers are the most suitable due to their fast start-up times and variable operating mode. Values of around 10% for PEM and 1.67% for AWE of the nominal power per second are quoted. An important and critical point is the lifetime of the stacks, especially in relation to the variable conditions. For AWE, the service life with acceptable efficiency losses is between 60,000 and 90,000 hours, for PEM lower at 20,000 to 60,000 hours.

Studies and certificates show that electrolyzers can handle variable renewable energy well. Only minor influences are associated with this. The operating limits of the electrolyzers are the most important factor in this context, although they can be influenced. In addition, there is no clear evidence that variable operation can lead to significant degradation (Martinez Lopez et al. 2023, pp. 10-12).

A final outlook supports the idea of expanding a system to include a battery storage system, which would allow a better use of renewables and could also reduce the size of the electrolyzer (Gutiérrez-Martín et al. 2023, p. 10).

2.6 Sale of green electricity and market mechanisms

The sale of green electricity is divided into different areas, the first is the electricity market. Common rules for the energy market apply at EU level. This market is cross-border and the infrastructure enables energy imports and exports between the individual countries which guarantees a secure, sustainable and affordable energy supply (European Commission 2024).

The next player is the German electricity market, which in turn consists of individual submarkets. The various players operate on these markets. The main driver of the price is the relationship between supply and demand. This platform is operated by the Federal Network Agency and centralizes the trading of generation and consumption. The special feature of electricity is that it must be consumed at the same time as it is generated, as large-scale storage systems reach their limits. Prices change throughout the day according to this principle. The sub-markets are the futures market, on which electricity deliveries are traded several years in advance. Negotiations take place on the day-ahead market for the following day. Even more precise trading takes place on the intraday market. Here, negotiations can take place up to 30 minutes before delivery, in some cases even up to 5 minutes before (Hu et al. 2018, pp. 3-5).

Balancing mechanisms are provided to guarantee a secure supply of electricity. Three types of balancing reserves are provided to keep the balancing group in equilibrium: The primary reserve within 30 seconds, the secondary reserve within 5 minutes and the tertiary reserve within a quarter of an hour. The control reserve is available in both the positive and negative range, this service is compensated es well as the sale of electricity (Bundesnetzagentur 2024b).

The merit order applies on the electricity market and in auctions which gives priority to the cheapest generation. Electricity prices are typically based on generation costs, according to which renewables with the lowest marginal costs are the cheapest. However, the merit order also has the effect of reducing the price of electricity on the market and conventional power plants may experience economic problems and may no longer be able to operate profitably thus might needing subsidies (Coester et al. 2018, p. 16).

Another way to sell renewable energies is via the EEG (Renewable Energy Sources Act, German: Erneuerbare-Energien-Gesetz). Under this law, photovoltaic and wind energy systems are compensated over 20 years at a fixed price per kWh. According to the EEG, the systems are divided into different segments for which different remuneration rates apply. In the case of PV, a distinction is made between systems with an output of up to 10, 40, 100, 400 and 1000 kW, as well as between partial and full feed-in. In 2023, the EEG remuneration was between 5.74 ct/kWh and 13.27 ct/kWh (Bundesnetzagentur 2024a). For PV and wind systems larger than 1 MW, the so-called tendering procedure applies where the lowest bid is awarded

the contract. The average value in 2023 was 6.47 ct/kWh for ground-mounted systems and 10.47 ct/kWh for rooftop systems. The average price for onshore wind turbines was 5.88 ct/kWh (Bundesnetzagentur 2024a).

For the production of green certified hydrogen with electrolyzers, no electricity with EEG subsidies may be used according to the EEG.

An alternative way to market the electricity is via PPAs, Power Purchase Agreements. These electricity purchase agreements have the advantage of concluding long-term contracts with a buyer where a fixed price is agreed and the producer has planning security. This can be particularly attractive for non-subsidized plants, as a prestigious guarantee of origin is also issued. In addition, plants that fall out of the EEG subsidy after 20 years can continue to be operated and a guaranteed price can be achieved. A PPA price calculated for January 2024 was between 5.1 ct/kWh and 6.4 ct/kWh, with a clear downward trend in 2023 (pv magazine 2024). A producer can also conclude a PPA at location A and use it for its second location B. However, this incurs grid charges and fees from the energy supplier. This option is therefore not necessarily attractive, even if the supply of green electricity can be ensured.

Direct marketing is a sales option where electricity is sold by a direct marketer or producer on the electricity exchange, following EEG rules. This method offers higher profit potential but also higher risk of falling below prices. The typical market situation for PV electricity is high surplus at midday, with relative low demand, making the chance of achieving above-average prices less promising.

According to the Federal Network Agency and SMARD, the average wholesale electricity price in the day-ahead market in 2024 was lower than in recent years, with values for 2020 at 3.05 ct/kWh, 2021 at 9.69 ct/kWh, 2022 at 23.54 ct/kWh, 2023 at 9.52 ct/kWh and Q1 2024 at 6.77 ct/kWh. Additional ancillary costs and a guarantee of origin for green electricity make purchasing more expensive then producing it yourself.

The forecast for the wholesale electricity price predicts a development in the medium price range of around 7.6 ct/kWh for 2030 and even lower at around 6.0 ct/kWh for 2050, with additional ancillary costs on top of this (vbw 2023). According to a forecast for the household electricity price for end customers, the values could stabilize at around 42 to 44 ct/kWh in 2035 (McKinsey & Company, Inc. 2024).

For both households and industry, it is always advantageous to achieve a high level of self-consumption and to draw as little as possible from the grid due to the gap between selling and purchase price.

3 Methodology

Simulations were carried out to model the system using certain specific values as a basis. The structure and correlations of the entire system are described in detail in chapter 3.1.

The data used can be divided into two categories: consumption data and generation data. The consumption data, including electricity and hydrogen consumption from the facility, was extrapolated in consultation with the company under review according to the forecasts for the year 2035. This is the target date by which the company aims to have transitioned to climate-friendly and CO_2-free production. In order to keep the company anonymous, some specific circumstances such as locations etc. are not explained in detail. All data used can be found in the electronic appendix. The generation data for wind energy and photovoltaic systems was generated using simulation software (PVsyst and HOMER), based on assumptions about the size of the systems and available areas.

The consumption and generation data were used to simulate an entire year with hourly resolution. To conduct the research, a discrete time-step simulation was developed in MATLAB based on the specific conditions and requirements of the company. A customized decision structure was developed for this purpose. In addition, a simulation was carried out with the software HOMER, whereby the settings were adapted to the discrete time-step simulation.

The results of both simulation methods were then evaluated and compared. In particular, key figures such as the degree of autarky were taken into consideration. Furthermore, the detailed result files played an important role in the analysis. For each hour, the values were calculated and analyzed to understand the impact on the generation and consumption side. The effects of these events on the three critical components, the hydrogen tank, the electrolyzer and the fuel cell, were examined.

Autarky, which is a key concept in this discussion, is defined as the proportion of total electrical consumption that can be covered by renewable energy without relying on the grid and is quantified as a percentage. Mathematically, autarky can be represented by the following formula 3:

$$Autarky = 1 - \left(\frac{Grid\ supply}{total\ consumption\ from\ facility}\right) \tag{3}$$

The two simulation variants were first compared with each other in order to assess their accuracy. For the specific setup with the assumed generation and consumption data and the specified decision process, both variants delivered valid results. However, the results of the equivalent system in HOMER differed despite identical input data and settings. This can be explained by the fact that the HOMER decision algorithm is based on the net present costs

(NPC) of the system and uses this to optimize the system. The decisions are made on this basis and the conditions set for the system. Despite these differences, consistent results were achieved in repeated simulations, which confirms the reliability. Care was taken to maintain the objectivity of the study and to minimize the influence of external conditions. However, the specific framework conditions of the plant and the company were considered. But there is a potential impairment of forecast accuracy due to unforeseen external influences. In addition, it should be noted that the results of this study are not directly transferable to other systems, as each system has its own structure and complexity.

The methods were chosen in order to carry out a comprehensive technical analysis of energy production and consumption for the company. By using simulations, it was possible to model different scenarios and examine their impact on the system.

Overall, the chosen methodology provided a solid basis for answering the questions of this study and provided valuable insights into the potential and challenges of an environmentally friendly energy supply in this specific context.

The two simulation variants are described in detail in the following chapters, starting with an overview of the overall system and the correlations.

3.1 Description of system structure and methodology

The structure of the entire system under consideration and which components and mechanisms are playing a role are explained and presented below. The assessment carried out is specifically designed for this particular system and the conditions. Chapter 3.2 will cover exclusively the details of the conditions. As mentioned in the introduction, assumptions were made and used as the basis for this scenario. There are different ideas with different priorities on how to deal with the hydrogen produced.

The basic idea for this system is to use renewable energies, especially wind energy and from photovoltaics, to produce electricity for the company's own consumption in order to be as self-sufficient as possible. In addition, the renewables should be oversized so that there is a significant surplus of electricity. The factor of generation by renewables compared to the plant's annual consumption is 2.1. In the underlaying scenario, it is planned to install approximately 71.3 MW of PV capacity, resulting in an annual yield of around 68.1 GWh. The majority of the PV systems will be installed as ground-mounted systems on the surrounding areas, half of which will be procured via a PPA. The remaining part will be installed on the rooftops of the factory.

The installed capacity of the wind turbines is 57.6 MW. The assumption is that 8 turbines in the vicinity of the facility can produce around 135.4 GWh/a. This installed capacity respectively generated yield is opposite to the extrapolated annual consumption of 96.4 GWh of the facility.

In the scenario under review this system shall now be completed with the addition of an electrolyzer for the production of green hydrogen, a hydrogen tank for intermediate storage and a fuel to convert the hydrogen produced back into electricity if required. The fuel cell is set up so that it jumps in when too little electricity is generated by wind and PV for the facility and there is enough hydrogen in the storage tank. The aim is to keep grid consumption as low as possible, ideally it should be zero. But achieving 100% autarky and thus no longer being dependent on the grid is a challenge that will be examined in this analysis.

In addition to the requirements to draw as little electricity as possible from the grid and to use the surplus of the renewable energy for the electrolyzer, the proportion of green electricity that has to be fed into the grid should also be kept as low as possible. The reason behind the assumption in this scenario, that renewables do not receive any EEG tariffs and only receive the minimum price when feeding into the public grid (see chapter 2.6).

Another specified condition in this system is that the entire load profile must be covered, either by renewables, the fuel cell or the grid. The facility consumes hydrogen for production purposes as well which must also be covered at all times.

The various ways in which the hydrogen produced can be used are divided into three sections. The first, as already mentioned here, is that the hydrogen is only used for intermediate storage and is converted back into electricity via the fuel cell when required. It should be borne in mind that the efficiency of this back-and-forth conversion is significantly poor. This means that a larger amount of the valuable green electricity is required in comparison to the directly usage or when using other ways of storing which will be explained in more detail in chapter 4.1.

Another use case is the sale of green hydrogen (see chapter 3.2.3). However, this share can no longer contribute to covering the dark doldrums via the fuel cell. The use case of selling the hydrogen to the mobility sector is included in this scenario as well.

The last possible case is the direct use of hydrogen in the mobility sector (see chapter 3.2.4). In this case, the company would have to build its own hydrogen filling station, which could be used to refuel the company's own fleet of trucks, for example.

Finally, an energy flow diagram provides an overview of the entire system and describes the individual energy flows involved (Figure 5). The individual losses of the separate sections are not considered at this point for a better and simpler overview.

The diagram shows generation from renewables in green on the left-hand side, while the middle block represents the facility, from which the individual energy flows such as electricity, heating and cooling originate. Added to this is the surplus energy that can be used in the hydrogen cycle with electrolyzer and fuel cell.

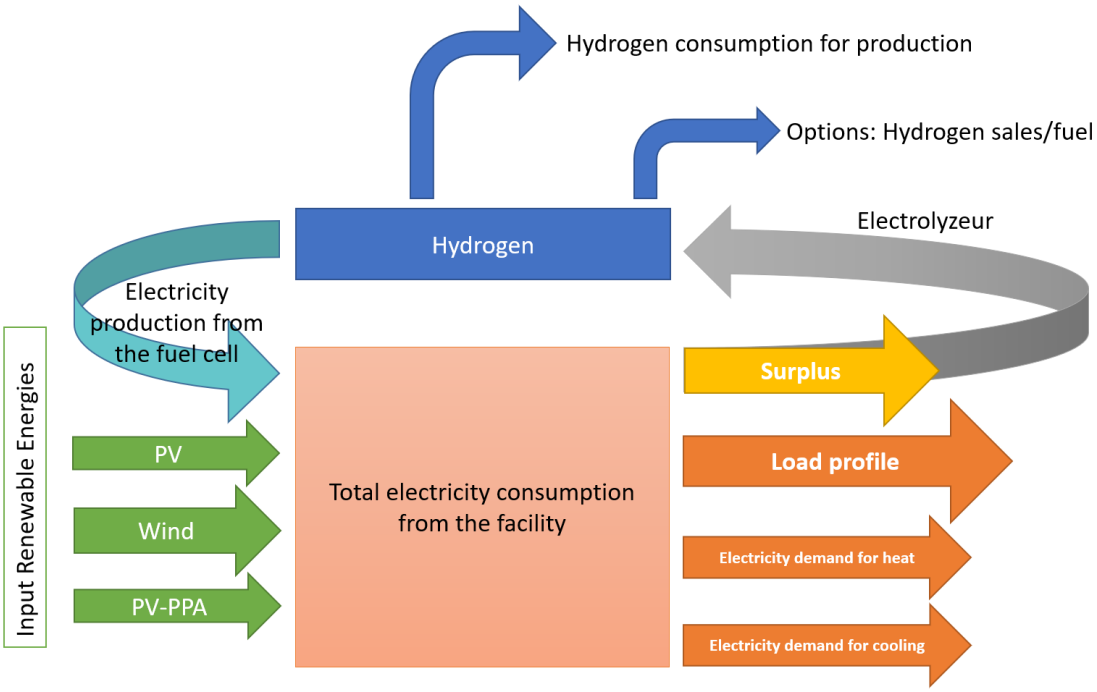

Figure 5: Energy flow chart of the entire system under consideration with generation and consumption

The following two sub-chapters provide a detailed presentation of the installed photovoltaic and wind power plants and explain how the data was generated. They form an essential part of the simulations.

3.1.1 PV installation

Some basic assumptions were made for the photovoltaic share of renewable energy generation based on discussions with the company. These assumptions are first presented and discussed, on the basis of which the figures and yields were then calculated. The PVSyst (PVsyst SA 2024) simulation software (version 7.4.6) was used to calculate the data. The results of these calculations are shown at the end of each passage in this section. They form the basis for the actual simulations carried out with the discrete time-step simulation and HOMER.

As shown in Chapter 2.5, it is advantageous for this project to use a PV system with an east-west orientation, as the generation of energy is better distributed throughout the day. As this project is only in the early phase and much of the construction and design of wind and PV systems is in the hands of the company, it is assumed here that an east-west orientation will be chosen for the PV system.

Weather and radiation data create the basis for the simulation and the calculated yields. Various databases are available for the project site, which use either satellite information or ground measurements to forecast long-term average values for global radiation and diffuse radiation. Data from the years 1994 to 2023 was used.

Hourly weather data is generated for the simulation (see appendix). This is based on the radiation values from the recognized sources for irradiation data PVGIS, SolarGIS, Meteonorm 8 and DWD (Deutscher Wetterdienst).

The average monthly sums of global radiation on the horizontal surface are weighted according to the number of years that the data sources consider for the long-term average of global radiation and combined to develop a database. Attenuating factors, such as air pollution or horizon shading by mountains, are not considered. The uncertainty of the average global radiation data (horizontal) was determined to be 4.7%.

Data from Meteonorm 8, SolarGIS, PVGIS and DWD were used as the basis for the mean daily temperature. The daily temperature is also calculated as a long-term average, weighted by the number of years for which the data is available. The wind speed data is based on data from Meteonorm 8.

The PV part is divided into different sections, the first one is the rooftop systems. There is enough space on the roofs of the production facilities to install a 2.74 MWp PV system. For this purpose, the modules are installed in an east-west direction (90°/270°, N=0°) with an inclination of 10° and one module in horizontal alignment. The module chosen is of the type TSM-DE14H-(II)-390 with a peak power of 390 Wp from the manufacturer Trina (see appendix). Monocrystalline silicon is to be used as the electrically active material. The selected inverter is the SG110-CX type from the manufacturer SUNGROW with a nominal output of 110 kW (see appendix). It is foreseen to connect 18 modules in series and 17 to 18 strings to one string inverter. This results in a DC-AC ratio of 1.1. The simulation with PVsyst resulted in an annual yield of 2.5 GWh, a performance ratio of 83% and a specific annual yield of 913 kWh/kWp for this setup.

The development of technologies that increase module efficiency, for example, has not been considered at this point. There will be further improvements in the coming years, similar to the current use of HJT (Heterojunction technology) and TOPCon (Tunnel Oxide Passivated Contact) technologies instead of PERC (Passivated Emitter and Rear Cell) technology. Although this will lead to an increase in efficiency, this aspect plays a minor role and is not considered at this point.

The next part is the ground-mounted PV system. There are several suitable areas in proximity of the production facilities which can be used for this purpose. In this study case a total of 35.01 MWp will be mounted on them where the modules will be installed in an east-west orientation (90/270°, N=0°) with an inclination of 12° and six modules in a horizontal alignment. The distance between the tables rows is 71.5 cm. This table configuration is currently the state of the art for an east-west orientation. The module used is of type CHSM78N(DG)/F-BH-625 with a peak output of 625 Wp from the manufacturer Astronergy. The modules are n-type mono-crystalline modules with a bifaciality factor of 80%. The modules use TOPCon technology (see appendix). The two modules from Trina and

Astronergy are classified as Tier 1 modules by Bloomberg New Energy Finance which is an expression of the quality of the manufacturers.

The inverter used is type SG350HX from the manufacturer SUNGROW with a nominal output of 320 kW (see appendix). It is foreseen to connect 24 modules in series and 25 to 26 strings to one string inverter. This results in a DC-AC ratio of 1.22. The simulation with PVsyst resulted in an annual yield of 33.5 GWh, a performance ratio of 87.6% and a specific annual yield of 957 kWh/kWp.

The final part consists of PPA PV systems. It is assumed that these systems are at least state of the art and also have a similar configuration to the ground-mounted systems described above. Therefore, the same values were assumed for these installations. The assumption made here is that an installed capacity of 33.55 MWp will generate an initial annual yield of 32.1 GWh based on the same configuration and co-location. This results in a generation of 65.6 GWh/a for the entire part of the ground-mounted PV systems.

3.1.2 Wind installation

In addition to a PV system with an east-west orientation, there is a further advantage to combining wind energy and photovoltaics in order to achieve better distributed energy generation as discussed in chapter 2.5.

A number of assumptions were also made for the wind share of renewable energy generation, which form the basis for the generation values. The wind turbines will all be in the vicinity of the plant site and not in other parts of Germany. Whether the entire generation is produced by the company's own wind farm or project rights are purchased as well. This distinction makes no difference in this analysis.

An Enercon E-126 with a rated output of 7.5 MW, a hub height of 135 m and a rotor diameter of 126 m was used as a reference turbine. It has an upwind rotor with active pitch control. The turbine's power curve covers a range of wind speeds from 3 m/s to 25 m/s. Further settings were left at their default values during the simulation.

Eight of these type E-126 turbines are installed for this study case which results in a total installed capacity of 60 MW. As in the previous chapter on the PV system, no technological progress was considered here. It is likely that there will still be ongoing progress in terms of increased efficiency and improvements in the wind sector. However, these improvements are marginal in contrast to the uncertainties of the assumptions made.

The yield analysis was carried out using the HOMER software which was used to generate the hourly yield values. The basis for this was the weather data from the NASA prediction of worldwide energy resources (POWER) database. The average monthly values of the wind speed at 50 m above the surface over a period of 30 years (1984 - 2013) were used (see appendix).

The analysis shows that the installed capacity of 60 MW generates an annual yield of 135.5 GWh. This allows for conclusions to be drawn about the full load hours. The definition of the full load hours of a wind turbine is the ratio of the energy yield to the nominal output and is given in hours per year. Ultimately, the full load hours are a measure of the degree of utilization of a wind turbine. The average value of the full load hours in this calculation is around 2260 h/a. This is well within the range for onshore wind turbines in Germany, which lies between values of 2,000 h/a and 2,600 h/a and imply a slight upwards trend for the future (Borrmann et al. 2020, p. 9).

The yield values generated by the wind and PV system with hourly resolution form the basis for the system modeling described in the following chapter. They are also part of the analysis with the HOMER software in chapter 3.3.

3.2 Developing a discrete time-step simulation in MATLAB

In order to model the system described in chapter 3.1 accurately and to make an exact decision according to the specific conditions, a customized program was developed using MATLAB. The program imports the relevant data with an hourly resolution for an entire year and calculates the resulting values.

The relevant data consists of the load profile of the entire facility, the load profile of hydrogen consumption for production purposes and the energy generation data from photovoltaic and wind energy systems.

The consumption data reflects the status quo and was extrapolated to the year 2035 based on the forecast growth and the expected increase in efficiency. The growth forecast and the expected increase in efficiency are based on the company's internal calculations, which were exclusively determined for this particular scenario. The degree of fulfillment for precisely this scenario can be discussed at another point.

The main focus of this study is on finding a way to reach the goal of being a CO_2 neutral and climate-friendly company by 2035. Therefore, the focus is on the degree of autarky and how the highest possible level can be achieved.

The program was written in the MATLAB environment with version R2023b and is part of the electronic appendix. The following scheme according to the specific conditions is the basis for the program and the system that must be simulated.

For this study case the system is divided into two main segments. In the first segment, there is a surplus of renewable energy to cover the facility's energy needs. In this case, the surplus electricity is used to operate an electrolyzer that produces green hydrogen as discussed in chapter 2.1. In the second segment, the generation of renewable energy is not sufficient to cover the facility's electricity needs. This occurs, for instance, during dark doldrums. Stored

hydrogen is then used in a fuel cell to generate electricity. If this electricity is not sufficient, additional electricity is drawn from the public grid.

The following decision tree (Figure 6) shows the exact diagram of the principles for the MATLAB code that the processes follow. The different cases are mapped exactly. The principles are clearly defined regarding the use of green energy from wind and PV and the specific conditions under which it can be used.

They follow these main specific terms:

1. Archive the highest possible level of autarky;
2. The surplus electricity from renewable energies is used for the electrolyzer to produce hydrogen;
3. As little electricity as possible is fed into the grid;
4. The fuel cell is used for reconversion during dark doldrums;
5. Further hydrogen production for sale to third parties or for other purposes;
6. The hourly hydrogen consumption of the facility must be covered at all times;
7. The electricity demand must be covered at all times.

In order to achieve $C0_2$ neutrality, the first goal is to achieve a high level of autarky. The electrolyzer is to be operated primarily with the surplus generated. The amount of electricity that must be fed into the grid should be kept as small as possible. The market mechanisms were discussed in Chapter 2.6 and the options for using them were presented. The hydrogen produced is to be used by the fuel cell to generate electricity during dark doldrums so that the public grid does not have to be used. Ultimately, the entire load profile as well as the hydrogen required for production must be covered. If this cannot be achieved using electricity from renewable sources or the hydrogen produced on-site, the grid must provide a temporary solution, possibly even operating the electrolyzer if there is not enough hydrogen in the tank.

The basis for all decisions is the relation between the load profile and electricity generation from renewable energies which is checked for each time step. All data with an hourly resolution was used for the completed analysis.

If the electricity generation from renewable energies is greater than the consumption of the system, the queries on the left-hand side of the decision tree are followed. In this case, the surplus is generally used to operate the electrolyzer and produce green hydrogen.

If the production of renewables is less than the consumption of the facility, the decisions are made on the right-hand side. This is where the previously produced hydrogen is generally converted back into electricity via the fuel cell and thus hydrogen is consumed. If the required output cannot be generated by the fuel cell, the grid must be included.

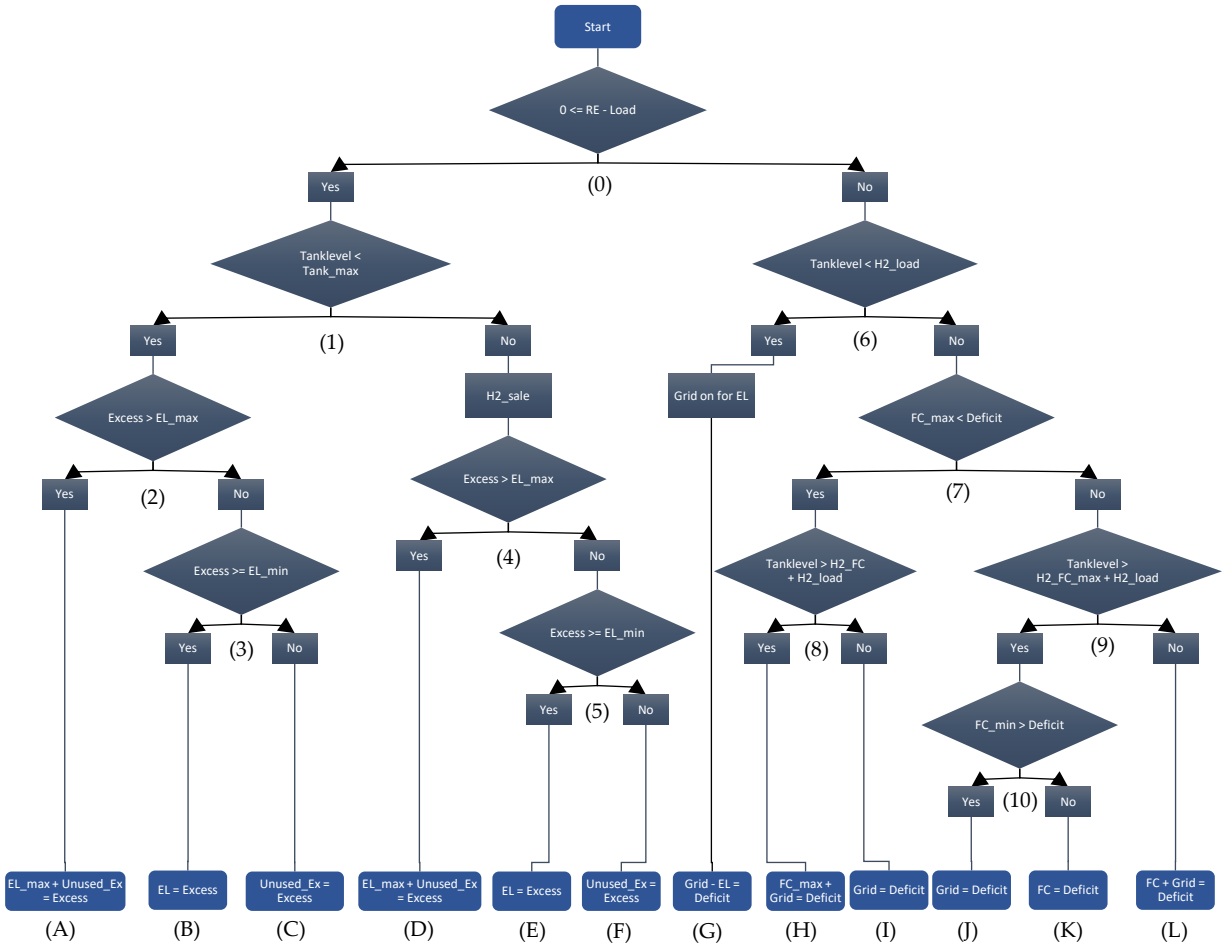

Figure 6: Decision tree for the processes in the MATLAB code for the time discrete simulation

Abbreviations:

RE	– Renewable energy
EL	– Electrolyzer
EL min/max	– Electrolyzer min/max power
FC	– Fuel cell
FC min/max	– Fuel cell min/max power

The following sections describe the individual decision paths in more detail. At the end of each decision path is an instruction on how to deal with the surplus or deficit and how each component is affected (A to L).

The beginning is at the top at *Start*. The first query is whether production is greater than consumption (0). If the answer is *Yes* (left side), the system checks whether the tank level is low enough to generate H_2 with the electrolyzer after deducting the hourly H_2 consumption (1). If the tank level is low enough, the next step is to check whether there is a greater surplus than the maximum power of the electrolyzer (2). If so, the electrolyzer is operated at maximum power. The maximum amount of H_2 that can be produced is also calculated and must not be

exceeded. The remaining surplus of electricity is not used and can be fed into the grid. H_2 is produced, the fuel cell remains off (A).

If the excess is not greater than the maximum electrolyzer power (2), the system checks whether the surplus is greater than the minimum power of the electrolyzer (3). If so, the electrolyzer runs at the excess power (B). If not, the surplus cannot be used, and the electrolyzer remains off (C).

If after the first query about the available surplus the answer to the following query (1) is negative (the H_2 tank is too full to operate the electrolyzer directly), 25% of the tank content is sold. This leaves space in the tank to produce new hydrogen and use the surplus. As before, it will be checked whether the surplus is greater than the maximum power or less than the minimum (4). If the surplus is greater than the maximum, the rest of surplus remains and the electrolyzer runs and produces hydrogen (D). If the surplus is at least above the minimum power (5), the electrolyzer runs at the corresponding power and the entire surplus is used (E). In the third case, the surplus is too low to operate the electrolyzer and it remains unused (F).

The decision paths on the right-hand side follow (after 0). This is where there is a deficit, and the load profile is greater than the electricity produced by renewables.

The first query then asks whether there is not enough hydrogen in the tank for the hourly consumption from the factory (6). If so, the electrolyzer is operated via the grid supply. In this case, the grid covers the entire power consumption of the facility as well (G).

If the tank is not too empty, the next query is whether the maximum output of the fuel cell is less than the deficit (7). If so, the tank level is queried again. Is there enough to operate the fuel cell (8)? If so, it starts up at maximum power and the remaining deficit is covered by the grid (H). If there is not enough hydrogen available, the fuel cell remains off and only the grid covers the load profile (I).

Back to the third query, whether the maximum output of the fuel cell is less than the deficit (7). If the result is *No*, the tank level is also queried here (9). If this is greater than the calculated hydrogen consumption of the fuel cell to cover the deficit, it is also checked whether the deficit is less than the minimum output of the fuel cell (10). If so, only the grid is activated (J). If not, the fuel cell starts up and covers the deficit (K).

If the result of the previous query about the tank level (9) is that the fuel cell only has some hydrogen available, it is operated with the corresponding power. The remaining deficit is covered by the grid (L).

At the end of the decision paths, there are twelve results to choose from (A to L), which can be achieved in various ways. The modeling in the MATLAB simulation is based on them. For all results according to the decision tree, the load profile is covered by the renewables, the fuel cell and the grid. The hourly hydrogen consumption is as well always covered by the plant for production.

The technical background of the system was outlined and a link to existing literature and studies from research and industry was shown. An overview of the entire system has also been provided. In addition, the decision tree has been explained in detail, which is an important basis for modeling the system in MATLAB. The following sub-chapters explain the individual cases, how to deal with a surplus or deficit of renewable energy and what options are being considered for using the green hydrogen produced.

3.2.1 Base Case 1 – green hydrogen production

This part represents the basis of the entire system. With the generation of green electricity through wind and PV systems and the oversizing compared to the facility's annual consumption, a surplus is generated.

This surplus will primarily be used to operate the electrolyzer. The electrolyzer then produces green hydrogen, which is temporarily stored in a tank. One limiting factor is the minimum output of the electrolyzer at which it must be operated. If the surplus is less than the minimum output, the electrolyzer cannot be used and the surplus must be fed into the grid. Another possibly limiting factor is linked to the requirement that the hydrogen demand for production must be covered at all times. If this is not possible because the hydrogen tank is empty, the grid must supply the electrolyzer. In this case, only as much hydrogen is produced as necessary or the electrolyzer is only operated at minimum power if the amount of H_2 required for production is less.

This green hydrogen is a valuable product and once declared completely green, it can serve as basis for a business model (see chapter 4.2). The choice of technology and the electrolyzer itself with its specific operating conditions also play an important role. This was discussed in the theoretical and technical principles (see chapter 2.2).

3.2.2 Case 2 – H_2 reconversion to electricity

The second case builds on the first one, the production of green hydrogen. Supplementary to the described system a fuel cell is added. Its function is to use the temporarily stored hydrogen in the event of a dark doldrums and to cover the deficit. Again, there are requirements that make this task more difficult and push the degree of autarky down. Like the electrolyzer, the fuel cell also has a minimum power at which it can be operated. If this is not reached, it cannot be operated and the grid has to step in instead. This again reduces autarky. The situation is similar if the maximum output of the fuel cell is exceeded. In this scenario, the deficit exceeds the capacity of the fuel cell, such that the missing electricity has to be drawn from the grid.

The selection of technology and the fuel cell itself with its specific operating conditions play an important role once again. This was discussed in the theoretical and technical principles (see chapter 2.4).

3.2.3 Case 3 – sale of green H_2

If the hydrogen tank reaches its maximum capacity, the excess energy cannot be used by the electrolyzer. In this case, the production of hydrogen must be stopped temporarily. In order to use the excess energy efficiently, a certain proportion of the hydrogen stored in the tank is sold. This proportion is exactly 25% of the tank's current capacity. This means that the proportionate amount for sale is always slightly less than 25% of the maximum tank volume. As a result of this dynamic control, the surplus green electricity can continue to be used by the electrolyzer and does not have to be fed into the grid. Hydrogen is also preliminary produced for sale. This hydrogen must be stored temporarily or filled accordingly for transportation.

3.2.4 Case 4 – H_2 use as a fuel

Unlike the cases described above, the fourth case is not directly part of the investigation and is also not considered in the MATLAB code described. Case 4 is a consideration of how the produced hydrogen, which is not needed for production or the electrolyzer, can be utilized. Part of the assessment is to look into possible business models which can be established around this excess hydrogen and how reliable those could be. One possible usage could be as fuel for the company's truck fleet. Those trucks are responsible for transporting the manufactured goods and delivering them to customers within a radius of around 200 to 300 kilometers. This poses no problem; the hydrogen-powered Mercedes-Benz GenH2 truck from Daimler has already exceeded 1,000 km on one charge in a first test drive (Daimler Truck Holding AG 2023).

This would require a number of changes, not only would the truck fleet have to be converted by purchasing new hydrogen trucks, an on-site filling station would be required as well. There are always funding programs that support and subsidize such projects.

Fuel cells for heavy transport offer a few advantages. For example, the fueling/charging time is 15 times faster compared to battery-powered vehicles, the space required for the fueling infrastructure is 10 to 15 times less and, from around 100 km, the ratio of costs to energy capacity converted into range is much better (Fuel Cells and Hydrogen 2019, pp. 25-31). These arguments are countered by the price of hydrogen.

Nevertheless, further investigations and calculations are necessary at this point in order to create a more reliable evaluation on this scenario. It should be examined in more detail whether the quantities of hydrogen required for the trucks can be produced. Furthermore, an economic assessment of this scenario is of crucial importance. This would allow a better assessment of its feasibility and practicability.

3.3 Use of commercially available software HOMER

In addition to the discrete time-step simulation, the established simulation software HOMER Pro (version 3.18.0) was used as a further method of simulation. The software is used worldwide for the optimization of renewable energy systems (Bahramara et al. 2016). The following part outlines the main features of the software and describes the settings and assumptions selected for the system to be analyzed in this study case. The software was developed by HOMER Energy LLC from Boulder, Colorado, USA (HOMER Pro 2024).

According on the numerous publications in which HOMER has been used, it can be concluded that this software is one of the most widely used simulation programs for stand-alone and as well as grid-connected systems.

The program offers the option of simultaneously integrating a variety of components such as generators with conventional power generation and renewable energy sources. Thermal and electrical generators and consumers are covered as well. All consumption profiles, generation profiles and ambient conditions such as solar irradiation, ambient temperature and wind speed are included and calculated for a selected system of the customer's own design. The possible system designs are compared with each other, such as the size of PV and wind systems.

When optimizing the systems, HOMER focuses on the economic costs. Complementary to the internal optimization algorithm, HOMER also offers the option of carrying out a sensitivity analysis or the mapping of an existing system and restricting it under certain conditions.

For the modeling of the system in HOMER, the scenario was mapped in the software. The generation data for the PV part was used from the PVSyst output file and imported into HOMER. The load profile and the hydrogen profile for production were imported as well. In addition, the system components under consideration and their properties were stored in the HOMER database.

The following Figure 7 provides an overview of the system shown in HOMER. This corresponds to the system described in chapter 3.1.

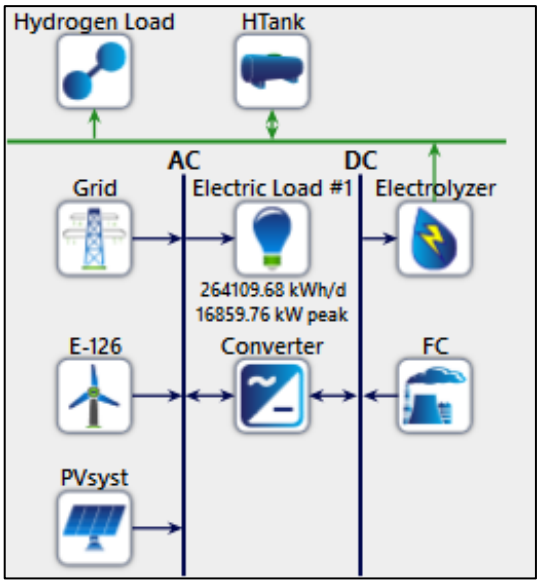

Figure 7: Schematic structure of the complete system in HOMER (HOMER Pro 2024)

The schematic figure shows the system with grid connection, the renewable energy sources wind and PV, converter, electrolyzer, hydrogen storage, fuel cell, load profile and hydrogen consumption profile.

The same assumptions were made and parameters set as for the time discrete simulation (section 3.2). As a result, two comparable simulation variants were obtained. A simple stand-alone system without hourly hydrogen consumption and a grid connection were created in advance. The generation and consumption data are the same as in the later simulation and were used to benchmark the two simulation variants. The result of the benchmarking was as follows (the deviations from the HOMER to the time-discrete simulation are shown):

- Power generation by the fuel cell: + 0.16%
- Electricity consumption by the electrolyzer: - 0.68%
- Hydrogen consumption of the fuel cell: + 0.2%
- Hydrogen production from the electrolyzer: + 0.15%

Those small deviations of less than 1% display sufficient accuracy and conformity between the two software options to be able to compare the two approaches.

The input parameters for the components for the electrolyzer were a minimum operation limit of 10% and an efficiency of 72% with an electricity consumption of 54.8 kWh/kg H_2 and a specific fuel consumption of 0.06 kg/kWh. This corresponds to common values according to the data sheets in the appendices. The minimum operation limit depends on the wiring of the individual electrolyzer modules and can be reduced even further by smart connections.

For the fuel cell, the minimum operation limit was set to 20% and an efficiency of 50% was set, which is typical for current fuel cell technologies according to the data sheets in the appendices.

4 Results

The technical feasibility and design of a specific system and the associated generation and consumption of electricity and hydrogen of the facility were modeled and analyzed. The main focus of this assessment is to elaborate the optimal design in regard to the sizes of the hydrogen tank, electrolyzer and fuel cell. It is investigated which combination of these components and sizes represents the most suitable design for the specific prerequisites of the company. The results are intended to create a basis for further evaluation and to indicate whether and how this approach using hydrogen as an energy storage system is promising for the future.

Finally, this analysis should provide an answer to the question posed at the beginning, how companies can efficiently use solar and wind energy to cover the load profile and produce green hydrogen while ensuring economic performance, focusing on a high degree of self-sufficiency and co-location strategies.

The results are presented below, along with the various cases and arguments that are part of the simulation. The analysis is based on the results of the PV and wind systems (see chapter 3.1.1 and 3.1.2).

In the scenario examined, an installed capacity of 71.3 MW PV and 60 MW wind was used, generating an initial annual yield of 203.5 GWh/a in total.

For the tank size, kilogram (kg) is used as the reference unit, as the volume varies depending on the pressure and other conditions. The alternative of specifying the tank size in Nm^3 is deliberately not chosen. Firstly, the specification in kg is easier to classify and can be better categorized than a very large volume. Secondly, by using kg, the reference value remains uniform and can later be converted into a volume with specific conditions.

4.1 Technical system design results

In the following chapter the results of the time discrete simulation, which was carried out with the specially developed algorithm in MATLAB are presented, beginning with a brief description and explanation of the input parameters used, which are essential for the analysis.

To start the simulation, the initial value of the hydrogen tank was set to 20% of the maximum capacity. This setting ensures the initial availability of hydrogen without the need of a completely full tank. The tank reserve has been set to 0.5% of the maximum tank volume. This tank reserve is intended to ensure that the system continues to function even when the tank is almost empty and that at least the hourly consumption can still be covered. This could otherwise become critical in the event of unforeseen consumption peaks if the fuel cell consumes too much hydrogen.

The efficiency of the electrolyzer is set at 72%, which corresponds to an energy consumption of 54.8 kWh/kg of hydrogen. With a slightly conservative approach, this value reflects the

efficiency of current electrolysis technologies on the market. The values used for the electrolyzer and the fuel cell correspond to the values in the data sheets, which can be found in the appendices. The minimum output of the electrolyzer was set at 10% of its capacity.

The efficiency of the fuel cell is set at 50%, which is typical for current fuel cell technologies. This value indicates how effectively the fuel cell can convert chemical energy into electrical energy. The minimum output of the fuel cell is 20% of its capacity.

Finally, the sales rate of 25% of the hydrogen from the tank was set. This enables flexible handling of hydrogen production and storage before the tank is full. This rate was introduced to prevent the tank from being completely filled. Otherwise, the electrolyzer would have to be switched off in the event of an electrical surplus. In this way, the surplus can be used as efficiently as possible at this point while hydrogen can be produced and stored for sale or other purposes. The analysis was carried out with these selected specific parameters for the simulation. They enable a comprehensive evaluation of the system performance under the most realistic conditions possible and help to effectively simulate the dynamics of the system.

The following parameters are crucial for analyzing the system and are used as a basis for dimensioning the components. These parameters have been identified as decisive:

- Degree of autarky
- Energy content of the tank
- Share of dark doldrums covered by the fuel cell and the grid
- Share of hydrogen sales

Furthermore, the operating hours of the electrolyzer and the fuel cell also play a role and should not be disregarded in the decision making.

The first decisive parameter is the degree of autarky which is defined as the proportion of the facility's energy requirements that is covered by renewable sources. This degree is determined by the ratio of energy covered from renewable sources to the facility's total energy consumption. The analysis is intended to show the extent to which autarky is achievable and whether there is an optimal degree of autarky that can be effectively achieved. One question is whether exceeding the optimum degree of autarky requires a significant increase in the size of the components without the additional gain in autarky being proportionate.

The next important parameter is the energy content of the tank. This is related to the time span and amplitude of power consumption that can be covered by the fuel cell. It raises the question of whether the tank should be designed in such a way that in the event of a dark doldrums and the worst-case scenario with maximum load over the entire period, the fuel cell should completely cover the deficit. The study also examines how the energy content and the corresponding tank size changes in relation to the duration in hours.

The share of the dark doldrums covered by the fuel cell and the share from the grid are included next. Those two parameters can provide information as to whether there is a point at which the share of the fuel cell is at its maximum and that of the grid at its minimum.

The operating hours of the electrolyzer and the fuel cell are important for the technical and economic feasibility of the system. Too many hours of downtime are not beneficial for the two devices from a technical point of view. In economic terms, the investment costs are amortized more quickly with higher operating hours.

The final parameter that plays a role in determining the size of the components is another economic aspect. The proportion of the hydrogen produced that can be sold and is not required for self-consumption or the electrolyzer. This can be used to create a business model showing where this system can become economically viable.

Those six described parameters are now examined in detail and the results are presented in the following chapter. First, an overall picture of how the three parameters tank size, electrolyzer size and fuel cell size relate to each other and in regard to autarky which is indicated by the coloring. The following Figure 8 shows a three-dimensional overview of the tank size in kg along the horizontal abscissa axis. The size of the electrolyzer in kW is shown in the ordinate axis, the size of the fuel cell in kW is shown in the vertical application axis.

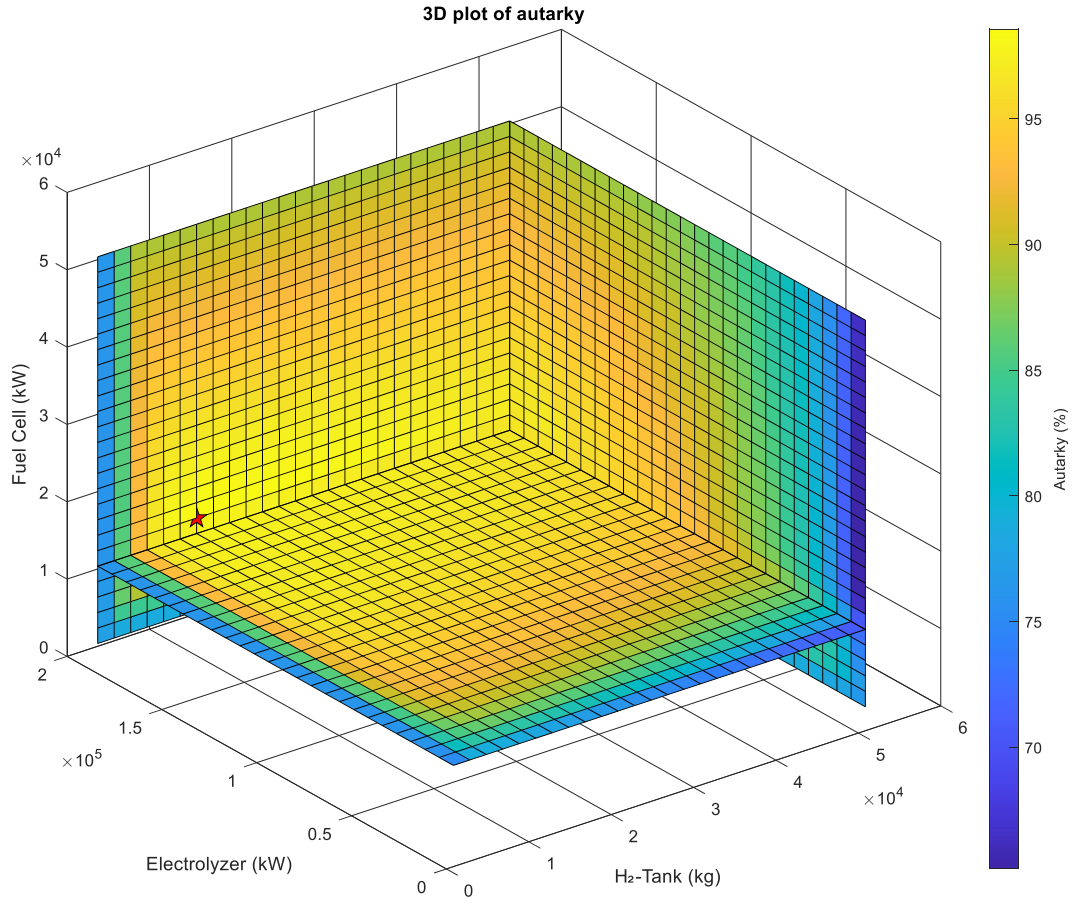

Figure 8: 3D-plot with an overview of tank size, electrolyzer and fuel cell in relation to each other with corresponding autarky and with red star as autarky maximum

For this first overview, the components were presented in a wide range of sizes in order to get a good impression of the behavior and the degree of autarky. The size ranges are as follows: tank size between 2,000 and 52,000 kg; electrolyzer size between 5 and 195 MW; fuel cell size between 2 and 52 MW.

The change in autarky is clearly visible. The light greenish area shows values around 90% of autarky. The orange areas show values above 90% and the yellow areas are above 95% autarky. The red star marks the maximum at 98.56%. It displays the first triplet of values that reaches this maximum value. No higher value above this can be achieved with the system with the size ranges and the principles for the use of renewables. The graph shows that, in principle, autarky increases as the tank grows, but only up to the maximum mentioned. The situation is similar with the size of the electrolyzer, autarky also increases with increasing values. A different behavior is visible with the fuel cell. Here, it reaches a maximum between around 10 and 25 MW. At values above this, autarky decreases again.

It is clear from this overview that the tank and the electrolyzer are crucial for achieving an autarky higher than around 90%. A further 3D plot (Figure 9) follows, in which a smaller range is shown: tank size between 2,000 and 26,000 kg; electrolyzer size between 10 and 40 MW; fuel cell size between 5 and 17 MW. The marked maximum (red star) shows a value of 96.18% autarky.

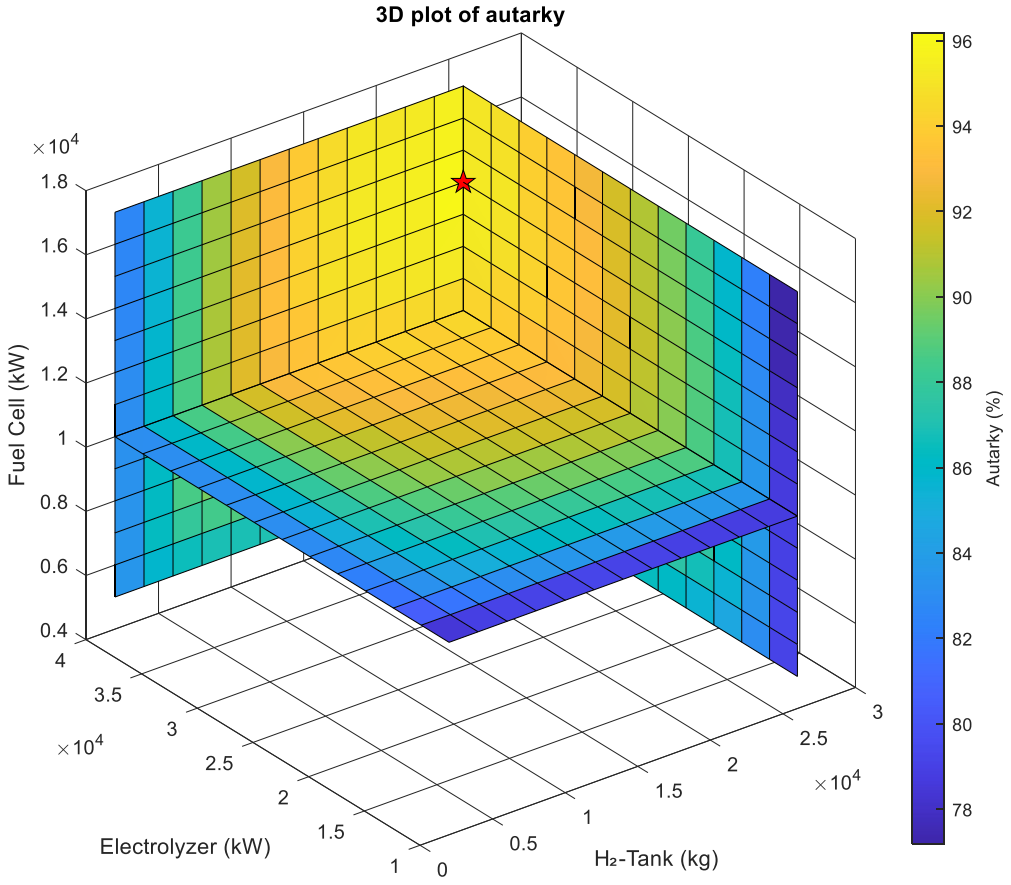

Figure 9: Section of 3D-plot with an overview of tank size, electrolyzer and fuel cell in relation to each other with corresponding autarky and with red star as autarky maximum

The data shows that a degree of autarky of around 90% can be achieved even with smaller components. The areas shown in yellow and orange in the diagram are already clearly above this value. In certain regions of the diagram, the degree of autarky can be increased to around 96% by selecting larger components.

The following pictures show the dependency of two parameters. The corresponding values can now also be identified more easily here. In the following three figures, the marked maximum (red star) indicates the highest possible autarky in the area concerned.

First, the tank and electrolyzer size are shown with the corresponding autarky (Figure 10). Here, as in Figure 9, the cut was made at a fuel cell size of 10 MW.

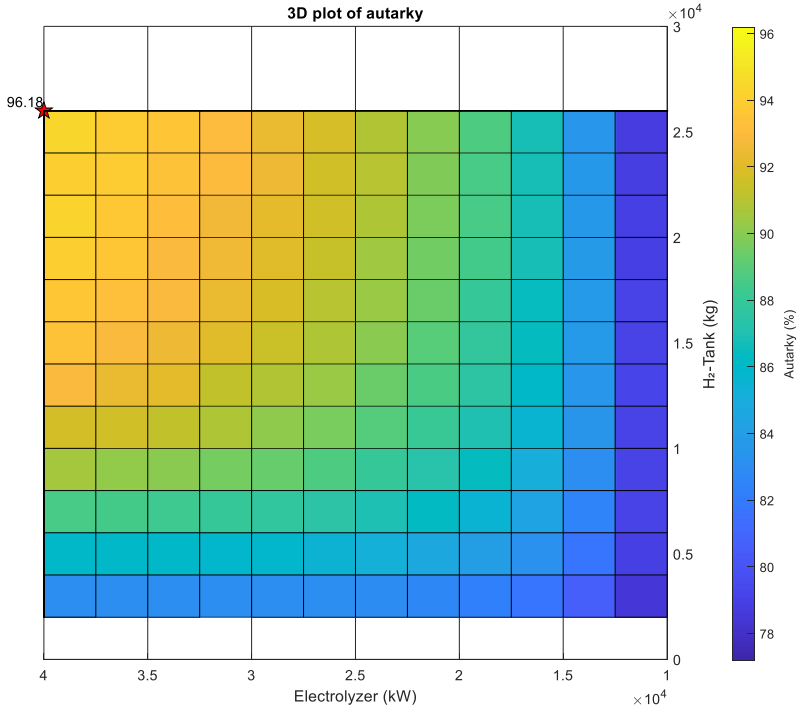

Figure 10: Section with tank size compared to the size of the electrolyzer at a fuel cell size of 10 MW with corresponding autarky and marked maximum

The next section (Figure 11) shows the electrolyzer size versus the size of the fuel cell with corresponding autarky. Here, as in Figure 9, the cut was made at the maximum tank size of 26,000 kg.

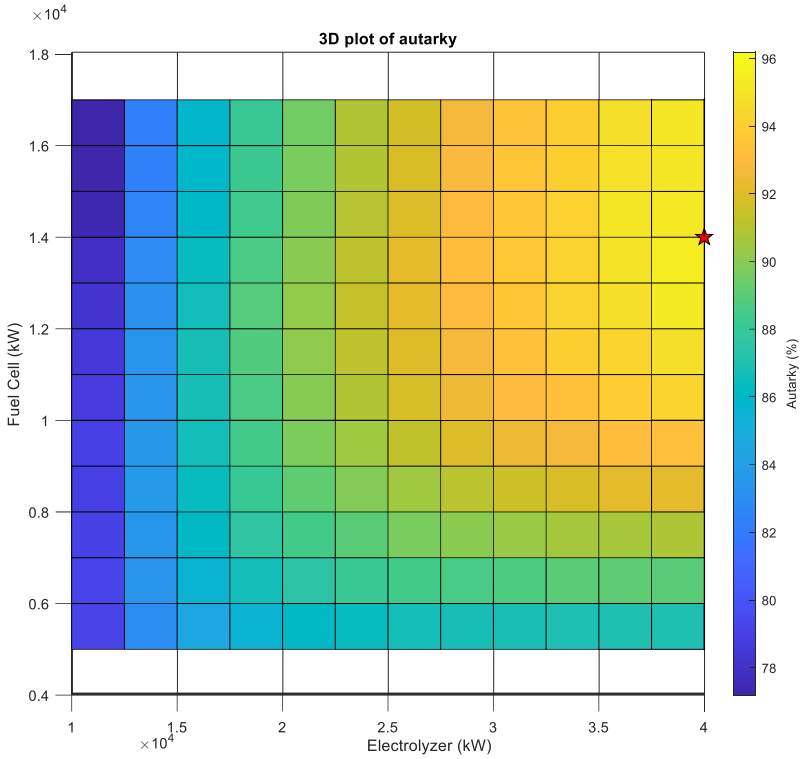

Figure 11: Section with electrolyzer size compared to the size of the fuel cell at a tank size of 26,000 kg with corresponding autarky and marked maximum

The last plot shows the tank size against the size of the fuel cell with corresponding autarky (Figure 12). Here, as in Figure 9, the cut was made at the maximum size of the electrolyzer with 40 MW.

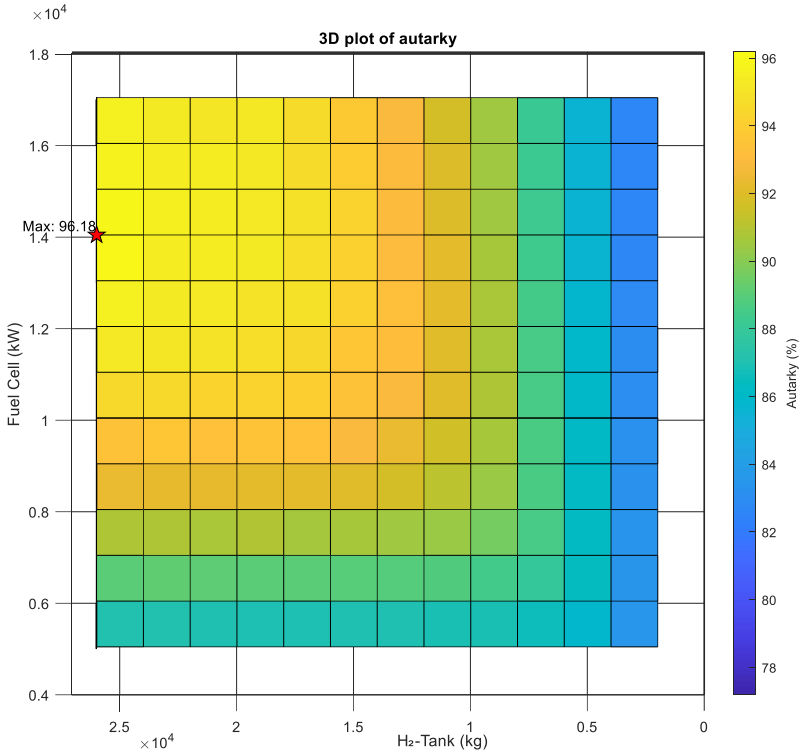

Figure 12: Section with tank size compared to the size of the fuel cell at an electrolyzer size of 40 MW with corresponding autarky and marked maximum

The last three plots showed how the autarky changes with increasing component size. This is the case if only one size increases, a similar change can also be seen when both components show an increase in size.

With a balanced ratio of the sizes of the various components, an autarky of more than 90% can be achieved. The size of components does not need to be exceptional big to achieve this. The term "big" is of course a relative description.

In the following, a detailed look will be taken at this appropriate tank size and the associated energy content. This consideration is also intended to show what options are available for the tank and what impact this has on its size.

First, the hydrogen required per hour to supply the fuel cell with a certain amount of energy is considered. This already shows the order of magnitude of the consumption. Table 4 below only shows the hydrogen consumption required for the fuel cell.

Table 4: Power of the fuel cell in relation to the amount of H_2 required

Power	Required H_2
[kW]	[kg]
2,000	120
4,000	240
6,000	360
8,000	480
10,000	600
12,000	720
14,000	840
16,000	960
18,000	1,080
20,000	1,200

These displayed quantities of hydrogen are required every hour. Assuming, for example, that there is only a dark doldrum for 10 hours overnight and the fuel cell has an output of 10 MW and thus supplies the plant, a total of 6,000 kg of hydrogen is required. This small hypothetical calculation is only intended to illustrate how quickly a larger quantity of hydrogen and therefore a correspondingly larger tank is required.

Based on this preliminary analysis, the data generated in MATLAB is then analyzed in relation to the tank size and the load profile respectively the deficits.

4.1.1 Hydrogen tank size and energy content

Based on the hourly data generated by the MATLAB simulations, the frequency and duration of the dark doldrums' cycles (deficits due to insufficient energy generation from wind and PV)

are determined. In the following sections, this serves as a basis for establishing a reasonable assumption for the tank size of the hydrogen.

The cycles of renewable energy generation often look like this: in the dark season, during the night, less electricity is generated than is consumed. There is a deficit over around 12 to 20 hours. The situation is similar in the brighter months of the year, but with slightly shorter dark doldrums. A total of 12 events per year show that there is no energy generation from renewables up to 36 hours. The longest period without energy generation in the data was 61 hours. However, this extreme event with over 36 hours without renewable energy production only appears three times in the data over an entire year.

The consumption data clearly shows that the load profile is significantly higher during the week than at the weekend. During the week, the load profile averages to 14 to 15 MW per hour. At the weekend, the load profile fluctuates between 5 and 6 MW on average per hour. This behavior is reflected in a similar way in the hydrogen load profile but does not correlate as strongly and frequently and shows deviations from this pattern. During the week, it frequently shows an average hydrogen consumption for production of around 16 to 19 kg per hour with the high load profile. At the weekend, the average hydrogen consumption for production falls to around 4.5 to 5.5 kg of hydrogen.

Based on this data, an appropriate size can now be determined. Therefore, the basis for the analysis is the worst-case scenario with 15 MW/h energy consumption and 19 kg/h of hydrogen consumption for production purposes.

In order to be able to cover the regular doldrums in electricity generation up to around 18 hours, the tank for supplying the fuel cell and for the worst-case scenario with 19 kg/hour hydrogen consumption for production would have to be able to hold around 16,202 kg.

The next scenario is the rare doldrums of up to 36 hours. In this case, the tank would have to have a capacity of around 33.087 kg. Here too, the maximum hourly consumption has been considered for production purposes as described above.

For the extreme case, which is only recorded three times in the data, the tank would have to have a capacity of around 55,145 kg. To be completely autarkic for 60 hours and to solve this scenario without drawing electricity from the grid does not seem economical. The more complete cycles a battery system runs through in a year, the more economical it becomes. This principle applies to electrolyzers and fuel cells as well as to hydrogen storage systems. The additional purchase costs for the increasing size of the storage tank must be covered by the cycles. However, as the extreme events described only occur very rarely, there is no basis for economic viability.

Table 5 shows the three cases described. The worst-case scenario is shown with the corresponding tank sizes and the energy content with the equivalent amount of hydrogen. The

efficiency of 50% of the fuel cell has already been considered here and not the lower calorific value of hydrogen of 33.33 kWh/kg.

Table 5: Tank sizes, time period and energy content for the worst-case scenario with hourly consumption of 15 MW and 19 kg hydrogen

Peak power	Duration	H_2 consumption fuel cell	H_2 consumption production	Tank size	Energy content of tank
[kW/h]	[hrs.]	[kg/h]	[kg/h]	[kg]	[kWh/Tank]
15,000	12	900	19	11,029	183,800
15,000	18	900	19	16,544	275,699
15,000	24	900	19	22,058	367,599
15,000	36	900	19	33,087	551,399
15,000	48	900	19	44,116	735,198
15,000	60	900	19	55,145	918,998

Various methods are available for storing hydrogen as discussed in chapter 2.3. One of the simplest methods is storage in a pressurized tank, as used in this project. In this case, the hydrogen is stored at a pressure of around 45 bar in a tank with a volume of 90 m^3. Based on this volume, the total number of tanks required to store the specified amount of hydrogen at different pressure levels can be calculated. In addition to the above-mentioned pressure of 45 bar, higher pressures of 350 bar and 700 bar are also used in practice. The following Table 6 illustrates the total volume that can be stored under these pressure conditions and the corresponding number of tanks required at each pressure.

Table 6: Tank volume, energy content, time period and number of tanks at different pressures

Duration	Tank size	Energy content of tank	Volume (45 bar)	No. of tanks (45 bar)	Volume (350 bar)	No. of tanks (350 bar)	Volume (700 bar)	No. of tanks (700 bar)
[hrs.]	[kg]	[kWh/Tank]	[m^3]	[pcs]	[m^3]	[pcs]	[m^3]	[pcs]
12	11,029	183,800	2,918	32.4	375	4.2	188	2.1
18	16,544	275,699	4,377	48.6	563	6.3	281	3.1
24	22,058	367,599	5,835	64.8	750	8.3	375	4.2
36	33,087	551,399	8,753	97.3	1,125	12.5	563	6.3
48	44,116	735,198	11,671	129.7	1,501	16.7	750	8.3
60	55,145	918,998	14,589	162.1	1,876	20.8	938	10.4

Note: the usual rounding up and down rules have been applied to the values. A decimal point was only added where more precise information was deemed necessary.

This calculation clearly shows what a difference it makes to store the hydrogen at a higher pressure and the number of corresponding tanks with a size of 90 m^3 is reduced. As the period length to be covered by the fuel cell increases, more space is required for the tanks. At a storage pressure of 45 bar, 32 tanks are still required to cover even just 12 hours of dark doldrums. At 350 bar and 700 bar, the numbers are significantly smaller. However, a higher storage pressure entails other aspects that must be considered as well. In addition to the energy required to achieve the corresponding pressure, legal regulations also come into place. Supplementary to a higher pressure for storage, the size of the fuel cell can also be reduced. This means that the entire load profile can no longer be matched with the fuel cell in the worst-case scenario shown. This raises the question of the consequences for autarky.

However, before the autarky curves in relation to the three parameters tank size, electrolyzer size and fuel cell size are discussed in detail, a final comparison regarding the hydrogen storage will be made.

4.1.2 Comparison with equivalent battery storage systems

In order to extend the analysis to other aspects, a brief comparative analysis with conventional battery energy storage systems (BESS) is carried out.

The question arises as to whether the current system with a hydrogen tank for intermediate storage is the only practicable option. Does a battery energy storage system offer a simpler alternative to store the electricity directly and release it when needed, bypassing the hydrogen conversion step? An important aspect to be investigated is the required size of such a battery storage system and its energy density compared to a system using hydrogen. An initial comparison of efficiencies will give a clear indication of which system could be more advantageous overall.

The efficiency of a battery storage system is specified at 75% to 98% (Yang et al. 2024, pp. 6-8). Assuming the battery system has an efficiency of 85%. This is compared to the overall efficiency of the system consisting of electrolyzer, hydrogen storage and fuel cell. The efficiencies of electrolyzers are in the range of around 50% to around 80%. As in the other simulation variant, an efficiency of 72% is assumed. The storage itself causes minimal energy losses; the efficiency is assumed to be 100% at this point. However, pressure losses and energy for compression can lead to losses, but these are not considered at this point. The fuel cell can achieve an electrical efficiency of 35% to 70%, depending on the type and use. In this study, an efficiency of 50% is assumed. This results in the following calculation for the hydrogen system with the mentioned values:

$$Efficiency_{total} = 0.72 \times 1 \times 0.5 = 0.36 \quad (4)$$

For both systems, only the direct efficiencies were considered. Further system losses are deliberately not included at this point in order to obtain an initial and simple comparison. The following Table 7 shows how clearly these two systems differ in terms of their efficiencies.

Table 7: Comparison of system efficiencies for BESS and Hydrogen

	Efficiency
	[%]
Battery-System	85
H_2-System	36

As a result, almost 2.4 times as much energy must be used in the hydrogen system to achieve the same energy output as for the battery system. This is a very important finding, especially in regard to areas such as mobility. In general, if it is already a major task to generate the necessary quantities of green electricity, it must be considered whether the hydrogen route and thus significantly higher electricity generation is necessary and possible, or whether a solution with batteries or other technologies is a more suitable alternative to hydrogen systems in certain places.

The following comparison with different BESS which are currently on the market shows how important the energy content respectively the density is (Table 8). As in the previous tables displayed, the values refer to a required peak output of 15 MW per hour, which must be covered over a certain period of time. If they are to be completely covered by a battery storage system, the number of storage systems with the given nominal output shown is required (Table 8). All battery storage systems are a container solution and fit into a 20-ft container. Further specific characteristics can be found in the appendices with the data sheets for the battery systems. The nominal capacity of the battery storage systems is in the lower MW range. Much larger storage systems that are not special solutions are not yet available on the market at the time of the study. To have a directly comparable component, a car battery from the Tesla Model Y with 77 kWh (Stöckel 2023) was included in the list. This gives a direct indication of the actual amount of energy required.

Table 8: Comparison of the required number of battery storage units in terms of energy content and tank size

Duration	Tank size	Energy content of tank	SUNGROW ST2236UX (2,236 kWh)	CATL - EnerC (3,720 kWh)	TRICERA energy HC-Container (3,600 kWh)	Tesla-Y Battery (77 kWh)
[hrs.]	[kg]	[kWh/Tan	[pcs]	[pcs]	[pcs]	[pcs]
12	11,029	183,800	82	49	51	2,387
18	16,544	275,699	123	74	77	3,581
24	22,058	367,599	164	99	102	4,774
36	33,087	551,399	247	148	153	7,161
48	44,116	735,198	329	198	204	9,548
60	55,145	918,998	411	247	255	11,935

This analysis shows how many battery containers are needed to cover the required energy of 15 MW. Around 50 to just over 400 battery storage systems are required to cover the capacity under consideration over the various time periods. The numbers for the CATL and TRICERA systems are similar, as the storage systems also have a comparable battery capacity of 3.72 and 3.6 MWh respectively. The SUNGROW battery system, on the other hand, has a lower capacity of 2.236 MWh and therefore a slightly larger number of containers required. The number of Tesla batteries shows how many of these cars would be needed.

A 20-ft container has the external dimensions (mm) 6,058 x 2,438 x 2,591 (LxWxH) and a volume of 33.1 m^3. If we now compare the energy density of the battery systems listed in Table 8 with the different pressure systems of the hydrogen storage tanks, the following picture can be obtained (Table 9).

Table 9: Energy density of battery storages and hydrogen tanks at different pressure levels

Component	Energy density
	[kWh/m^3]
H_2-Tank at 45 bar	63.0
H_2-Tank at 350 bar	490.0
H_2-Tank at 700 bar	979.9
SUNGROW - ST2236UX (2,236 kWh)	67.6
CATL - EnerC (3,720 kWh)	112.4
TRICERA energy - HC-Container (3,600 kWh)	108.8

It clearly shows what an advantage a hydrogen storage system with higher pressure offers. At only 45 bar, the energy density is similarly low to that of the battery storage systems. The

CATL and TRICERA systems have a slightly higher energy density than the SUNGROW system. However, if we compare the hydrogen storage systems at 350 and 700 bar with BESS, there is a distinct difference. At a pressure of 350 bar, the energy density is around 7.8 times higher than with a storage tank at 45 bar. At a storage pressure of 700 bar, this factor even rises to around 15.5. This significant difference is also reflected in the number of tanks required to cover certain dark doldrums (see Table 6).

4.1.3 Autarky curves of electrolyzer, hydrogen storage and fuel cell

The autarky curves of the three components tank, electrolyzer and fuel cells were examined. In this scenario the size of one component was varied and the other two components were kept at the corresponding values. The baseline values are as follows: tank size of 12,000 kg, size of the electrolyzer 30 MW, size of the fuel cell 10 MW.

Figure 13 shows the first curve with a varying tank size between 2,000 kg and 26,000 kg and the other two parameters were kept at the above-mentioned baseline values.

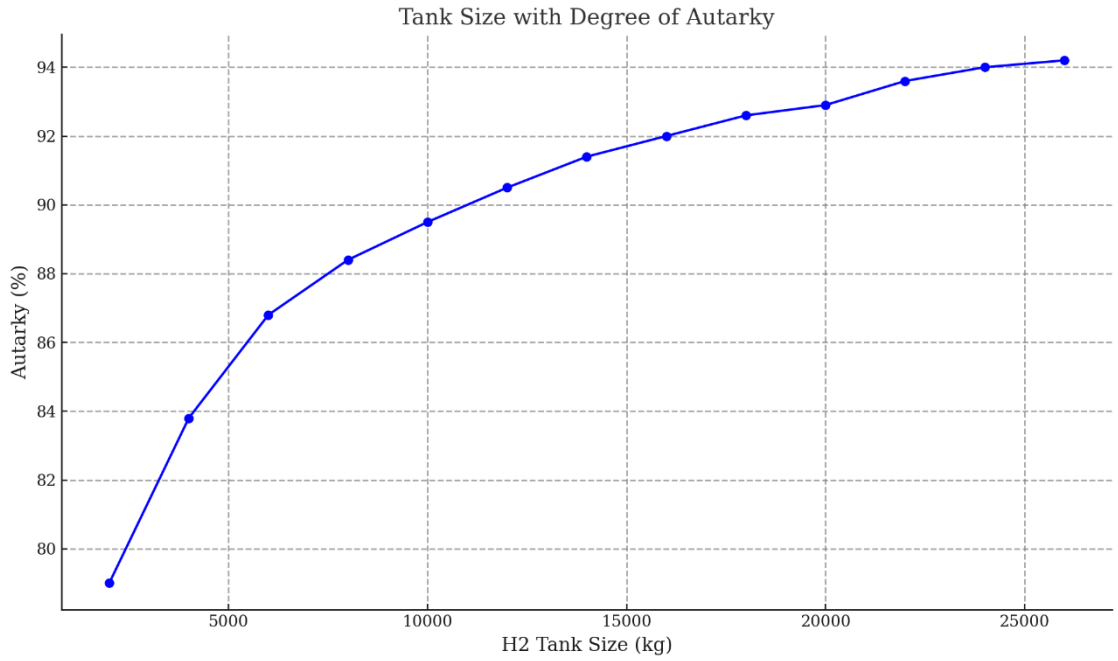

Figure 13: Variations of tank size with the corresponding degree of autarky

The autarky curve is asymptotic and tends on the long run towards 98.5% autarky as the tank size increases. The next Figure 14 shows the autarky curve with varying electrolyzer size. Again, the other two parameters were fixed at the corresponding baseline values.

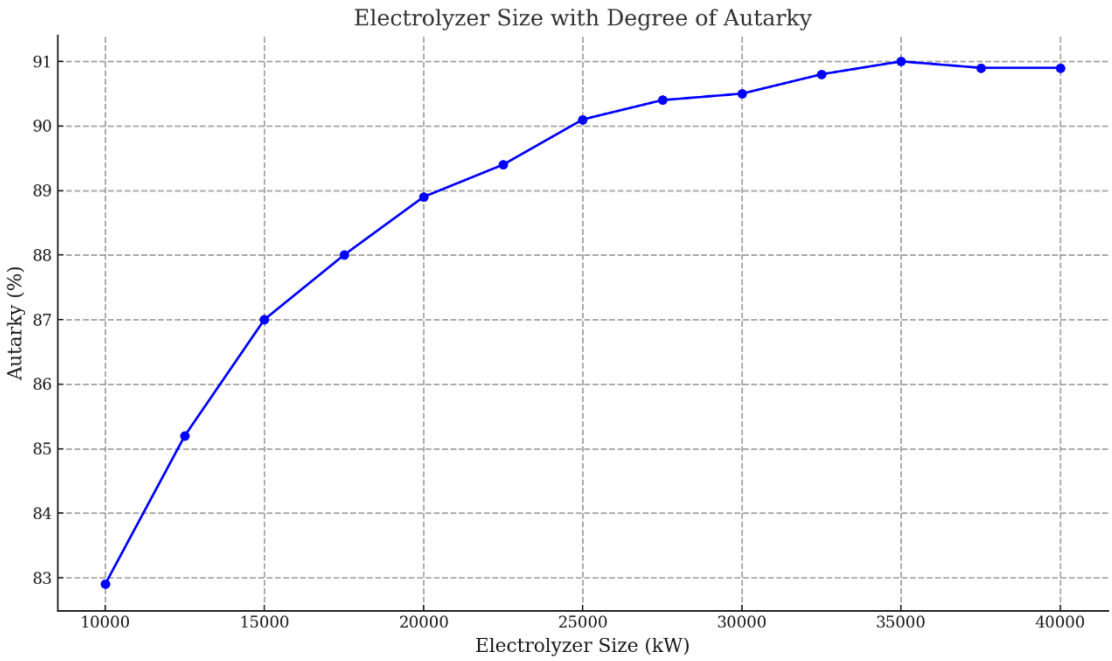

Figure 14: Variation of electrolyzer size with the corresponding degree of autarky

At the end of the curve, from a size of 35 MW from the electrolyzer, the values drop again very slightly and autarky decreases. Until then, the autarky increases with enlarging size up to 91%.

The last Figure 15 of the autarky curves shows the varying size of the fuel cell. The two other sizes of the tank and the electrolyzer were kept at the baseline values of 12,000 kg and 30 MW respectively. This results in the following picture:

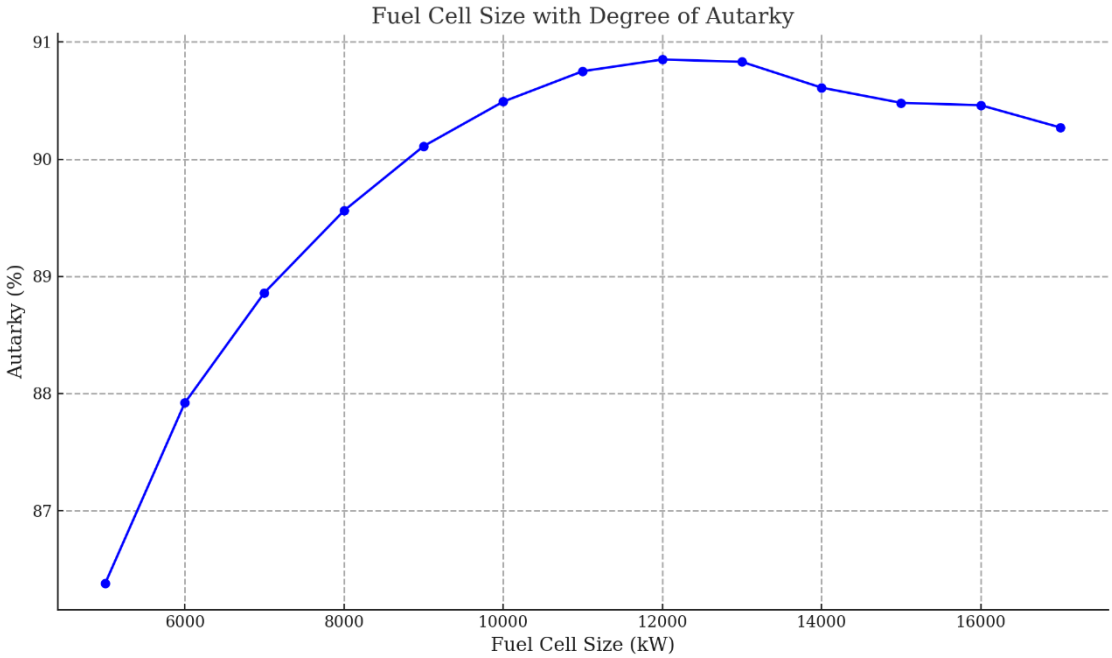

Figure 15: Variation of fuel cell size with the corresponding degree of autarky

This figure shows that there is a clear maximum of autarky. This is at a fuel cell size of 12 MW and is just under 91%. For larger fuel cell sizes, the autarky values drop again significantly. This phenomenon, which occurs in the fuel cell as well as in the electrolyzer and the autarky curves, can be explained (see chapter 5.1). All data from the simulations used to create the tables and figures can be found in the electronic appendix.

With the selected electrolyzer and fuel cell sizes of 30 MW and 10 MW, the autarky reaches 96%. This is also consistent with the values in Figure 8 and Figure 9.

4.1.4 Share of dark doldrums covered by the fuel cell and the grid

Another relevant consideration in the analysis is the proportion of the annual deficit covered by the fuel cell and the grid. From the simulated values, the data is examined to see how the respective coverage share changes with the size of the tank, electrolyzer and fuel cell. The corresponding values can be seen in the following Figure 16 to Figure 18. The corresponding autarky values of the individual plots can be taken from the figures before. As with the autarky curves, only one component was varied in size and the other two were left at fixed values. The initial values are as follows: tank size of 12,000 kg, size of the electrolyzer 30 MW, size of the fuel cell 10 MW.

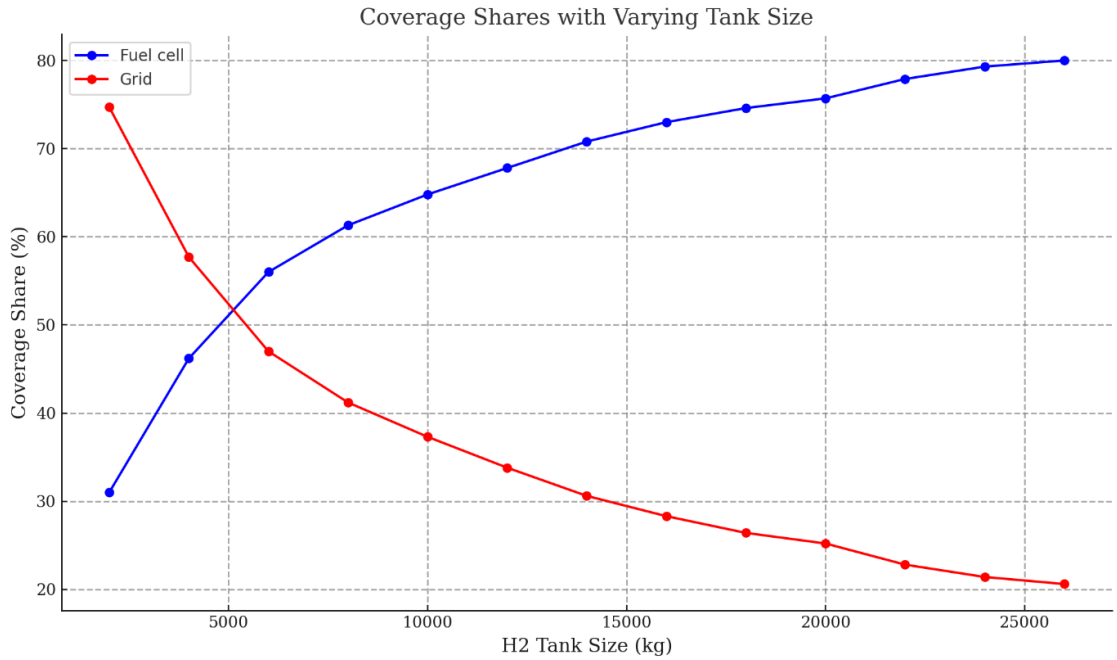

Figure 16: Coverage shares of the fuel cell and the grid with different tank sizes

When considering different tank sizes, the proportion of the deficit covered by the fuel cell is steadily increasing. This trend continues up to a certain point and finally approaches an approximate limit value of just over 80%. The share from the grid decreases accordingly to around 20%.

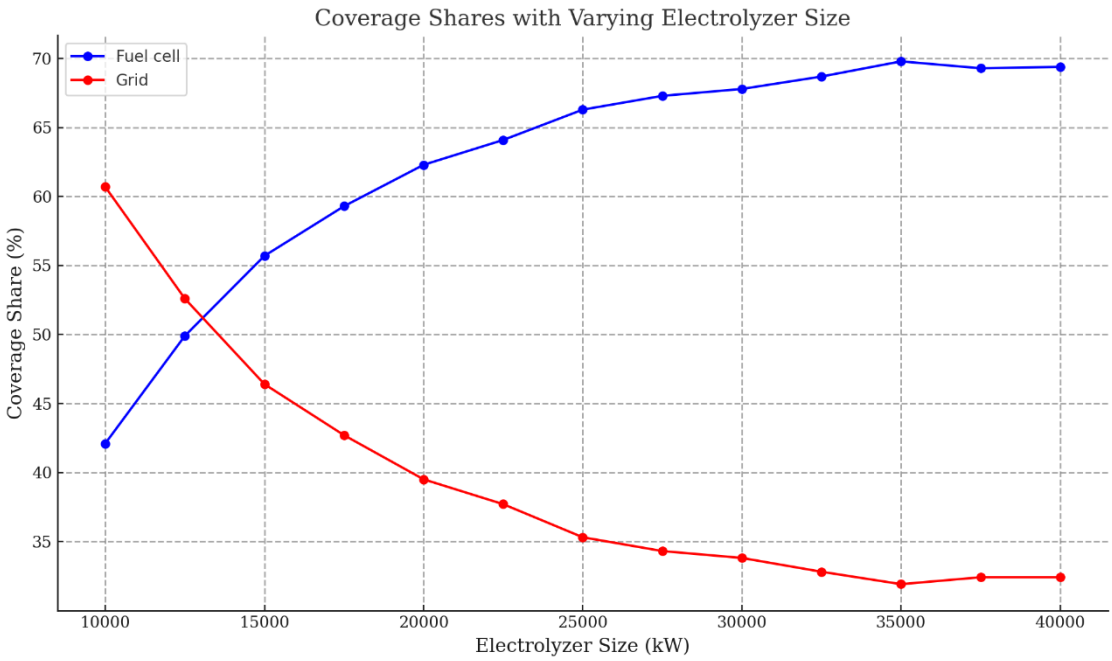

Figure 17: Coverage shares of the fuel cell and the grid with different electrolyzer sizes

When looking at different electrolyzer sizes, it can be seen that the proportion of deficit coverage by the fuel cell increases steadily and reaches a maximum (Figure 17). After that, the values fall respectively rise again very slightly. The maximum share of the fuel cell is around 70%, corresponding to around 30% of the grid.

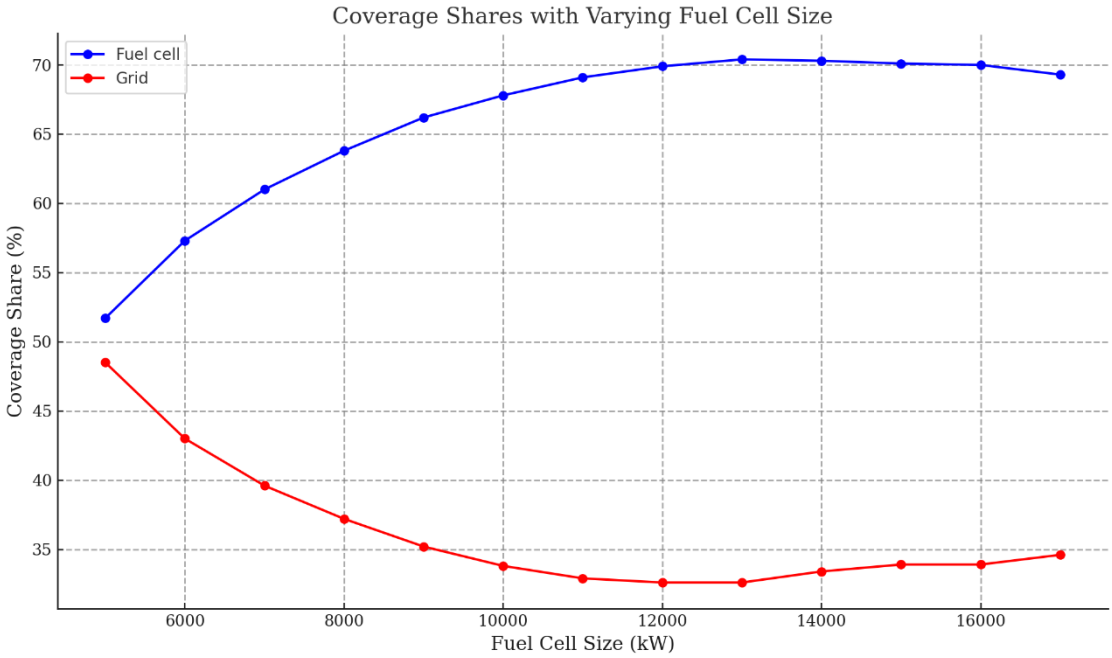

Figure 18: Coverage shares of the fuel cell and the grid with different fuel cell sizes

The behavior is similar for the different sizes of the fuel cell (Figure 18). The share of the fuel cell rises to a maximum of around 70% and then falls again slightly. As a result, the share of the grid falls to a minimum of around 30% and then rises again slightly.

Before the sales shares of hydrogen are analyzed in more detail in the next chapter, the operating hours of the electrolyzer and the fuel cell will be discussed. Table 10 displays the hours per year for each assessed scenario with the two baseline values and one varied value which is displayed in the table.

Table 10: Operating hours of electrolyzer and fuel cell for the different component sizes

Tank size	Electrolyzer operating hours	Fuel cell operating hours	Electrolyzer size	Electrolyzer operating hours	Fuel cell operating hours	Fuel cell size	Electrolyzer operating hours	Fuel cell operating hours
[kg]	[hrs/a]	[hrs/a]	[kW]	[hrs/a]	[hrs/a]	[kW]	[hrs/a]	[hrs/a]
2,000	5,296	1,744	10,000	5,829	1,893	5,000	4,792	3,157
4,000	5,131	2,105	12,500	5,616	2,127	6,000	4,809	3,052
6,000	5,046	2,342	15,000	5,389	2,305	7,000	4,837	2,922
8,000	5,000	2,477	17,500	5,295	2,418	8,000	4,869	2,814
10,000	4,965	2,562	20,000	5,198	2,494	9,000	4,903	2,723
12,000	4,927	2,643	22,500	5,119	2,553	10,00	4,927	2,643
14,000	4,912	2,720	25,000	5,048	2,611	11,00	4,962	2,583
16,000	4,897	2,776	27,500	4,986	2,628	12,00	5,009	2,524
18,000	4,872	2,810	30,000	4,927	2,643	13,00	5,060	2,522
20,000	4,864	2,840	32,500	4,878	2,672	14,00	5,113	2,546
22,000	4,848	2,898	35,000	4,832	2,697	15,00	5,139	2,553
24,000	4,840	2,931	37,500	4,785	2,685	16,00	5,139	2,521
26,000	4,832	2,950	40,000	4,752	2,686	17,00	5,139	2,473

In the left section, the tank size is varied, the size of the electrolyzer and the fuel cell remain at the baseline values. The operating hours per year of the electrolyzer and fuel cell are shown as well. The values for the electrolyzer vary around 5,000 hours, those for the fuel cell between just under 2,000 and almost 3,000 hours per year. The values of the two components are in opposite directions: as the tank is enlarged, the electrolyzer hours decrease and those of the fuel cell increase. The delta of the hours between the smallest and the largest value of the tank is significantly smaller for the electrolyzer with 464 hours in contrast to that of the fuel cell with 1,206 hours.

In the middle section of the table, the size of the electrolyzer is changed and the other two components are fixed. Here, the change in operating hours is again in the opposite direction. The delta of the electrolyzer values has increased to 1.077. The values range between just under 6,000 and just under 5,000 hours. The delta of the fuel cell has become smaller with 793 hours. The values lie between just under 2,000 and just under 2,700 hours.

The right-hand section of the table shows the operating hours when the fuel cell size is changed. Here too, the values are in opposite directions. The operating hours of the electrolyzer are around 5,000 and show a delta of 347. The values for the fuel cell range between just over 3,000 and just under 2,500 hours. The delta is now 684 hours.

For all three variants, the operating hours per year of the electrolyzer are around 5,000, while those of the fuel cell are significantly lower at around 2,000 to 3,000 hours.

4.2 Share of hydrogen sales - business model

This work focuses on the technical feasibility and design of the system. Particular attention is paid to analyzing how effectively this system works under specific conditions and how the various components interact with each other to achieve an optimal technical design. However, some economic aspects will also be discussed without going into depth.

The first crucial aspect is the distinction between the different types of hydrogen: grey, blue and green as discussed in chapter 2.1. Another aspect which is currently very important and decisive is the price trend. Political events can have a strong influence on this which the following Figure 19 indicates. The political conflicts erupted in February 2022 and in this context the company's purchase price from the beginning of January 2022 already shows a price increase, in the following year the price increase is more than three times as high.

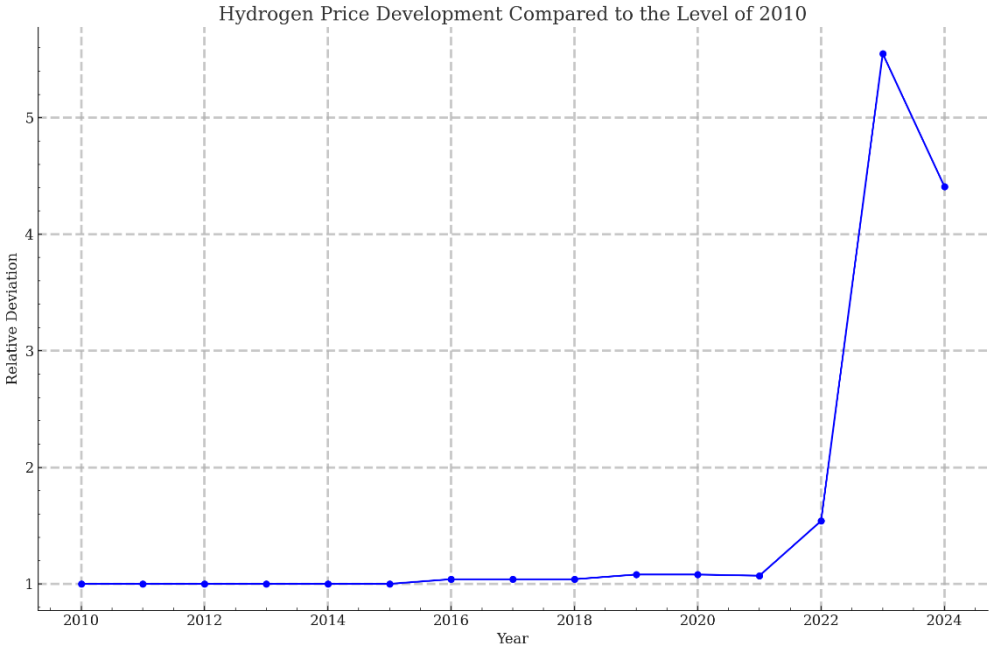

Figure 19: Development of the company's hydrogen purchase prices over the last 14 years in relation to the 2010 level

The company's purchase prices of grey hydrogen from the last 14 years show the changes. The 2010 level was chosen as the basis and the relative changes in the coming years are presented. The price development strongly suggests that it is advisable to at least examine the possibilities

of in-house hydrogen production more closely. This analysis should show whether and when the result is in favor of in-house hydrogen production or not.

This increase after the turn of the year from 2021 to 2022 is outlined in studies as well, with the increase clearly applying to both green and grey hydrogen. The national production costs in Germany (Hydex, marginal cost-based, excl. transportation) in 2021 were 5.26 €/kg for green hydrogen and 3.02 €/kg for grey hydrogen on an annual average. The following year, the price rose to 9.66 €/kg for green hydrogen and 5.67 €/kg for grey hydrogen on an annual average. Between grey and green hydrogen prices was a factor of 1.74 in 2021 and 1.70 in 2022 (Düsterlho et al. 2023, pp. 12-13). However, not all cost-causing factors were included in the price of green hydrogen. If these are taken into account, the gap will increase further (Doucet et al. 2023b).

The explanations and purchase data of recent years underline the growing attraction of producing hydrogen in-house as compared to buying it, especially as the costs of the latter have risen significantly.

If the cost of generating electricity from the company's own photovoltaic and wind power plants remains competitive and allows for surplus production of green hydrogen, there is the possibility of a viable business model that may even include the sale of surplus production.

For the following calculation, the annual average price of 7.99 €/kg for 2023 in Germany is used (Doucet et al. 2023a). As the prices of green hydrogen are subject to greater fluctuations, the annual average is used and not a recent price. At the moment, the price for green hydrogen is 7.73 €/kg (as of 24.4.2024, EEX Hydrix).

For this purpose, the hydrogen values from a scenario with a tank of 12,000 kg, an electrolyzer with 30 MW and a fuel cell with 10 MW are used as a basis.

The hydrogen figures are shown in the following Table 11.

Table 11: Hydrogen figures from the time discrete simulation for a 12,000 kg tank, 30 MW electrolyzer and 10 MW fuel cell

	Annual H_2	**Unit**
Fuel cell H_2 consumption	123,317	kg
Production H_2 consumption	1,101,653	kg
Quantity H_2 of sales	584,293	kg
Total	1,809,263	kg

This means that 67.6 % of the hydrogen is used for consumption in production and by the electrolyzer, while the remaining 32.4 % is the surplus potential for sale.

According to the Federal Network Agency, the average feed-in tariffs for ground-mounted systems in 2023 were 6.47 ct/kWh and 10.47 ct/kWh for rooftop systems. However, both show

a downward trend. The average value for onshore wind energy is 5.88 ct/kWh (Bundesnetzagentur 2024a). The scenario used mainly obtains electricity from ground-mounted PV systems and wind turbines. A conservative approach was chosen, and 5 ct/kWh was used as electricity price for further calculations.

To ensure that the path to hydrogen is economical and to feed the surplus electricity into the grid for 0.05 €/kWh is not the better solution, the hydrogen produced must be sold for a minimum price. The pure hydrogen production costs are 2.74 €/kg (at 54.8 kWh/kg H_2 and 0.05 €/kWh). The other components that influence this internal LCOH were not considered. If the production price for the consumption part as well as for the sales part is now set to 2.74 €/kg, the selling price of the surplus hydrogen is derived from this and is calculated as follows:

$$\frac{Consumption_{Fuel\ cell} + Consumption_{Production} + Sales\ share}{Sales\ share} \times LCOH =$$

$$\frac{(1{,}101{,}653 + 123{,}317 + 584{,}293)\ kg}{584{,}293\ kg} \times 2.74 \frac{€}{kg} = 8.48 \frac{€}{kg} \quad (5)$$

At this sales price of 8.48 €/kg and a sales volume of 584.293 kg H_2, the production costs of the entire quantity of hydrogen produced would already be covered. With an average price for green hydrogen of 7.99 €/kg in 2023, this value is slightly higher, but only just under half a euro. Since this analysis does not consider the purchase price for the hydrogen used in production, which is now eliminated by in-house production, it can be concluded that profitability could be achieved through this hydrogen sale. However, this requires a more detailed economic analysis.

4.3 Comparable results from HOMER

The system under consideration was entered into HOMER accordingly and the scenarios were generated corresponding to the optimization algorithm of HOMER. As described in chapter 3.3, the same generation and consumption data as in the time-discrete simulation were used as the basis. In addition, the parameters for the components were set to the same values.

For a better understanding of the results from HOMER, a few details need to be outlined first. The optimization of the systems by HOMER is based on economic feasibility. Furthermore, technical design and optimization are conceived in such a way that the system itself is functional and fulfils the specified conditions. This means that the demand for electricity and hydrogen consumption in the scenario is met to the specified degree. However, there is (as for now) no mechanism to use the surplus electricity for further hydrogen production and to sell this excess production. It was therefore only possible to obtain results that covered the demand as well as possible while the remaining surplus electricity was fed into the grid. Such a hydrogen system can only be simulated to a limited extent with these mechanisms. As shown

in chapter 4.1, the overall efficiency is that low it only produces the most necessary hydrogen. Hydrogen is never a cost-effective option at this point and is not produced beyond what is really necessary. The results look accordingly. The limits of the system were defined as follows, within which the optimization of HOMER was carried out:

- Range of the electrolyzer: 15 to 25 MW
- Range of the fuel cell: 5 to 12 MW
- Range of the tank: 9,000 to 21,000 kg

No further meaningful results have been produced for larger or smaller ranges. This resulted in a number of outcomes, each with a degree of autarky of 91.9%. Higher values could not be achieved. The maximum unmet hydrogen load was set to 2% and the maximum annual capacity shortage was set to 1%. The maximum annual capacity shortage is defined as the maximum allowable value of the capacity shortage fraction, which is the total capacity shortage divided by the total annual electrical load (HOMER Pro 2024).

The generation by renewables was set as a fixed parameter for all results. Only the three components vary in size. Tank sizes from 14,000 kg to 21,000 kg can be found. For the electrolyzer, the size varies between 16 MW and 25 MW, while only the smallest size of 5 MW was used for the fuel cell. The following system will be presented:

- tank size of 15,000 kg
- 20 MW electrolyzer
- 5 MW fuel cell

There is no comparable result with approximately the same sizes as in the time-discrete simulation.

The simulation results show a renewable fraction of 91.9% and in the same range of just over 90% as the results of the time-discrete simulation. Table 12 shows the detailed results from HOMER.

Table 12: Results from the HOMER simulation with a 15t tank, 20 MW electrolyzer and 5 MW fuel cell

Production	MWh/a	%	Consumption	MWh/a	%
Fuel cell	16,262	6.9	**Load**	96,400	42
Wind	135,381	58.0	**Grid sales**	72,473	31.5
PV	68,080	29.2	**Electrolyzer**	60,740	26.5
Grid	13,739	5.9	**Total**	229,613	100
Total	233,462	100			

It can be seen that the fuel cell only contributes a fraction of the energy required, in the same order of magnitude the grid is required as well. The consumption side shows that 31.5% of the energy is surplus and is fed into the grid. Whereas 26.5% of the energy is used by the

electrolyzer. The operating hours of the electrolyzer are 5,334 hrs./a, those of the fuel cell 3,264 hrs./a.

The hydrogen results of the simulation are listed in Table 13.

Table 13: Hydrogen results from the HOMER simulation with 15 t tank, 20 MW electrolyzer and 5 MW fuel cell

Production	kg/a	%
Electrolyzer	1,108,719	100
Consumption		
Fuel cell	975,701	89
Hydrogen load	121,018	11
Total	**1,096,719**	**100**
Unmet hydrogen load	2,299	0.21

The fuel cell consumes almost 90% of the hydrogen, the remaining amount is needed for production. Only 0.21% of the hydrogen requirement cannot be served.

The following Figure 20 displays the electrical consumption with the distribution of the various generation sources.

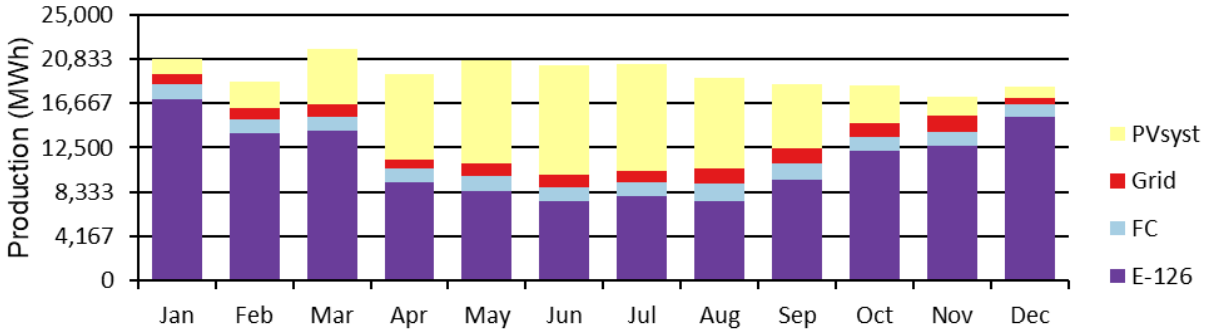

Figure 20: Distribution of the various generation sources for supplying the electrical load (HOMER Pro 2024)

The proportions of wind (E-126) and PV reflect the seasonal pattern with wind and solar distribution. Every month, the fuel cell and the grid support consumption to a small extent.

The 15,000 kg tank has an energy storage capacity of 500,000 kWh and can operate the 5 MW fuel cell autonomously for 45 hours. At the beginning of the year the tank is 20% full as the system was set up, by the end of the year the tank is completely full. This means that over the course of a year more hydrogen is produced than is consumed.

These results of an optimization by HOMER will be discussed later in chapter 5.3 and brought into perspective with the results of the time-discrete simulation. Firstly, a critical examination of the methods and limitations of this entire study follows first.

4.4 Error consideration

Following this examination and presentation of the results, a critical discussion must be held on the limitations and possible errors associated with the study presented.

An important feature of this analysis is the data which create the foundation of the simulations and thereby the results. All the data used has a resolution of one hour. This changes the values of the real time. By adding up the consumption and generation over an hour, the peaks and dips are possibly reduced, and in some cases, they disappear completely. Any peaks or dips in consumption or electricity generation from renewables are leveled out and therefore only have a minor impact.

This is particularly noticeable when the PV system is generating electricity. In this case, power generation can drop significantly within a few seconds to minutes due to a simple cloud passing by and then continue at the previous level. This and similar effects are smoothed out by the relatively low resolution of one hour. Corresponding effects occur during conversion into hydrogen and back into electricity as well. The electrolyzer and the fuel cell each have a minimum operating limit. A higher resolution of the data could result in them not starting or starting later, as the limits are not exceeded. As a result, no hydrogen or electricity is produced. The grid may have to step in for the fuel cell or there may be a lack of hydrogen again at a later point in time, which in the worst case would have to be produced by drawing electricity from the grid.

This peak shaving introduces a blurring into the analysis that needs to be considered. It was not possible to use a higher resolution of the data, as in some cases no data were available with a higher resolution. The lowest denominator was therefore an hourly resolution.

Another factor that was not considered is the possible shutdown times of the wind turbines. For example, the turbines are shut down to prevent and reduce bird collisions or other endangered species such as bats. These shutdown requirements imposed by the authorities are intended to protect species and are often a requirement of turbine installation. Whether, and in which periods, must be specifically checked for each project by the relevant experts or authorities. If corresponding shutdown periods are imposed for this project, this would have an impact on the energy production of the wind turbines. This would potentially reduce production and probably result in a different generation profile. These requirements could also have an impact on the wind farm design. However, this could not be considered in this hypothetical scenario.

The weather data used for the generation of wind and PV systems poses a further uncertainty in the analysis. The corresponding weather data has its own uncertainty. A weather forecast for a time that lies several years in the future is fundamentally subject to uncertainty. However, if a forecast is made over a longer period, the deviations balance each other out and the predicted values apply to the long-term average with less uncertainty. There is an uncertainty

of 4.7% for the resources used in the analysis of the PV data. In addition to the resource data, the assumptions in terms of costs and the load profile are regarded as the greatest source of uncertainty in such simulations (Bahramara et al. 2016, p. 12).

Another uncertainty lies in the chosen procedure. The consumption data from the status quo was used and extrapolated for 2035 according to the company's forecasts. This procedure is subject to the uncertainty that this selected scenario does not necessarily correspond to real developments. However, this approach was deliberately chosen to be able to analyze the system under certain conditions and to derive initial findings from this assessment.

Other aspects that were not considered in the analysis due to the much higher uncertainty of the scenario itself are possible technological developments and losses as well as degradation of the systems.

The last aspect that should be critically noted at this point is the chosen approach in the time discrete simulation for hydrogen sales. The mechanism implemented here is that a fixed amount of 25% of the tank content is sold before it is full. This ensures that the surplus electricity can be utilized as well as possible. However, this procedure may not always correspond to reality. As a result, it may happen that the surplus cannot be used as well as shown and the sales share of hydrogen gets smaller. However, this aspect is regarded as marginal, as hydrogen can be removed from the tank using a filling station in tank bottles, for example.

5 Discussion and evaluation

The results of the two simulation variants were previously presented and explained. The results are divided into three areas: the figures from the discrete-time step simulation, the share of hydrogen sales results and the results from HOMER.

For the discrete-time simulation, particular attention was paid to the decisive parameters in the first section. After an initial overview with the variance of the three components tank, electrolyzer and fuel cell over a very large range, it was already possible to conclude from this which combination of variables achieves good results with an autarky of around 90% (see Figure 8).

The size of the tank and its energy content were then analyzed in detail to determine the amplitude and time period over which the dark doldrums can be covered by hydrogen and the fuel cell. The periods that need to be covered and frequently occur in the analyzed data are between 12 and 30 hours. To cover a peak load of 15 MW, a tank of around 11,000 kg to 33,000 kg is required. The evaluation showed that a storage tank with 45 bar is unsuitable to cover dark doldrums of 12 hours; a tank with 350 or 700 bar would only require 4 or 2 tanks. A comparison with battery systems follows next. The analysis of the efficiency of the battery system is 85% compared to 34% for the hydrogen system. However, a comparison of the battery system with pressurized storage systems regarding the energy density gives a completely different picture. At 350 and 700 bar, pressurized storage systems have an energy density 4.5 and 9 times higher than the battery storage systems. Next came a detailed analysis of the autarky curves. It was found that the curves level off with increasing component size and in some cases even decrease slightly. This shows that a system with large components does not necessarily have the best autarky.

The next decisive parameter in the investigation is the proportion of dark doldrums covered by the fuel cell and by the grid. The fuel cell curve reaches its maximum between 70% and 80% in the selected component size range. The operating hours of the electrolyzer and fuel cell conclude the first part of the results. For different component sizes, the operating hours of the electrolyzer vary between 4,580 and 5,800 hours per year, while the operating hours of the fuel cell vary between 1,700 and 3,150 hours per year.

The next section of the results is the financial part, which emphasizes the importance of producing green hydrogen in-house and the increase in purchase prices for grey hydrogen (Düsterlho et al. 2023, pp. 9-10). Although there is still a difference between green and grey hydrogen, the gap is shrinking. At certain component sizes, around 32% of hydrogen can be sold. If this share is sold at a price of 8.48 €/kg, the total production costs of the hydrogen produced can be covered.

Finally, the results of the simulation with HOMER are presented, which, in contrast to the discrete-time simulation, do not use excess electricity for further hydrogen production. The

optimization algorithm provides many results of which a system with a 15,000 kg tank, a 20 MW electrolyzer and a 5 MW fuel cell is presented. This system has a degree of autarky of 91.9%, with the fuel cell contributing 6.9% to the energy supply and the grid 5.6%. The fuel cell uses almost 90% of the hydrogen produced, the rest is used for production.

The two simulation approaches were used to model the designed system. The study's question of how companies can efficiently use solar and wind energy to cover the load profile and produce green hydrogen while ensuring economic performance, with a focus on a high degree of self-sufficiency and co-location strategies, will be discussed under the mentioned aspects.

5.1 Evaluation of the time-discrete simulation

The first part of the results evaluation is focused on the time-discrete simulation, which was carried out using the MATLAB software.

Figure 21 below shows that even a triplet of the three components with a smaller size can achieve a degree of autarky of 90%. This figure shows a marker with X, Y and Z-values for a tank size of 12,000 kg, 30 MW electrolyzer and 10 MW fuel cell.

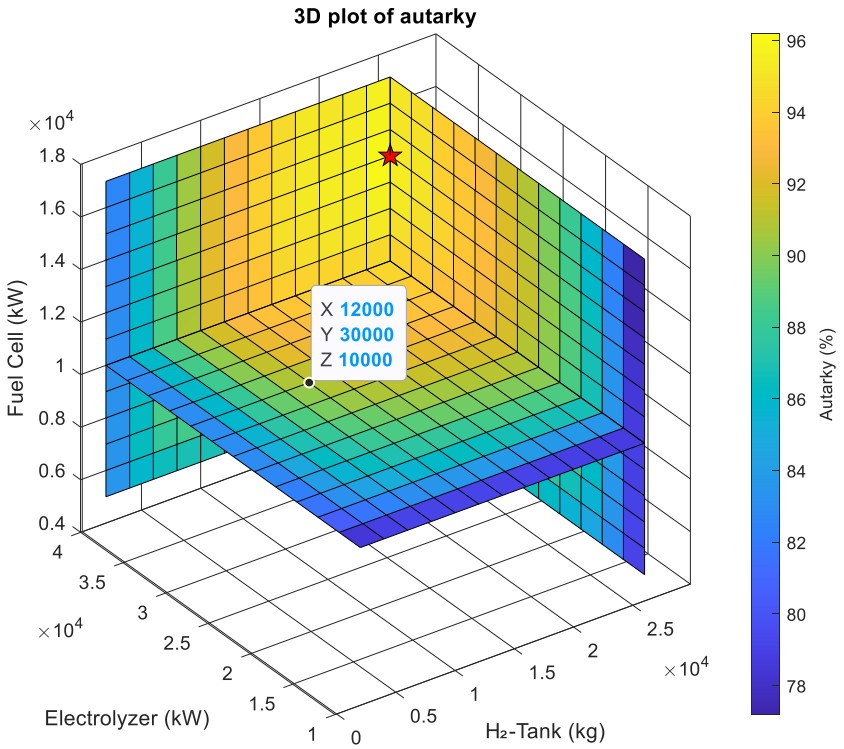

Figure 21: Section of 3D-plot with an overview of tank size, electrolyzer and fuel cell in relation to each other with corresponding autarky and with a red star as autarky maximum and a selected point

It is clearly shown how it is possible to achieve 90% autarky with the selected combination of components. With a selection of larger components, autarky values of over 95% can also be achieved which is indicated with the red star as the maximum. However, the following discussion of the decisive parameters provides arguments as to why this is not necessarily the optimal design and why sacrificing some autarky might be the better option.

By considering the amplitude of the power to be covered, the tank size and the energy content, it is apparent that the tank eventually needs to be big in size. We are talking here about a quantity of 11 to 33 tons if the entire peak power over 12 to 36 hours is to be completely covered by the fuel cell. It is interesting to see how autarky relates to this. Table 6 has shown how many tanks are required according to the period of time over which the tank is to supply the power. Comparisons were also made for the different pressure levels. Operating the storage tank at only 45 bar does not appear to be a practical approach. With a pressure tank of several hundred bar, the number of tanks looks much more realizable than at only 45 bar.

If the comparison with a battery storage system is now added, the difference in the efficiency values is clear. Compared to a hydrogen system, the efficiency of battery storage systems is higher. However, the energy density must be considered as well (see Table 9). This comparison clearly shows that a hydrogen system of these dimensions with a pressure storage system at 350 or 700 bar is advantageous. The storage tanks have an energy density 4.5 to 9 times higher than a battery storage. At least 50 of the battery storage units, each with a 20 ft container, would have to be installed on site to cover the peak power of 15 MW for just 12 hours.

Further conclusions can be drawn from the autarky curves. The autarky increases steadily as the tank is enlarged, while the two other components, electrolyzer and fuel cell, were kept at their baseline values of 30 MW and 10 MW. The initial value of the tank size is 12,000 kg. The curve strives asymptotically towards its limit value which is just slightly under 100%. At a size of around 11,000 kg, an autarky of 90% is already achieved.

Looking at the two other autarky curves, in which the size of the electrolyzer and the fuel cell is changed, one finding stands out. Each curve has a maximum, followed by slight decrease. This phenomenon can be explained.

By varying the size of the electrolyzer, the autarky increases up to a size of 35 MW of the electrolyzer, after which it decreases again slightly. The parameters of the minimum output of the electrolyzer and fuel cell have an influence in this respect. The hourly hydrogen consumption for on-site production plays a role as well. If the tank is empty and the hourly hydrogen demand has to be covered, but the surplus electricity is too low (below the minimum output of the electrolyzer) or there is a deficit, the grid has to step in to operate the electrolyzer to produce the necessary hydrogen. This slightly reduces the degree of autarky as the electrolyzer size increases. Another mechanism that plays a role as well depends on the operating hours and the tank size. If the parameters of the minimum power of the electrolyzer and fuel cell are set to zero and the hourly hydrogen consumption as well, the degree of autarky goes towards 92.8% with increasing electrolyzer power and no longer shows this behavior with a maximum and subsequent drop.

This phenomenon in the fuel cell's autarky curve, where the size of it is varied, can be explained in a similar way. In this case, it can be seen that the autarky decreases again after the fuel cell has reached 12 MW. The ratio of energy generation by the fuel cell to energy

consumption by the electrolyzer reaches a maximum and then drops again. As a result, the degree of autarky declines again as well. In addition, the share of grid consumption is higher with a larger fuel cell, as the minimum output of the fuel cell (20% of the maximum output) is reached later, and the grid must therefore be used more often.

Furthermore, the fuel cell also consumes the available hydrogen from the tank more quickly and the grid must step in again more rapidly in the event of a prolonged dark doldrums.

If the minimum output parameters of the electrolyzer and fuel cell are also set to zero, as is the hourly hydrogen consumption described in the previous paragraph, the degree of autarky approaches 92.7% as the fuel cell output increases.

One conclusion can be drawn from this behavior is that autarky does not increase significantly with the size of the fuel cell or electrolyzer. This should be considered when discussing how large the storage system should be in order to be able to cover a dark doldrum with a correspondingly large fuel cell. The question arises as to whether it is advantageous to dimension the fuel cell in such a way that it can cover the entire output during dark doldrums and the facility is thus autonomous. The entire year should also be considered as well as the coverage share of the fuel cell.

The behavior of how the share of coverage that the fuel cell can provide over the course of the year changes allows a further conclusion to be drawn at this point. In each case, the behavior was examined when one of the three components were varied in size. The curve approaches 70% to 80% share of coverage in each case. However, these values do not increase. The remaining share is covered by the grid in each case. The electrolyzer and fuel cell curves again show the phenomenon where the curve reaches a maximum and then drops slightly (see Figure 17 and Figure 18). This can also be explained by the minimum operating limit of the electrolyzer and the fuel cell. If hydrogen is required and the tank is empty and there is only a slight surplus of electricity, the grid must step in. If the operating limit increases, the grid consumption increases as well. Similarly, if the fuel cell increases in size, so does its minimum operating limit. If the limit rises, the grid consumption increases as well.

It can be concluded that the fuel cell can cover only around 70% of the dark doldrums. Just with a tank size of around 24,000 kg is it possible to reach 80%. However, the degree of autarky must be considered in this context. Due to this enormous size of the tank, only around 3% to 4% autarky is gained.

The operating hours of the electrolyzer and fuel cell conclude the first part of the results (see Table 10). As the component size changes with the same delta, the operating hours of the two components change differently. The minimum operating limits again play a role at this point. If a component becomes too large and the autarky decreases slightly, the delta of the operating hours decreases as well.

Another behavior stands out. The operating hours of the electrolyzer decrease as the tank size increases. This phenomenon can be well explained. A closer look at the data shows that this phenomenon is related to when the tank is empty. According to the principles of the time-discrete simulation, the hourly hydrogen demand must be always covered by the system. This means that the grid must step in more frequently to operate the electrolyzer and produce the required hydrogen. This is the case a few hours a year when there is no surplus or not enough hydrogen in the tank. Which explains the decreasing operating hours of the electrolyzer as the tank size increases. There are two sides to this phenomenon: On the one hand, a higher number of operating hours is good for the system; on the other hand, these are covered by the public grid and not by renewable energy. As a result, autarky does not increase as much as it would if this case could be avoided. However, this would violate the established rules (see chapter 3.1 and 3.2), according to which the hydrogen demand must be covered at all times.

From the previous consideration, it can be stated that a good degree of autarky can be achieved even with smaller component sizes. An increase in size does not necessarily mean that the degree of autarky increases. The analysis has shown that the exact opposite is the case when a certain point is exceeded. The consideration of the tank size and the energy content, as well as the comparison of the different storage options, shows that hydrogen pressure storage is the best choice and has the highest energy density. In addition, the space consumption and the number of storage tanks is an argument to support this.

Another aspect is the share of the dark doldrums that the fuel cell can cover. Around 70% coverage is achieved at approximately 11 MW; no significant improvement can be seen if the fuel cell is increased.

The operating hours also provide a further argument in favor of a limited size of electrolyzer and fuel cell. The larger the component, the lower the operating hours. To achieve good capacity utilization, the components should not be excessively large.

5.2 Evaluation of the financial aspect

This section of the results deals with the financial aspects of the share of hydrogen sales. Although the focus of this work is on the technical aspects and the design, reference will also be made to a financial part resulting from the technical assessment.

The purchase prices shown for grey hydrogen over the last 14 years reveal a clear picture. Due to the massive price increase, it is extremely important to consider producing in-house hydrogen. If investments are also made in CO_2-free production and green electricity production, the consideration should also be extended to green hydrogen. In the scenario shown, with a 12,000 kg tank, a 30 MW electrolyzer and a 10 MW fuel cell, about 32% of the hydrogen produced can be sold. If this proportion is now sold for 8.48 €/kg, it would cover the entire production costs of the hydrogen produced in-house. This does not consider the fact that the purchase of hydrogen is no longer necessary and therefore these costs are eliminated.

On the other hand, the calculated LCOH only includes the electricity costs that would otherwise be generated by selling the electricity from wind and PV. Further shares of the LCOH were not considered in this initial analysis.

Compared to the average price for green hydrogen of 7.99 €/kg in Germany in 2023, the calculated price of 8.48 €/kg is only slightly higher. If the other financial aspects, such as the savings for the purchase of hydrogen, are considered, this could possibly result in a promising business model. However, further analysis is required.

Only the electricity costs are included in the production costs of the hydrogen since it is one of the major cost drivers. CAPEX and OPEX play a relevant role as well. The larger the electrolyzer, the lower the specific CAPEX costs (Agora Industry and Umlaut 2023, pp. 15-23). Mathematically, the LCOH can be described as follows:

$$LCOH = \frac{LHV}{\eta_{sys,LHV}} \left(\left(\frac{\frac{i}{100} \times \left(1 + \frac{i}{100}\right)^{n}}{\left(1 + \frac{i}{100}\right)^{n} - 1} + \frac{OPEX}{100} \right) \frac{CAPEX}{\tau} + E \right) \quad (6)$$

LCOH	Levelized cost of hydrogen	$\eta_{sys,LHV}$	System efficiency related to the
LHV	Lower heating value [kWh/kgH2]	τ	Full load hours [h]
i	Discount rate [%]	OPEX	Operational expenditures [%
n	Lifetime [a]	CAPEX	Capital expenditures [€/kW]
E	Electricity cost [€/kWh]		

(Fraunhofer ISE 2018, p. 199)

However, if the production costs would rise by 1-2 cents/kg, the necessary sales price would be significantly higher. The relationship is not linear, as only around a third of the hydrogen can be sold but the entire 100% of the hydrogen needs to be covered by the revenues.

A look to the American states and the LCOH prices of green hydrogen for 20-100 MW electrolyzers there gives hope that prices will potentially fall significantly here once the market in Europe has gained even more momentum. The LCOH for green hydrogen production with PEM is: 4.38 to 6.77 €/kg without subsidy, with subsidy the values are significantly lower. For alkaline electrolysis, the LCOH values are between 3.48 €/kg and 5.31 €/kg without subsidies, with subsidies they are even lower (Lazard 2023, p. 32).

5.3 Evaluation of the results of HOMER

HOMER's results relate to a system with a 15,000 kg tank, 20 MW electrolyzer and 5 MW fuel cell. The significant difference between this system and the discrete-time simulation system lies in the underlying mechanisms. The optimization of HOMER does not provide for any additional hydrogen production than necessary. Furthermore, as already mentioned, the efficiency of a hydrogen system is relatively low at 34%. Hydrogen is therefore under the current circumstances not a cost-effective option.

The optimization process involved setting various conditions to achieve the highest degree of autarky in the system. The highest level that was exceeded was 91%, no system could reach 92% with any combination of components and range. The smallest fuel cell of 5 MW was sufficient for all systems. No larger one was provided for a system, whereas the other two components occurred in different sizes in the various results.

A closer look at the three components - storage system, electrolyzer and fuel cell - reveals a few things. The tank level and the associated frequency (Figure 22) show that there is sufficient hydrogen in the tank for the most part and that the tank is empty only 2% of the time. The frequency increases slightly the higher the tank level is. This can also be explained by the relatively small fuel cell, which consumes less than a fuel cell twice as large as in the discrete-time simulation even at full power.

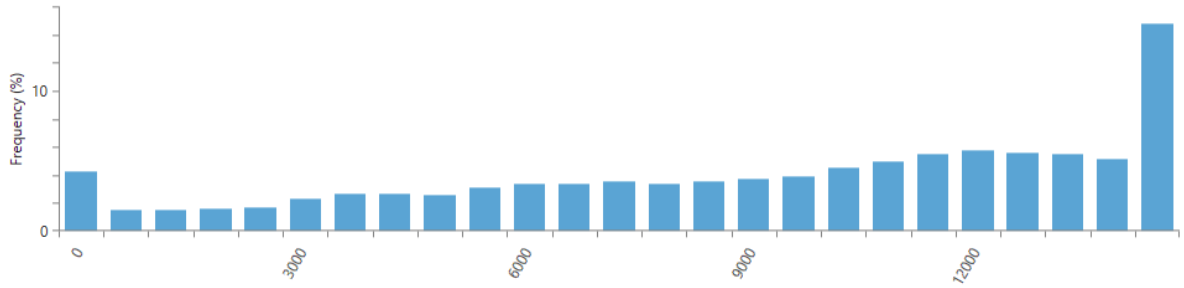

Figure 22: Various tank levels up to 15,000 kg with associated frequency (HOMER Pro 2024)

The average tank levels in relation to the individual months of the year show how the tank is around two-thirds full in the months of January to July (Figure 23). From August to November, the average level drops significantly to around 40%. The tank level then rises again slightly in December.

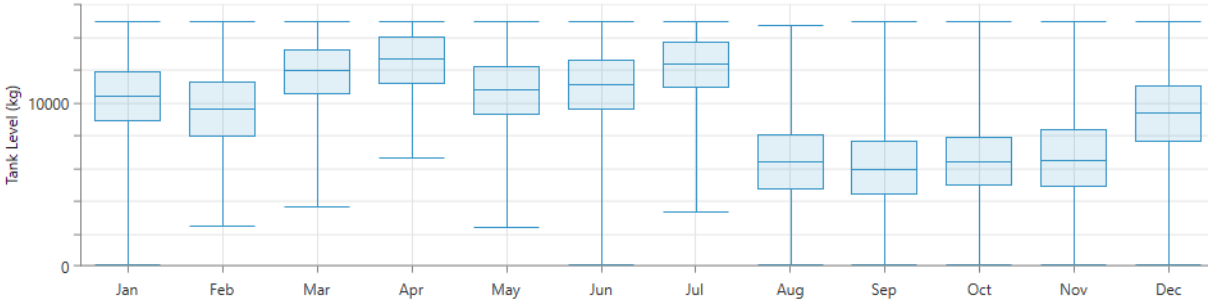

Figure 23: Average monthly tank level with uncertainty over a year (HOMER Pro 2024)

If this is set in relation to the electricity production of the various generation sources (Figure 20), adding that the fuel cell consumes a little more hydrogen and the electrolyzer produces slightly less hydrogen due to the slightly lower electricity production, this leads to a significantly lower average level in the months of August to November. Figure 24 clearly shows how the tank is completely empty more often in the fall as well. The hourly data shows how the hourly consumption for production cannot be covered at these times in every moment.

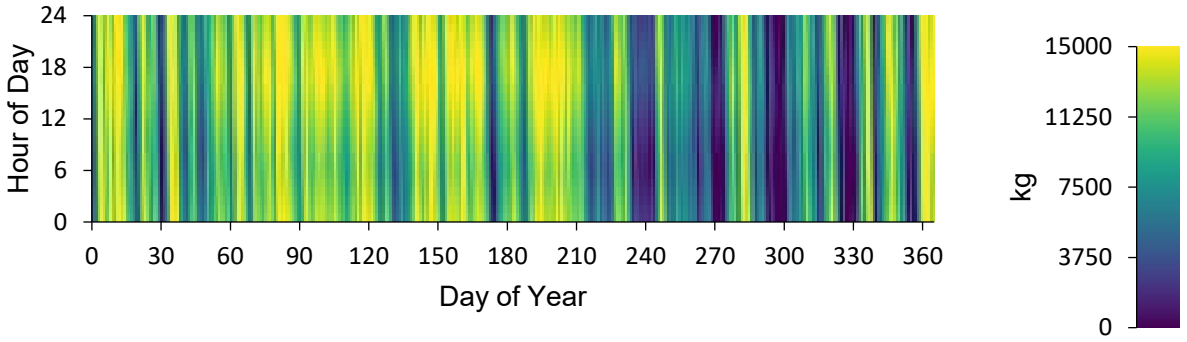

Figure 24: Tank level distributed over the year with hourly resolution (HOMER Pro 2024)

Figure 25 and Figure 26 show the operating times of the electrolyzer and the fuel cell with the respective amplitude over the year. The electrolyzer mainly produces hydrogen during the day from around March to September. Only occasionally is it operated at earlier or later times. From October to February, the operating times are spread over the entire day. The power at which the electrolyzer is operated is approximately around its maximum of 20 MW.

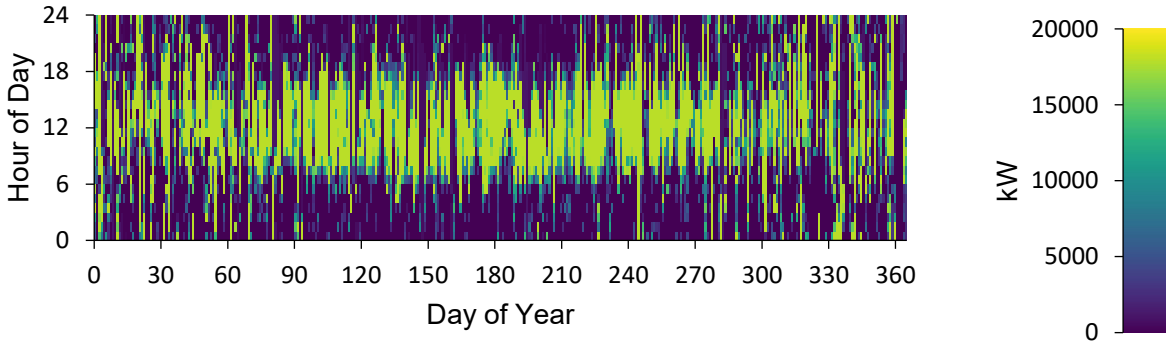

Figure 25: Electrolyzer input power over a year with hourly resolution (HOMER Pro 2024)

The operating times of the fuel cell paint a corresponding picture. From around March to September the operating times are mainly the night and only occasionally during the day. In the other half of the year, the operating hours are spread more throughout the entire day.

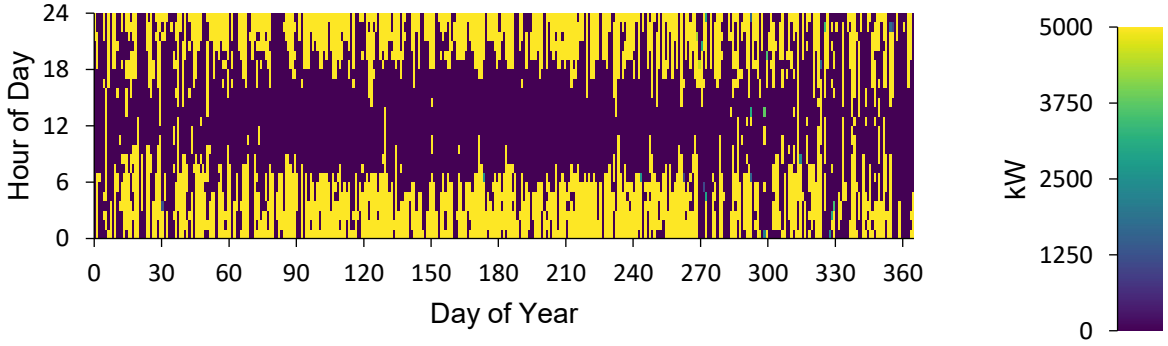

Figure 26: Fuel cell generator output over a year with hourly resolution (HOMER Pro 2024)

This phenomenon also corresponds with electricity generation from wind and PV (see appendix T). PV generation is clearly concentrated during the day and in summertime. Wind generation is better distributed throughout the day. In the winter months, electricity generation is longer and with a higher amplitude.

The grid is mainly only required for support at night, whereas surpluses are mainly fed into the grid during the day (see appendix U). In winter, electricity is also occasionally fed into the grid for longer periods, including overnight.

5.4 Overall assessment of the system and the decisive parameters

Finally, an overall assessment of the system, the decisive parameters, the financial part as well as the results from HOMER is carried out.

A system can be derived from the analysis of the time-discrete simulation as a basis that has a good degree of autarky of over 90% and considers the phenomena and correlations described in chapter 4 as well. Simply increasing the size of the components in order to achieve a higher degree of autarky is not a feasible solution. At the beginning of Chapter 4.1, the following parameters were highlighted which are relevant for the decision of a system. These were:

- Degree of autarky
- Energy content of the tank
- Share of dark doldrums covered by the fuel cell and the grid
- Share of hydrogen sales

These parameters were examined in detail. It was found that a degree of autarky of over 90% is associated with relatively large components. When looking at the tank size and the energy content, it became evident that a larger fuel cell does not necessarily lead to greater autarky, which in turn requires a larger tank. There are several ways to store hydrogen at different pressure levels. The higher the pressure, the fewer tanks are required, but in any case, several tanks are needed.

The proportion of the annual deficit that the fuel cell can cover also depends on its size. It has been shown that the fuel cell can't cover more than around 70% of the deficit. Accordingly, around 30% must be covered by the grid. In addition, the sales share of the hydrogen produced indicates a trend. The value decreases with increasing fuel cell size to around 30% and stagnates at this level.

With these results as a basis, the following component sizes can be concluded:

- Tank size: 12,000 kg
- Size of the electrolyzer: 30 MW
- Size of the fuel cell: 10 MW

A combination of these component sizes allows an adequate autarky of 90.5% and considers the parameters described above. The tank size and energy content, the proportion of the deficit

covered by the fuel cell and the proportion of the hydrogen produced that could be sold are in comparable good to very good ranges possible in this system.

At this point, the various storage options will be considered again, and the component sizes selected above will serve as the basis (Table 14). Accordingly, the 10 MW of the fuel cell is used as the maximum peak, which must be covered over a certain period of time. Correspondingly, the various battery storage systems are considered as well. The analysis is based on the assessments in Table 5, Table 6 and Table 8. As a reminder, a single tank in this system has a volume of 90 m³.

Table 14: Comparison of the different battery and hydrogen storage systems in relation to the 10 MW fuel cell with corresponding duration and energy content

Duration	Tank size	Energy content of tank	No. of tanks (45 bar)	No. of tanks (350 bar)	No. of tanks (700 bar)	SUNGROW ST2236UX (2,236 kWh)	CATL - EnerC (3,720 kWh)	TRICERA energy HC-Container (3,600 kWh)
[hrs.]	[kg]	[kWh/Tank]	[pcs]	[pcs]	[pcs]	[pcs]	[pcs]	[pcs]
10	6,191	103,166	18.2	2.3	1.2	46	28	29
15	9,286	154,750	27.3	3.5	1.8	69	42	43
18	11,143	185,699	32.8	4.2	2.1	83	50	52
20	12,381	206,333	36.4	4.7	2.3	92	55	57
24	14,857	247,599	43.7	5.6	2.8	111	67	69

Note: the usual rounding up and down rules have been applied to the values. A decimal point was only added where more precise information was deemed necessary.

This leads to the evaluation presented in the following three tables, starting with an overview of renewable energy sources in Table 15.

Table 15: Overview of installed renewable energies and their annual power generation as well as the facility's annual consumption

Installed capacity		Annual generation		Facility's annual consumption
PV	Wind	PV	Wind	
[MW]	[MW]	[GWh/a]	[GWh/a]	[GWh/a]
71.3	60.0	68.1	135.4	96.4

A total of 203.5 GWh/a is generated by renewables with a total installed capacity of 128.9 MW. This means that the renewables are oversized by a factor of 2.1 compared to the factory's annual consumption.

This results in the following scenario (Table 16) with the values for energy generation and consumption:

Table 16: Energy values on the producer and consumer side from time-discrete simulation with a 12,000 kg tank, 30 MW electrolyzer and 10 MW fuel cell

Explanation	Value	Unit	Percentage
Generation from RE	203,471	MWh/a	100
RE for load profile matching*	69,310	MWh/a	34.1
RE surplus after load profile matching	134,151	MWh/a	65.9
Energy consumption electrolyzer	99,304	MWh/a	
Energy generation fuel cell	18,359	MWh/a	
Fuel cell operating hours	2,643	hrs./a	
Energy consumption from grid	9,169	MWh/a	

* This means that 71.9% of the load profile is already covered by RE.

In this scenario, 74% of the surplus energy from renewable energies is used to operate the electrolyzer. The remaining surplus energy of 34,847 MWh per year respectively 26% cannot be used directly and is therefore fed into the public electricity grid.

During dark doldrums, the fuel cell covers 67.8% of the energy requirement related to the annual volume, while the grid supplies the remaining 32.2%. The simulation shows that the electrolyzer operates at its maximum capacity for 1,964 hours per year, which indicates a considerable surplus of renewable energy. In addition, the fuel cell reaches its full capacity for 141 hours per year.

The results, including detailed hydrogen consumption and production, are documented in Table 17.

Table 17: Hydrogen values on the producer and consumer side from time-discrete simulation with a 12,000 kg tank, 30 MW electrolyzer and 10 MW fuel cell

Explanation	Value	Unit	Percentage
Hydrogen consumption for production	123,317	kg	6.8
Hydrogen consumption from the fuel cell	1,101,653	kg	60.8
Hydrogen production by the electrolyzer	1,812,108	kg	100
Quantity of hydrogen sales	584,293	kg	32.2
Electrolyzer operating hours	4,927	hrs./a	

Slightly more than 60% of the hydrogen produced is consumed by the fuel cell, with a further 7% used for production purposes on site. This leaves around 32% of the green hydrogen for

sell. The full load hours of the electrolyzer are in a comparatively good range. At present, they are more likely to be in the region of 3000 hrs./a (Agora Industry and Umlaut 2023, p. 6).

In conclusion, it can be stated that a system with a hydrogen tank of 12,000 kg, an electrolyzer with 30 MW output and a fuel cell with 10 MW output can achieve acceptable values.

With this design, an autarky of just over 90% can be reached. By oversizing the renewable energies with a factor of 2.1 compared to the facility's annual consumption, around 72% of the load profile can be covered directly. A further 19% is covered by the fuel cell and the remaining 9% by the grid. The analysis has shown that the shares of the fuel cell and the grid will not be much better.

The financial analysis of this system has shown that the sales portion of the hydrogen must be sold for at least 8.48 €/kg in order to cover the production costs of the total amount of hydrogen. Compared to the average price of green hydrogen in Germany in 2023 at 7.99 €/kg, this value is only slightly higher and offers potential to close the gap.

The result presented by HOMER does not include the mechanism of using surplus electricity for further hydrogen production. This results in a system with

- 15,000 kg tank,
- 20 MW electrolyzer,
- 5 MW fuel cell.

Such a setup achieves an autarky of 91.9%. For hydrogen storage at 45 bar, 44 tanks would be required, at 350 bar 6 tanks would be needed and at 700 bar only 3.

The fuel cell contributes 6.9% of the total electricity, the grid 5.9%. If this is correlated as in the discrete-time simulation, the fuel cell only covers 53.9% of the dark doldrums, while the grid covers 46.1%.

Further key figures from the HOMER simulation are shown in Table 18.

Table 18: Energy values on the producer and consumer side from HOMER results with a 15,000 kg tank, 20 MW electrolyzer and 5 MW fuel cell

Explanation	Value	Unit	Percentage
Load profile matching by renewables	66,399	MWh/a	68.9
Energy generation fuel cell	16,262	MWh/a	16.9
Energy consumption from grid	13,739	MWh/a	14.2
Grid sales	72,473	MWh/a	31.5
Fuel cell operating hours	3,264	hrs./a	
Electrolyzer operating hours	5,334	hrs./a	

The operating hours of the fuel cell are over 3,000 hours and those of the electrolyzer over 5,000 hours. These values are noticeably higher than those of the discrete-time simulation. This is partly related to the significantly smaller component size but they are as well in reasonable ranges (Agora Industry and Umlaut 2023, p. 6).

The most developed electrolyzer technologies in use today are AWE and PEM, which offer a wide working mode and the maturity required for project execution. PEM is quick and dynamic, but because precious metals are used, it comes with higher prices. AEM and SOEC are still under development or have only recently been launched on the market. The short service life is another drawback. Most arguments are in favor of AWE and PEM, with AWE having a financial advantage, although it is a little bit less dynamic than PEM.

For hydrogen storage, pressure vessels are the most promising as they are mature, established on the market and relatively affordable. Type 1 or 2 storage tanks meet the requirements for pressure levels of 350 or 700 bar and show the lowest number of tanks required.

In fuel cell technology, the PEMFC has the necessary flexibility and a large operating mode. In addition, the lifetime is in the upper range. However, the power output is not yet quite at the required level. Other alternatives are the two high-temperature fuel cells MCFC and SOFC. Due to their high temperatures, they can score with good efficiencies in combined heat and power generation, but are significantly slower than the PEMFC with start times of 10 minutes and 60 minutes respectively. This is a significant limitation for the modeled scenario.

Renewable energy sources need to have overcapacity compared to consumption in order to produce enough hydrogen for fuel cells to cover a significant part of the dark doldrums. However, the exact amount of overcapacity required to avoid excessive power being fed into the public grid still needs to be investigated further. A similar approach was taken with a slightly different setup (Sorrenti et al. 2023).

It was shown that a degree of autarky of 100% is technically difficult to achieve with the conditions and restrictions of the setup. The use of more than one type of storage would reduce oversizing of storage or generation capacity and enable a higher degree of autarky (Bhandari and Shah 2021, p. 2).

The overview of the main conclusions is followed by a critical assessment of these results. This assessment will explore the practical implications within the context of the previously discussed theoretical framework.

5.5 Further review of critical elements

The study demonstrated how a complex system can be operated with renewable energy and green hydrogen as a storage medium. The results shall now be set in relation to the theory and the literature mentioned. The analysis with different simulation variants provided valid

results that could model the scenario presented and fulfill the requirements. However, a completely autarkic system could not be achieved within this framework.

A key factor in this constellation is the continuous hydrogen consumption for the facility's production. Expanding in-house production to operate a fuel cell would be advantageous. A comparison of the various storage systems shows that pressurized storage systems offer advantages due to their high energy density and thus fewer tanks.

The energy consumption for hydrogen production and conversion is quite high. Hydrogen is therefore more suitable for long-term storage and in large quantities. A combination of a battery and hydrogen is a suitable and effective solution for the transition phase. In this way, short and long-term storage can be combined (Yang et al. 2024, p. 18). With such an approach, the battery could step in during short-term bottlenecks and the fuel cell would not have to be kept on standby all the time, which would save electricity as well. The fuel cell can then be used during longer and predictable dark doldrums, such as at night.

Some aspects were not examined further in the study and they should be integrated in more detailed studies. Nevertheless, for this first evaluation, these topics were left out. Further studies must show whether and to what extent this limits the project and what impact the results have. Some aspects should be briefly highlighted at this point.

Issues relating to approval regulations always pose major hurdles and expenses. Electrolyzers are currently plants that require a planning approval (Planfeststellungsbeschluss). The duration and expense of the procedures are currently considered a relevant obstacle for these undertakings.

The background to this topic is that in July 2023, the German government decided to update the National Hydrogen Strategy (NWS) and set the goal of increasing domestic electrolysis capacity for green hydrogen to at least 10 GW by 2030. On November 22, 2023, the Federal Ministry for the Environment, Nature Conservation, Nuclear Safety and Consumer Protection presented the draft bill for the third ordinance amending the Ordinance on Installations Requiring a Permit (4th BImSchV). The aim of the amendment is to facilitate approval procedures for electrolyzers to produce hydrogen. The threshold for carrying out a simplified approval procedure in accordance with Section 19 BImSchG is to be set at a nominal electrical output of 5 megawatts or more. Below the threshold of 5 megawatts of rated electrical output, there would be no need for approval under immission control law (BMUV 2023).

Electrolyzers are currently classified as chemical plants. This means that at least a general preliminary EIA (environmental impact assessment) must be carried out. This and the threshold values to be introduced for handling the approval procedures are currently still being discussed.

The water consumption and treatment for the electrolyzer are crucial aspects to consider when planning a project. Even if the issue of water and water treatment is only considered a minor

cost driver for a project, these aspects should be examined more closely (Agora Industry and Umlaut 2023, p. 24). Demineralized, purified water is required for electrolysis, with data sheets showing that between 9.5 and 11.9 liters of water are consumed per kg of hydrogen at nominal output. For simplicity, 10 liters of water are assumed for 1 kg of hydrogen. With an annual production of 1,812,108 kg H_2, this results in an annual water consumption of 18,121,080 liters respectively 18,121 m^3. With an average hydrogen production of 5.090 kg/d, this results in a water consumption of 50.902 l/d or 51 m^3/d.

Assuming the cost of 0.002 €/l water (average water price in 2023), this amounts to a cost of just over 36,000 €/a, which is not a large sum in relative terms. However, the amount of water is an aspect that should be given more attention in the future studies. It must be mentioned at this point, especially in the context of climate change and summers with periods of drought, that water shortages can occur and other areas, such as drinking water supply and agriculture, would always be given priority in terms of water consumption.

The same problem also applies on a smaller scale to fuel cells, where water or water vapor is the by-product. The technology used determines in what form (liquid or gaseous) and in what quantities water is produced.

Another topic that should be considered is the further use of surplus electricity. The possibility of using the surplus at other company facilities that cannot be used by the factory or the electrolyzer was part of the considerations. However, this option is not feasible at this point and was not pursued any further due to high grid fees. Compared to 2023, the grid fees in 2024 have already risen noticeably. One main driver is the massive increase in costs for so-called system services. These are costs for energy that grid operators need to operate the grids as safely and reliably as they currently do. Another option is to store the surplus electricity with an additional battery storage system. This would not need to be as large as assumed in the previous studies. Any battery storage system would improve the degree of autarky and reduce the proportion of electricity that is fed into the grid.

At this point, it can also be recommended that a system with different approaches is the most promising. The path of solving everything with just one technology will not be the optimal one. It would be worth considering other PPAs that would utilize electricity from other regions as well. This would possibly allow electricity generation to be better distributed and regional weather conditions would not have so much influence.

6 Conclusion and outlook

In a final step, the overview of the research results allows a summary of the most important findings with regard to their added value for theory and practice. In addition, limiting factors of the research conducted will be identified and recommendations for further assessment and research will be given. The summary of the results also offers a channeled perspective on the research gap identified in the introduction of this study and allows a targeted answer to the underlying research question.

The aim of the study was to analyze the presented system on the generator and consumer side and to determine the size of the three key components - electrolyzer, storage and fuel cell - in order to achieve the highest possible level of autarky.

The software HOMER and a code for a time-discrete simulation, developed in-house with the special requirements of the defined system, were used for the analysis and the results were compared with each other. The result of the investigation is a size range of the components in which they achieve the highest possible self-sufficiency of just over 90%. With an electrolyzer of 30 MW, a storage unit of 12,000 kg and a fuel cell of 10 MW, the following values can be achieved. The fuel cell can cover a maximum proportion of the dark doldrums of around 70%. Furthermore, a surplus of hydrogen can be produced, which accounts for around 30% of the total volume and can be used, for example, for resale to third parties. The results from HOMER are similar in size but differ slightly. A system with a 20 MW electrolyzer, a storage tank of 15,000 kg and a fuel cell with 5 MW achieves a degree of autarky of around 91%. However, no surplus hydrogen is produced due to the algorithm's limitation.

The initial question of how companies can use solar and wind energy efficiently to cover their load profile and produce green hydrogen while ensuring economic viability, with a focus on a high degree of self-sufficiency and co-location strategies, was answered satisfactorily. Corresponding values can be given for the three decisive components. Although the results of HOMER and the discrete-time simulation differ, they agree in terms of magnitude and the level of autarky and are therefore sufficiently satisfactory if the difference in the algorithms is considered.

The results of this research can contribute to the investigation and the aforementioned research gap regarding hybrid systems and the connection with hydrogen topics. Low self-discharge and possible high energy density make hydrogen an attractive solution, and in combination with other technologies such as battery storage, it could also counteract excessive oversizing of renewables or the storage system.

Storage facilities such as high-pressure tanks for hydrogen usually require approval procedures that take time. This should be considered when planning such a project. These and other recommendations for further investigations and reviews of specific issues follow.

Optimizing the mix of wind and PV generation capacity can lead to improved utilization of the renewables. However, in the scenario examined, this is limited by the possibilities on site. Nevertheless, optimizing the overcapacity in relation to the best possible use of energy for load profile matching and the operation of the electrolyzer offers potential. As a further aspect in this context, it should be mentioned that in terms of the most favorable distribution of renewables, it could be beneficial to regulate the purchase of electricity through a nonlocal PPA. This has the potential to ensure that generation from the company's own PV and wind systems does not occur at the same time, which means that higher power peaks can be avoided and larger shares of the renewables can be used for load profile matching. Subsequently, a complete yield assessment with an optimized layout of wind and PV systems should be prepared.

The investigation with high-resolution data of generation and consumption in a minute-by-minute resolution or higher could provide further insights, as the fluctuation due to wind and irradiation variability can have an impact on the electricity for load profile matching and the operation of the electrolyzer and fuel cell.

With regard to the storage system, it may make sense to operate a battery storage system in combination with a hydrogen storage, as already mentioned before. This could have a positive impact on the size of the storage system, improve the operation of the electrolyzer and further increase the degree of autarky. The possible use of excess heat from the electrolyzer and the fuel cell can improve efficiency. This requires further analysis of how well this process could be integrated into the existing structures, with the temperature level depending on the choice of electrolyzer and fuel cell type.

As this project matures, it's crucial to consider additional components and processes, such as electricity consumption in compression machines for pressure storage tanks and the need for a water treatment system for the electrolyzer. Even if these factors were initially classified as minor cost aspects, they should be taken into account and can considerably impact the project's overall outcome. Further research could take a closer look at the benefits of the surplus hydrogen. For example, it can be sold to a hydrogen filling station or even used for the company's own hydrogen truck fleet. This major undertaking with the necessary elements requires its own investigation.

One part that has so far been completely unaddressed are the natural gas-powered combined heat and power (CHP) units that have been used to generate electricity, heat and cooling. A follow-up study could investigate whether the CHP units could also be converted to run on hydrogen. The question arises as to whether it is economically viable to convert the CHP units. Another possibility would be to operate CHPs with pure hydrogen instead of fuel cells. In this case, the efficiency of CHP units would be around 80% compared to 50% for fuel cells.

In summary, it can be concluded that the full potential of H_2 is far from being exhausted and further research could help to discover and utilize it for a path towards climate neutrality.

References

Agora Industry and Umlaut (2023). Levelised cost of hydrogen. Making the application of the LCOH concept more consistent and more useful. Available online at https://www.agora-energiewende.org/publications/levelised-cost-of-hydrogen (accessed 5/18/2024).

Arsad, A. Z./Hannan, M. A./Al-Shetwi, Ali Q./Mansur, M./Muttaqi, K. M./Dong, Z. Y./Blaabjerg, F. (2022). Hydrogen energy storage integrated hybrid renewable energy systems: A review analysis for future research directions. International Journal of Hydrogen Energy 47 (39), 17285–17312. https://doi.org/10.1016/j.ijhydene.2022.03.208.

Azaioud, Hakim/Desmet, Jan/Vandevelde, Lieven (2020). Benefit Evaluation of PV Orientation for Individual Residential Consumers. Energies 13 (19), 5122. https://doi.org/10.3390/en13195122.

Bahramara, S./Moghaddam, M. Parsa/Haghifam, M. R. (2016). Optimal planning of hybrid renewable energy systems using HOMER: A review. Renewable and Sustainable Energy Reviews 62, 609–620. https://doi.org/10.1016/j.rser.2016.05.039.

Bhandari, Ramchandra/Shah, Ronak Rakesh (2021). Hydrogen as energy carrier: Techno-economic assessment of decentralized hydrogen production in Germany. Renewable Energy 177, 915–931. https://doi.org/10.1016/j.renene.2021.05.149.

BMUV (2023). Referentenentwurf einer Dritten Verordnung zur Änderung der Verordnung über genehmigungsbedürftige Anlagen. Bundesministerium für Umwelt, Naturschutz, nukleare Sicherheit und Verbraucherschutz. Available online at https://www.bmuv.de/gesetz/referentenentwurf-einer-dritten-verordnung-zur-aenderung-der-verordnung-ueber-genehmigungsbeduerftige-anlagen (accessed 5/19/2024).

BMWi (2020). Nationales Reformprogramm 2020 - Die Nationale Wasserstoffstrategie. Bundesministerium für Bildung und Forschung, pp. 5-12.

Borrmann, Rasmus/Knud, Rehfeld/Kruse, Dennis (2020). Volllaststunden von Windenergieanlagen an Land. Deutsche WindGuard. Available online at https://www.windindustrie-in-deutschland.de/publikationen/aktuell/volllaststunden-von-windenergieanlagen-an-land-entwicklung-einfluesse-auswirkungen (accessed 5/10/2024).

Bundesnetzagentur (2024a). EEG-Förderung und -Fördersätze. Available online at https://www.bundesnetzagentur.de/DE/Fachthemen/ElektrizitaetundGas/Erneuerbare Energien/EEG_Foerderung/start.html (accessed 5/17/2024).

Bundesnetzagentur (2024b). So funktioniert der Strommarkt. Available online at https://www.smard.de/page/home/wiki-article/446/384 (accessed 5/31/2024).

Cigolotti, Viviana/Genovese, Matteo/Fragiacomo, Petronilla (2021). Comprehensive Review on Fuel Cell Technology for Stationary Applications as Sustainable and Efficient Poly-Generation Energy Systems. Energies 14 (16), 4963. https://doi.org/10.3390/en14164963.

Coester, Andreas/Hofkes, Marjan W./Papyrakis, Elissaios (2018). Economics of renewable energy expansion and security of supply: A dynamic simulation of the German electricity market. Applied Energy 231, 1268–1284. https://doi.org/10.1016/j.apenergy.2018.09.143.

Couto, António/Estanqueiro, Ana (2020). Exploring Wind and Solar PV Generation Complementarity to Meet Electricity Demand. Energies 13 (16), 4132. https://doi.org/10.3390/en13164132.

Daimler Truck Holding AG (2023). Daimler Truck #HydrogenRecordRun: Mercedes-Benz GenH2 Truck knackt 1.000-Kilometer-Marke mit einer Tankfüllung flüssigem Wasserstoff. Available online at https://www.daimlertruck.com/newsroom/pressemitteilung/daimler-truck-hydrogenrecordrun-mercedes-benz-genh2-truck-knackt-1000-kilometer-marke-mit-einer-tankfuellung-fluessigem-wasserstoff-52369346 (accessed 6/4/2024).

Das, Himadry Shekhar/Tan, Chee Wei/Yatim, A.H.M./Lau, Kwan Yiew (2017). Feasibility analysis of hybrid photovoltaic/battery/fuel cell energy system for an indigenous residence in East Malaysia. Renewable and Sustainable Energy Reviews 76, 1332–1347. https://doi.org/10.1016/j.rser.2017.01.174.

Doucet, Felix/Düsterlho, Eric von/Schäfers, Hans/Jürgens, Lucas/Schütte, Carsten/Barkow, Hagen/Neubauer, Nicolas/Heybrock, Britta/Jensen, Nanke (2023a). Grüner Wasserstoff für die Energiewende. Teil 4: Der Industriesektor. Available online at https://norddeutsches-reallabor.de/presse/ (accessed 5/4/2024).

Doucet, Felix/Jürgens, Lucas/Barkow, Hagen/Schütte, Carsten/Neubauer, Nicolas/Düsterlho, Eric von/Schäfers, Hans (2023b). Decarbonization of the Industry - (Demand and Cost Comparisson of Green Hydrogen in Germany). Available online at https://www.researchgate.net/publication/371378025_Decarbonization_of_the_Industry_-Demand_and_Cost_Comparison_of_Green_Hydrogen_in_Germany (accessed 5/4/2024).

Düsterlho, Eric von/Bannert, Jonas/Doucet, Felix/Lichtenberg, Lia Maria/Heybrock, Britta (2023). Grüner Wasserstoff für die Energiewende. Teil 1: Grüner Wasserstoff als Markt der Zukunft. Available online at https://norddeutsches-reallabor.de/presse/ (accessed 5/4/2024).

E-Bridge (2024). H2-BAROMETER - Unabhängige Bewertung der Wasserstoffwirtschaft in Deutschland. Available online at https://e-bridge.de/wp-content/uploads/2024/05/E-Bridge_Wasserstoff-Barometer_Ausgabe-1_2024.pdf (accessed 5/4/2024).

European Commission (2024). Electricity market design. Available online at https://energy.ec.europa.eu/topics/markets-and-consumers/market-legislation/electricity-market-design_en (accessed 5/31/2024).

Fabianek, Paul/Madlener, Reinhard (2023). Techno-Economic Analysis and Optimal Sizing of Hybrid PV-Wind Systems for Hydrogen Production by PEM Electrolysis in California and Germany. SSRN Electronic Journal. https://doi.org/10.2139/ssrn.4274802.

Ferraz de Andrade Santos, José Alexandre/Jong, Pieter de/Da Alves Costa, Caiuby/Torres, Ednildo Andrade (2020). Combining wind and solar energy sources: Potential for hybrid power generation in Brazil. Utilities Policy 67, 101084. https://doi.org/10.1016/j.jup.2020.101084.

Fraunhofer ISE (2018). Industrialisierung der Wasser-elektrolyse in -Deutschland: -Chancen und -Herausforderungen für nachhaltigen Wasserstoff für Verkehr, Strom und Wärme. Available online at https://www.ipa.fraunhofer.de/content/dam/ipa/de/documents/Publikationen/Studien/Studie-IndWEDe.pdf (accessed 5/18/2024).

Fraunhofer ISE (2024). Energy-Charts. Fraunhofer-Institut für Solare Energiesysteme ISE; Freiburg. Available online at https://www.energy-charts.info/charts/power/chart.htm?l=de&c=DE&year=2023&interval=week&legendItems=4x0fvn0&source=sw (accessed 5/29/2024).

Fraunhofer ISI & ISE (2019). Eine Wasserstoff-Roadmap für Deutschland, pp. 1–6. Available online at https://www.ieg.fraunhofer.de/content/dam/ieg/documents/pressemitteilungen/2019-10_Fraunhofer_Wasserstoff-Roadmap_fuer_Deutschland.pdf (accessed 5/21/2024).

Fuel Cells and Hydrogen (2019). Hydrogen roadmap Europe. A sustainable pathway for the European energy transition. Luxembourg, Publications Office of the European Union.

Grigoriev, S. A./Fateev, V. N./Bessarabov, D. G./Millet, P. (2020). Current status, research trends, and challenges in water electrolysis science and technology. International Journal of Hydrogen Energy 45 (49), 26036–26058. https://doi.org/10.1016/j.ijhydene.2020.03.109.

Gutiérrez-Martín, F./Díaz-López, J. A./Caravaca, A./Dos Santos-García, A. J. (2023). Modeling and simulation of integrated solar PV - hydrogen systems. International Journal of Hydrogen Energy. https://doi.org/10.1016/j.ijhydene.2023.05.179.

Harrabi, Naziha/Souissi, Mansour/Aitouche, Abdel/Chaabane, Mohamed (2018). Modeling and control of photovoltaic and fuel cell based alternative power systems. International

Journal of Hydrogen Energy 43 (25), 11442–11451. https://doi.org/10.1016/j.ijhydene.2018.03.012.

Hassan, I. A./Ramadan, Haitham S./Saleh, Mohamed A./Hissel, Daniel (2021). Hydrogen storage technologies for stationary and mobile applications: Review, analysis and perspectives. Renewable and Sustainable Energy Reviews 149, 111311. https://doi.org/10.1016/j.rser.2021.111311.

Hassan, Qusay/Algburi, Sameer/Sameen, Aws Zuhair/Salman, Hayder M./Jaszczur, Marek (2023). A review of hybrid renewable energy systems: Solar and wind-powered solutions: Challenges, opportunities, and policy implications. Results in Engineering 20, 101621. https://doi.org/10.1016/j.rineng.2023.101621.

HOMER Pro (2024). HOMER Software. Available online at https://homerenergy.com/products/pro/index.html (accessed 5/15/2024).

Hu, Jing/Harmsen, Robert/Crijns-Graus, Wina/Worrell, Ernst/van den Broek, Machteld (2018). Identifying barriers to large-scale integration of variable renewable electricity into the electricity market: A literature review of market design. Renewable and Sustainable Energy Reviews 81, 2181–2195. https://doi.org/10.1016/j.rser.2017.06.028.

Hussin, S. M./Salam, Z./Abdullah, M. P./Rosmin, N./Said, D. M./Rasid, M. (2019). Future hybrid of photovoltaic and fuel cell for Langkawi SkyCab. Journal of Electronic Science and Technology 17 (4), 100016. https://doi.org/10.1016/j.jnlest.2020.100016.

IKEM (2020). Wasserstoff - Farbenlehre Rechtwissenschaftliche und rechtspolitische Kurzstudie. Institut für Klimaschutz, Energie und Mobilität e.V. (IKEM), pp. 8-12. Available online at https://www.ikem.de/wp-content/uploads/2021/01/IKEM_Kurzstudie_Wasserstoff_Farbenlehre.pdf (accessed 5/20/2024).

Jamal, Taskin/Shafiullah, G. M./Dawood, Furat/Kaur, Arshdeep/Arif, Mohammad T./Pugazhendhi, Rishi/Elavarasan, Rajvikram M./Ahmed, Shams Forruque (2023). Fuelling the future: An in-depth review of recent trends, challenges and opportunities of hydrogen fuel cell for a sustainable hydrogen economy. Energy Reports 10, 2103–2127. https://doi.org/10.1016/j.egyr.2023.09.011.

Kalinci, Yildiz/Dincer, Ibrahim/Hepbasli, Arif (2017). Energy and exergy analyses of a hybrid hydrogen energy system: A case study for Bozcaada. International Journal of Hydrogen Energy 42 (4), 2492–2503. https://doi.org/10.1016/j.ijhydene.2016.02.048.

Khan, Asif/Javaid, Nadeem (2020). Optimal sizing of a stand-alone photovoltaic, wind turbine and fuel cell systems. Computers & Electrical Engineering 85, 106682. https://doi.org/10.1016/j.compeleceng.2020.106682.

Khan, Tahir/Yu, Miao/Waseem, Muhammad (2022). Review on recent optimization strategies for hybrid renewable energy system with hydrogen technologies: State of the art,

trends and future directions. International Journal of Hydrogen Energy 47 (60), 25155–25201. https://doi.org/10.1016/j.ijhydene.2022.05.263.

Khatib, F. N./Wilberforce, Tabbi/Ijaodola, Oluwatosin/Ogungbemi, Emmanuel/El-Hassan, Zaki/Durrant, A./Thompson, J./Olabi, A. G. (2019). Material degradation of components in polymer electrolyte membrane (PEM) electrolytic cell and mitigation mechanisms: A review. Renewable and Sustainable Energy Reviews 111, 1–14. https://doi.org/10.1016/j.rser.2019.05.007.

Krishnan, Subramani/Corona, Blanca/Kramer, Gert Jan/Junginger, Martin/Koning, Vinzenz (2024). Prospective LCA of alkaline and PEM electrolyser systems. International Journal of Hydrogen Energy 55, 26–41. https://doi.org/10.1016/j.ijhydene.2023.10.192.

Lahnaoui, Amin/Stenzel, Peter/Linssen, Jochen (2017). Tilt Angle and Orientation Impact on the Techno-economic Performance of Photovoltaic Battery Systems. Energy Procedia 105, 4312–4320. https://doi.org/10.1016/j.egypro.2017.03.903.

Lange, Jelto/Schulthoff, Michael/Puszkiel, Julián/Sens, Lucas/Jepsen, Julian/Klassen, Thomas/Kaltschmitt, Martin (2024). Aboveground hydrogen storage – Assessment of the potential market relevance in a Carbon-Neutral European energy system. Energy Conversion and Management 306, 118292. https://doi.org/10.1016/j.enconman.2024.118292.

Lazard (2023). LCOE+. Available online at https://www.lazard.com/media/2ozoovyg/lazards-lcoeplus-april-2023.pdf (accessed 5/17/2024).

Lindberg, Oskar/Arnqvist, Johan/Munkhammar, Joakim/Lingfors, David (2021). Review on power-production modeling of hybrid wind and PV power parks. Journal of Renewable and Sustainable Energy 13 (4). https://doi.org/10.1063/5.0056201.

Malek, Abdul/Lu, Xu/Shearing, Paul R./Brett, Dan J.L./He, Guanjie (2023). Strategic comparison of membrane-assisted and membrane-less water electrolyzers and their potential application in direct seawater splitting (DSS). Green Energy & Environment 8 (4), 989–1005. https://doi.org/10.1016/j.gee.2022.06.006.

Martinez Lopez, V. A./Ziar, H./Haverkort, J. W./Zeman, M./Isabella, O. (2023). Dynamic operation of water electrolyzers: A review for applications in photovoltaic systems integration. Renewable and Sustainable Energy Reviews 182, 113407. https://doi.org/10.1016/j.rser.2023.113407.

McKinsey & Company, Inc. (2024). Zukunftspfad Stromversorgung. Perspektiven zur Erhöhung der Versorgungssicherheit und Wirtschaftlichkeit der Energiewende in Deutschland bis 2035. Available online at https://www.mckinsey.com/de/~/media/mckinsey/locations/europe%20and%20middle%20east/deutschland/news/presse/2024/2024-01-

17%20zukunftspfad%20stromversorgung/zukunftspfad%20stromversorgung_inhalt_print_240222.pdf (accessed 5/31/2024).

Mubarak, Riyad/Weide Luiz, Eduardo/Seckmeyer, Gunther (2019). Why PV Modules Should Preferably No Longer Be Oriented to the South in the Near Future. Energies 12 (23), 4528. https://doi.org/10.3390/en12234528.

Muñoz Díaz, María Teresa/Chávez Oróstica, Héctor/Guajardo, Javiera (2023). Economic Analysis: Green Hydrogen Production Systems. Processes 11 (5), 1390. https://doi.org/10.3390/pr11051390.

Nanadegani, Fereshteh Salimi/Sunden, Bengt (2023). Review of exergy and energy analysis of fuel cells. International Journal of Hydrogen Energy 48 (84), 32875–32942. https://doi.org/10.1016/j.ijhydene.2023.05.052.

O'Hayre, Ryan/Cha, Suk-Won/Colella, Whitney/Prinz, Fritz B. (2016). Fuel Cell Fundamentals. Wiley.

Okundamiya, M. S. (2021). Size optimization of a hybrid photovoltaic/fuel cell grid connected power system including hydrogen storage. International Journal of Hydrogen Energy 46 (59), 30539–30546. https://doi.org/10.1016/j.ijhydene.2020.11.185.

Preuster, Patrick/Alekseev, Alexander/Wasserscheid, Peter (2017). Hydrogen Storage Technologies for Future Energy Systems. Annual review of chemical and biomolecular engineering 8, 445–471. https://doi.org/10.1146/annurev-chembioeng-060816-101334.

Prognos and Consentec (2022). Klimaneutrales Stromsystem 2035. Wie der deutsche Stromsektor bis zum Jahr 2035 klimaneutral werden kann, pp. 7-13. Available online at https://static.agora-energiewende.de/fileadmin/Projekte/2021/2021_11_DE_KNStrom2035/A-EW_264_KNStrom2035_WEB.pdf (accessed 6/4/2024).

pv magazine (2024). Enervis PPA-Price-Tracker für Photovoltaik: Jahresende bringt abermals fallende PPA-Preise. Available online at https://www.pv-magazine.de/2024/01/04/enervis-ppa-price-tracker-fuer-photovoltaik-jahresende-bringt-abermals-fallende-ppa-preise/ (accessed 5/31/2024).

PVsyst SA (2024). PVsyst. Version 7.4.6. Group of Energy Institute of the Sciences of the Environment. Available online at www.pvsyst.com (accessed 5/29/2024).

Reksten, Anita H./Thomassen, Magnus S./Møller-Holst, Steffen/Sundseth, Kyrre (2022). Projecting the future cost of PEM and alkaline water electrolysers; a CAPEX model including electrolyser plant size and technology development. International Journal of Hydrogen Energy 47 (90), 38106–38113. https://doi.org/10.1016/j.ijhydene.2022.08.306.

Saba, Sayed M./Müller, Martin/Robinius, Martin/Stolten, Detlef (2018). The investment costs of electrolysis – A comparison of cost studies from the past 30 years. International

Journal of Hydrogen Energy 43 (3), 1209–1223. https://doi.org/10.1016/j.ijhydene.2017.11.115.

Salehmin, Mohd Nur Ikhmal/Husaini, Teuku/Goh, Jonathan/Sulong, Abu Bakar (2022). High-pressure PEM water electrolyser: A review on challenges and mitigation strategies towards green and low-cost hydrogen production. Energy Conversion and Management 268, 115985. https://doi.org/10.1016/j.enconman.2022.115985.

Sazali, Norazlianie/Wan Salleh, Wan Norharyati/Jamaludin, Ahmad Shahir/Mhd Razali, Mohd Nizar (2020). New Perspectives on Fuel Cell Technology: A Brief Review. Membranes 10 (5). https://doi.org/10.3390/membranes10050099.

Sharaf, Omar Z./Orhan, Mehmet F. (2014). An overview of fuel cell technology: Fundamentals and applications. Renewable and Sustainable Energy Reviews 32, 810–853. https://doi.org/10.1016/j.rser.2014.01.012.

Shiva Kumar, S./Lim, Hankwon (2022). An overview of water electrolysis technologies for green hydrogen production. Energy Reports 8, 13793–13813. https://doi.org/10.1016/j.egyr.2022.10.127.

Sorrenti, Ilaria/Zheng, Yi/Singlitico, Alessandro/You, Shi (2023). Low-carbon and cost-efficient hydrogen optimisation through a grid-connected electrolyser: The case of GreenLab skive. Renewable and Sustainable Energy Reviews 171, 113033. https://doi.org/10.1016/j.rser.2022.113033.

Stöckel, Marc (2023). Tesla Model Y: Alle wichtigen Infos zu Akku, Reichweite und Ladezeit. GIGA. Available online at https://www.giga.de/artikel/tesla-model-y--2fx2pmrwvc (accessed 6/5/2024).

Sufaid Khan, Muhammad/Khattak, Rozina/Khan, Abbas (2024). Fuel Cell Technology (FCT): An Overview. In: Chemical Kinetics and Catalysis - Perspectives, Developments and Applications [Working Title]. IntechOpen.

Tuinema, Bart W./Adabi, Ebrahim/Ayivor, Patrick K.S./García Suárez, Víctor/Liu, Lian/Perilla, Arcadio/Ahmad, Zameer/Rueda Torres, José Luis/Meijden, Mart A.M.M./Palensky, Peter (2020). Modelling of large-sized electrolysers for real-time simulation and study of the possibility of frequency support by electrolysers. IET Generation, Transmission & Distribution 14 (10), 1985–1992. https://doi.org/10.1049/iet-gtd.2019.1364.

vbw (2023). Prognos Strompreisprognose 2023. Vereinigung der Bayerischen Wirtschaft e. V. Available online at https://www.vbw-bayern.de/Redaktion/Frei-zugaengliche-Medien/Abteilungen-GS/Wirtschaftspolitik/2023/Downloads/vbw_Strompreisprognose_Juli-2023-3.pdf (accessed 5/31/2024).

Velik, Rosemarie (2014). East-South-West Orientation of PV Systems and Neighbourhood Energy Exchange to Maximize Local Photovoltaics Energy Consumption. Available

online at https://www.researchgate.net/publication/263285002_East-South-West_Orientation_of_PV_Systems_and_Neighbourhood_Energy_Exchange_to_Maximize_Local_Photovoltaics_Energy_Consumption (accessed 5/29/2024).

Wietschel, Martin/Weißenburger, Bastian/Rehfeldt, Matthias/Lux, Benjamin/Zheng, Lin/Meier, Jonas (2023). Preiselastische Wasserstoffnachfrage in Deutschland – Methodik und Ergebnisse. Hypat Working Paper 01/2023, pp. 25-26. Available online at https://publica.fraunhofer.de/entities/publication/0f1e7d3e-fb5f-400d-aa83-4f5495253e91/details (accessed 5/21/2024).

Yang, Miao/Hunger, Ralf/Berrettoni, Stefano/Sprecher, Bernd/Wang, Baodong (2023). A review of hydrogen storage and transport technologies. Clean Energy 7 (1), 190–216. https://doi.org/10.1093/ce/zkad021.

Yang, Yuchen/Wu, Zhen/Yao, Jing/Guo, Tianlei/Yang, Fusheng/Zhang, Zaoxiao/Ren, Jianwei/Jiang, Liangliang/Li, Bo (2024). An overview of application-oriented multifunctional large-scale stationary battery and hydrogen hybrid energy storage system. Energy Reviews 3 (2), 100068. https://doi.org/10.1016/j.enrev.2024.100068.

Zhang, Dongke/Zeng, Kai (2015). Distributed Energy Systems Based on Water Electrolysis Driven by Renewable Electricity. In: Jinyue Yan (Ed.). Handbook of Clean Energy Systems. Wiley, 1–12.

Acknowledgement

I would like to take this opportunity to thank all those who have accompanied and supported me during the time of my thesis. First and foremost, I would like to thank 8.2 Obst & Hamm GmbH, who made this work possible in the first place. Thanks to their network of contacts, they made it possible for me to work on this topic in such a practical way.

I would like to thank my supervisor from HAW Hamburg, Prof. Dr. Timon Kampschulte, who always made time for me and provided me with advice and support right from the start. I would also like to thank Dr. rer. nat. Henrik Zahn, my supervisor from 8.2 Obst & Hamm GmbH, who never got tired of answering my many questions, gave me further interesting food for thought in countless conversations and was not hesitant to give me feedback and thus steer my work in the right direction.

On behalf of the company, I would like to thank M.B. for the fruitful collaboration. Without the great support in all questions, countless conversations and constructive discussions with P.S. and S.W. as external supervisors, the work would not have been possible. I would also like to thank T.S. and S.G. for their support with all questions regarding the consumption data and processes of the facility.

Finally, I would also like to thank my colleagues from 8.2 for their support and help with this project.

Declaration of Authorship

I hereby declare that I have composed this thesis independently and without any external assistance. Any passages of text that are based directly or indirectly on publications or lectures by other authors are indicated as such.

Hamburg, June 18, 2024

Signature

Appendix

Appendix A - Datasheet Accelera PEM Fuel Cell Power System

Stationary Solutions

Fuel Cell Power Systems

accelerate the shift™

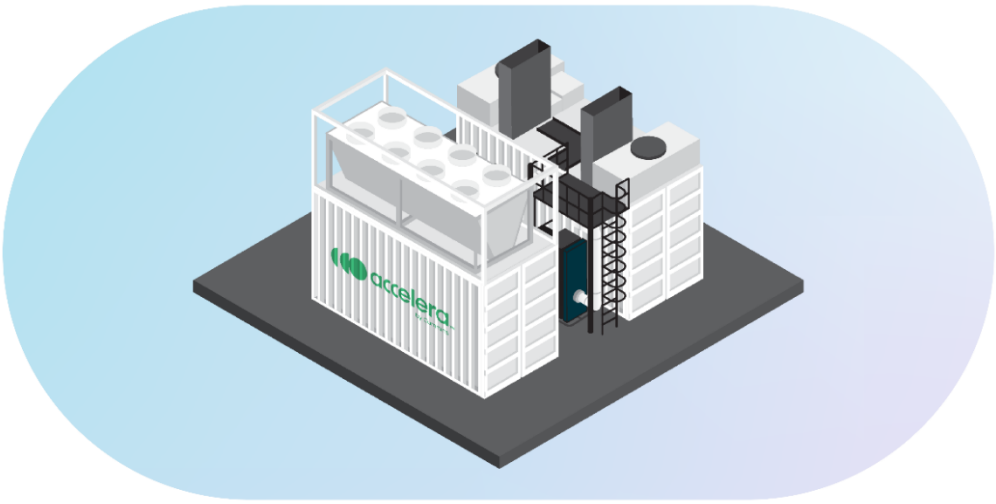

Features

36 x Advanced MEA PEM stacks

Advanced system controls - remote monitoring capability

Rapid start-up + dynamic response

Unlimited start-stop cycles

Low pressure air delivery system

No water required for humidification

No nitrogen required for shutdown

Plug + play design - ready to accept H2 + output AC power

Robust + reliable

Cummins Inc
Box 3005, Columbus, IN 47202-3005 U.S.A.
Bulletin 6519699 Produced in U.S.A. Rev 2/24

accelera™ by Cummins

Stationary Solutions

Fuel Cell Power Systems

Scalable + Reliable Power

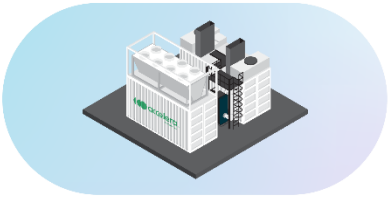

Benefits

- Proprietary PEM stack technology - with high durability components designed for demanding conditions.
- Modular & scalable - enables MW scale power plant deployments starting with a few hundred kWs.
- Integrated package - allows for easy on-site installation, reduced construction time + costs.
- Trusted service support network - provides rapid on-site predictive service to assure reliable power to critical applications.

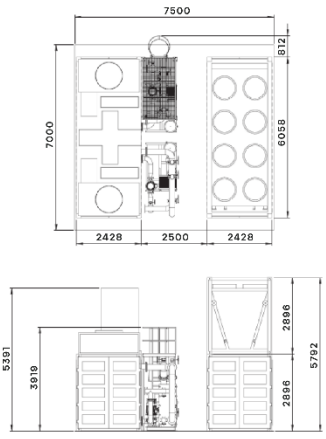

Can deliver anything above 100kW in a similar package

Specifications

Power Ratings	1,440 kW (NP)[1], 1,000 kW (ESP)[2], 1,000 kW (LTP)[3], 900 kW (PRP)[4], 800 kW (COP)[5]
Turndown [Partial Load] Ratio	100%
Ramp Rate	Black-start capable <180s (Off to full power[8]) <30s (Hot-standby/Partial to full power)
Max Electrical Efficiency[6]	50-55%
System Output + Frequency[7]	3-phase AC power 50/60 Hz
System Design Life	20 Years+
Installation & Layout Options	Outdoor installation with 3 layout options
Approximate Weight (Total)	30 tons
Fuel Quality	ISO 14687
Inlet Fuel Pressure	10-20 bar(g)
Fuel Flow Rate[6]	56-70 g/kWh
Ambient Operating Conditions[9]	2-40 °C (-25) °C operation achievable with cold climate package

[1] Name plate; [2] Emergency standby power (200hrs/yr; 24hrs continuous); [3] Limited time prime (500hrs/yr; 72hrs continuous); [4] Prime power (<4,000hrs/yr; load factor ~70%); [5] Continuous power (unlimited hrs/yr; base load); [6] Varies with operational profile; [7] Voltage determined by customer; DC output also available; [8] Without a battery energy storage system [9] hot and cold climate packages are available. Combined heat and power systems are available.

We are Accelera
And we're on a mission to transition the world's most economically critical industries to zero-emissions power.

Learn more at **accelerazero.com**

Appendix B - Datasheet Ballard PEM Fuel Cell

BALLARD™

FCwave™

Fuel Cell Power for Stationary Power Applications

Ballard's FCwave ™ hydrogen fuel cell solution, provides zero-emission, uninterrupted backup power to a wide range of power-intensive stationary applications and industries including data centers, health care centers, commercial buildings, charging points for electric vehicles, or shore connections at ports.

Available from 200kW to MWs, FCwave™ can meet stationary power needs for markets with scalable power requirements.

Based on more than 44 years of field experience and over 150 million kilometers of in service vehicles, the FCwave™ leverages Ballard's proven technology to deliver a reliable, scalable and flexible power solutions.

Features

Reliable and always-available power

Fuel cells provide the highest level of reliability supplying seamless and uninterrupted power. With gigawatts of fuel cell systems produced to date, the technology has demonstrated its reliability in all operating conditions.

Modular and scalable solution

Available in 200kW modules, FCwave™ facilitates scalable power up to 1.2 MW and allows for flexible integration with minimal use of space. FCwave™ modules, can easily be coupled in parallel to meet power output requirements and can be delivered as stand-alone modules or as a containerized solution.

Safe Operation

FCwave™-XD is developed, tested and prepared for installation with an uncompromising focus on safety. The fuel cell module is CE marked, which certifies that the solution meets the highest safety, health, and environmental protection standards.

Technology Leadership

The same Ballard fuel cell technology has already proved itself in more than 3,600 fuel cell electric trucks and buses deployed worldwide.

Ease of Integration

The FCwave™-system is developed for easy installation. Integrated into a simplified and streamlined cabinet with easy-to- access doors and all interfaces accessible from the front for service and maintenance.

No risk

Fuel cell backup power systems are solid state power generators with few moving parts and no degradation in standby mode regardless of temperature. Diagnostic connections allow customers to monitor performance data remotely and plan for preventative maintenance.

Low Lifecycle Cost

Low total-cost-of-ownership, achieved through product performance optimization, common components across product platforms and low maintenance requirements

Product Specifications

Performance	
Rated power	200kW
Minimum power	50kW
Peak fuel Efficiency	53.5 %
Operating voltage	350 - 720 V DC
Rated current [1]	2 x 300 A or 1 x 550
System cooling output	Max 65° C
Stack technology	
Heat management	Liquid cooled
H2 Pressure	3.5 - 6.5 Barg
Physical	
Dimensions (l x w x h) [2]	1210 mm x 738 mm x 2195 mm
Weight (estimate) [3]	1050 kg
Environmental protection	IP44
Engine room (DNV CG-0339)	+0°C – +45°C
Minimum start-up temperature	0°C
Short-term storage temp	-20°C – +60°C
Reactants and Coolant	
Type	Gaseous hydrogen
Composition	As per SAE spec. J2719. ISO 14687:2019, grade D or GB/T 3244-2018
Oxidant	Air
Composition	Particulate, Chemical and Salt filtered
Coolant [4]	Water or 50/50 glycol
Safety Compliance	
Certifications	CE Marked
Enclosure	Sealed secondary barrier for hydrogen
Monitoring	
Control interface	Ethernet, CAN
Emissions	
Exhaust	Zero-emission

[1] System output is 2 x 300 A (1 x 550A output still under development). [2] Target size. [3] Includes: framed skid base, fuel cell stacks, plumbing and wiring, H2 enclosure, cooling system, air system, electrical panel, and miscellaneous (sensors, cable tray, etc.). [4] Customer coolant type.

Here for life™

Ballard Power Systems
9000 Glenlyon Parkway
Burnaby, BC V5J 5J8
Canada

Ballard Power Systems
Majsmarken 1
DK-9500 Hobro
Denmark

Contact us
marketing@ballard.com
ballard.com

Appendix C - Datasheet FuelCellEnergy Solid Oxide Fuel Cell

FuelCell Energy

3 Great Pasture Road, Danbury, CT 06810
Phone: (203) 825-6000 | Email: info@fce.com
Website: fuelcellenergy.com

Data Sheet

Solid Oxide Fuel Cell

A 250 kW fuel cell system for low-carbon, resilient distributed energy generation

FuelCell Energy's Solid Oxide Fuel Cell (SOFC) system generates 250 kW of reliable, efficient, and low-carbon power. The fuel flexible system is capable of running on natural gas, biogas, or hydrogen. The system's superior fuel efficiency to combustion-based power generation can improve a customer's return on investment. A clean emissions profile, small footprint, and quiet operation make the fuel cell easy to site in urban areas.

Key Benefits

- Fuel flexible
- Hydrogen ready
- Microgrid capable
- High efficiency
- Low emissions
- Scalable design

Appendix

Specifications subject to change without notice.

	Natural Gas Fuel	Biogas[1] Fuel (60% Methane)
Net Power Output[2]	250 kW	
Part Power Capability	10 - 100%	
Dynamic Response	10% per minute	
Voltage / Frequency	480 VAC / 60 Hz	
Heat Output, maximum[5]	382,000 BTU/h	471,000 BTU/h
Efficiency, Electrical / Overall (LHV)[2,3]	62% / 90%	58% / 90%
Fuel Consumption	1,491 SCFH @ 1025 BTU/SCF	2,694 SCFH @ 606 BTU/SCF
Dual Fuel Option	Natural Gas & Hydrogen	Natural Gas & Biogas
Fuel Blending Range[4] (Performed Onboard)	0 - 100% H_2	0 - 100% Biogas
Fuel Inlet Pressure	15 - 20 psig	
Water Consumption / Discharge	None during normal operation	
NO_x and CO Emissions	0.01 lb/MWh	
VOC, PM10, SO_x Emissions	Negligible	
CO_2 (electric only)[6]	715 lb/MWh	Dependent on biogas source[6]
CO_2 (with full heat recovery)[6,7]	494 lb/MWh	Dependent on biogas source[6]
Ambient Temperature Range	-20°F to 104°F	
Noise	< 72 dBA @ 10 ft, option for < 65 dBA	
Codes & Standards	ANSI/CSA FC1-2021: Stationary Fuel Cell Power Systems UL1741SA-2016: Inverters for Use with Distributed Energy Resources	

Dimensions

Length	35' 3"
Width	8' 3"
Height	10' 6"
Weight	80,000 lbs

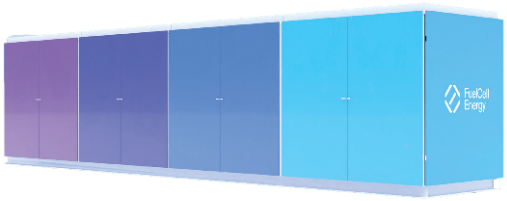

[1]Biogas must be pre-conditioned to meet FCE's fuel composition requirements. FCE can supply the pre-conditioning system, if desired.
[2]Power and efficiency are rated at beginning of operation and will decrease by approximately 10% over the life of the fuel cell stack module.
[3]Biogas system efficiency depends upon % methane in fuel. Rating based on 60% methane. Minimum methane % is 55%.
[4]Performance at 50% H2: 250 kW / 56% electrical efficiency. Performance at 100% H2: 180 kW / 50% electrical efficiency.
[5]Maximum heat recovery based on cooling the exhaust to 120 F.
[6]Carbon intensity for operation on biogas dependent on biogas source.
[7]CO_2 emissions with full heat recovery is based on the total electric and thermal energy available from the system.

FuelCell Energy

3 Great Pasture Road
Danbury, CT 06810
(203) 825-6000

fuelcellenergy.com

Appendix D – Total Renewable Power Output over a year from HOMER

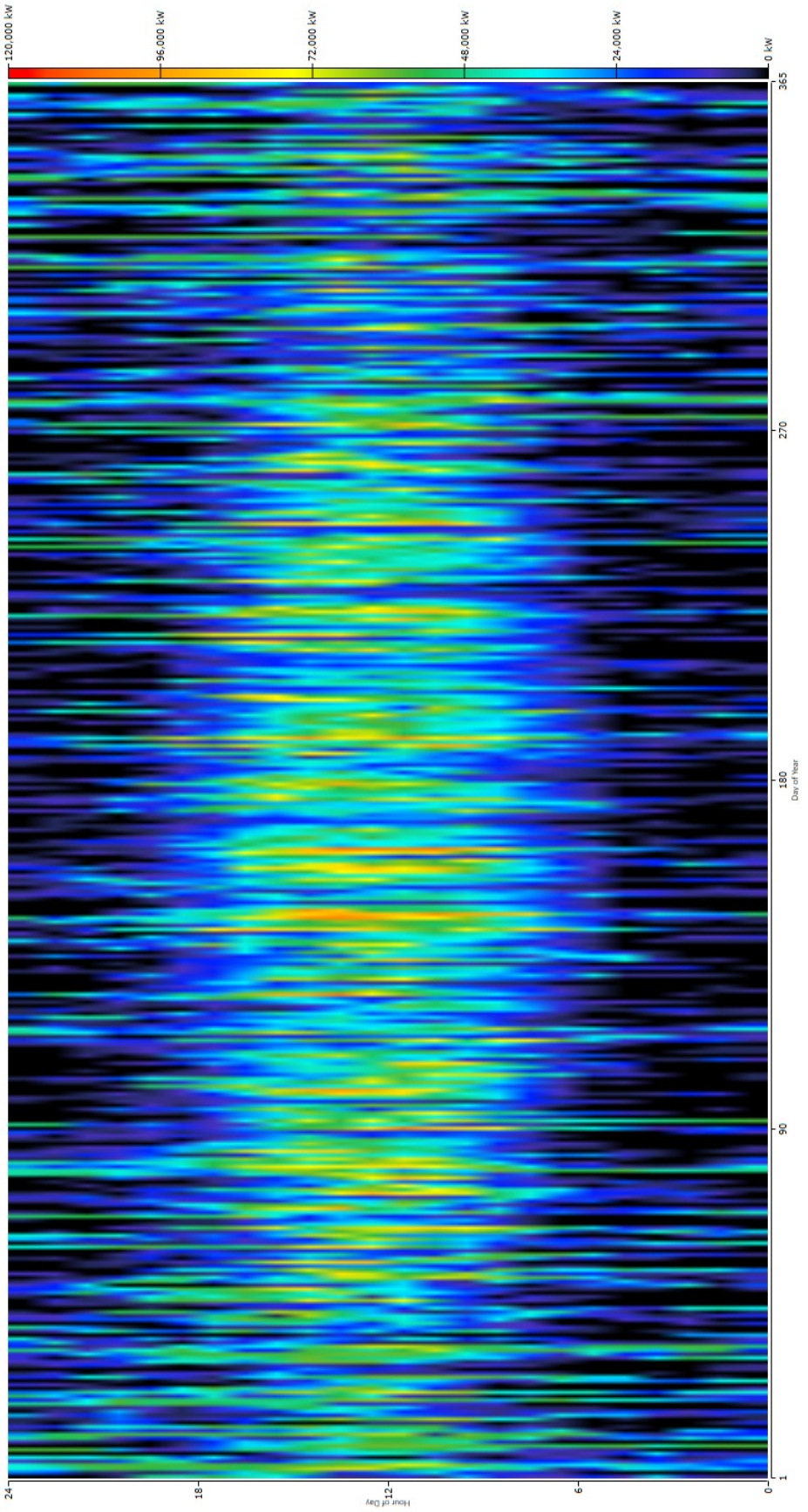

Appendix E – Public Wind and PV net electricity generation in Germany in 2023

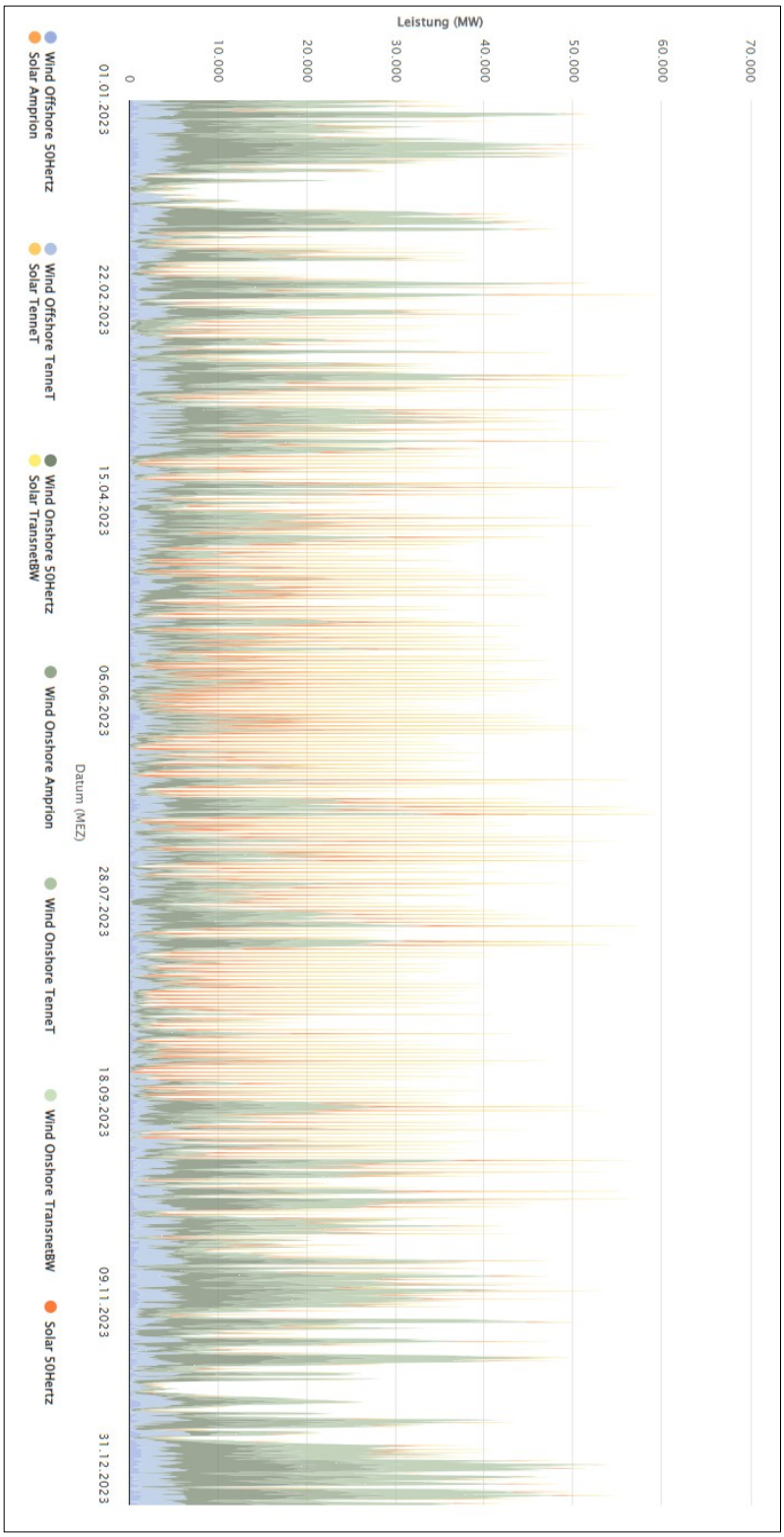

(Fraunhofer ISE 2024)

Appendix F - Irradiation data

Horizontal global irradiation

Period of measurement	1996-2015	1994 - 2021	2004-2023	2005-2020	1996-2015	1994 - 2021	2004-2023	2005-2020	
weighting factor	20	28	20	16	20	28	20	16	
Source	Meteonorm 8	Solargis	DWD	PVGIS SARAH2	Meteonorm 8	Solargis	DWD	PVGIS SARAH2	Average
Global Irradiation	Horizontal	Horizontal	Horizontal	Horizontal	Horizontal	Horizontal	Horizontal	Horizontal	Horizontal
	kWh/m²	kWh/m²	kWh/m²	kWh/m²	kWh/m²	kWh/m²	kWh/m²	kWh/m²	kWh/m²
Month	average daily sum	average daily sum	average daily sum	average daily sum	average monthly sum	average monthly sum	average monthly sum	average monthly sum	average monthly sum
January	0.75	0.77	0.71	0.78	23.3	23.9	22.2	24.0	23.4
February	1.45	1.48	1.42	1.45	40.7	41.6	39.9	40.6	40.8
March	2.57	2.69	2.63	2.62	79.8	83.3	81.7	81.4	81.7
April	4.08	4.23	4.20	4.38	122.5	126.8	126.0	131.5	126.5
May	5.04	5.13	5.15	5.14	156.1	159.1	159.6	159.2	158.5
June	5.50	5.52	5.71	5.64	164.9	165.5	171.3	169.1	167.4
July	5.16	5.15	5.40	5.43	160.0	159.6	167.4	168.2	163.2
August	4.48	4.51	4.46	4.55	139.0	139.7	138.2	140.9	139.4
September	3.19	3.19	3.30	3.37	95.8	95.6	98.9	101.0	97.5
October	1.87	1.89	1.87	1.93	58.1	58.6	57.9	59.9	58.6
November	0.89	0.95	0.89	1.01	26.6	28.4	26.6	30.3	27.9
December	0.57	0.59	0.57	0.66	17.8	18.4	17.6	20.5	18.5
Annual average	**3.0**	**3.0**	**3.0**	**3.1**	**1,084.6**	**1,100.7**	**1,106.9**	**1,126.6**	**1,103.3**

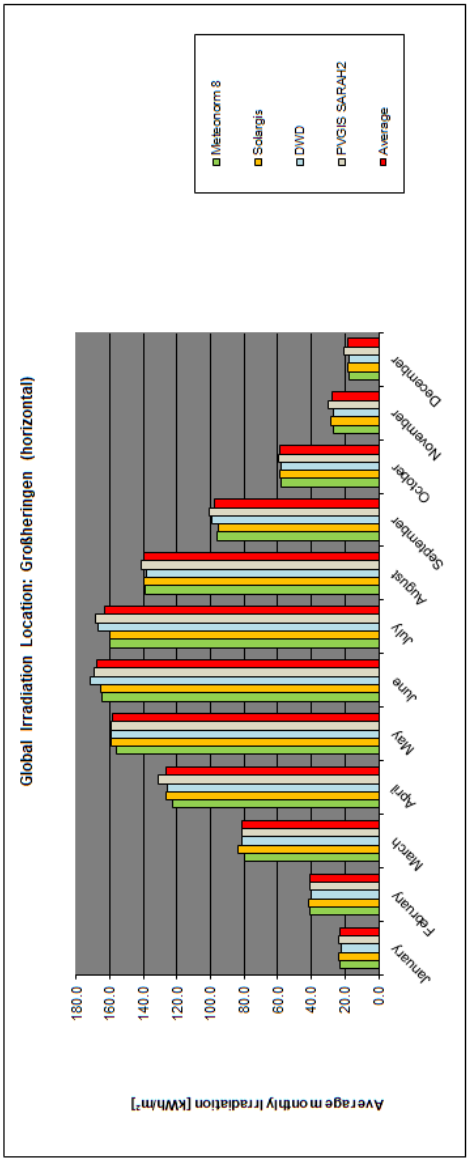

	diffuse irradiation (into the horizontal)								
Period of measurement	1996-2015	1994 - 2021	2004-2023	2005-2020	1996-2015	1994 - 2021	2005 - 2023	2005-2020	
weighting factor	20	28	19	16	20	28	19	16	
Source	Meteonorm 8	Solargis	DWD	PVGIS SARAH2	Meteonorm 8	Solargis	DWD	PVGIS SARAH2	Average
Diffus Irradiation	Horizontal	Horizontal	Horizontal	Horizontal	Horizontal	Horizontal	Horizontal	Horizontal	Horizontal
	kWh/m²	kWh/m²	kWh/m²	kWh/m²	kWh/m²	kWh/m²	kWh/m²	kWh/m²	kWh/m²
Month	average daily sum	average daily sum	average daily sum	average daily sum	average monthly sum	average monthly sum	average monthly sum	average monthly sum	average monthly sum
January	0.50	0.49	0.50	0.53	15.6	15.3	15.5	16.3	15.6
February	0.85	0.85	0.88	0.86	23.7	23.9	24.8	24.1	24.1
March	1.36	1.43	1.44	1.42	42.1	44.2	44.7	44.0	43.8
April	1.99	2.05	1.97	2.01	59.8	61.6	59.1	60.4	60.4
May	2.55	2.48	2.48	2.44	79.1	77.0	76.8	75.7	77.2
June	2.85	2.75	2.67	2.68	85.4	82.4	80.2	80.3	82.2
July	2.72	2.66	2.64	2.67	84.4	82.5	81.7	82.7	82.8
August	2.43	2.28	2.18	2.22	75.3	70.7	67.5	69.0	70.7
September	1.73	1.65	1.57	1.65	51.9	49.5	47.2	49.6	49.6
October	1.05	1.05	1.01	1.06	32.5	32.6	31.5	32.9	32.4
November	0.54	0.58	0.56	0.61	16.2	17.5	16.9	18.3	17.2
December	0.36	0.39	0.39	0.44	11.1	12.2	12.2	13.6	12.2
Annual average	**1.6**	**1.6**	**1.5**	**1.6**	**577.1**	**569.5**	**558.1**	**567.1**	**568.2**

					Average daily temperature				
					20	28	20	16	
					Meteonorm 8	Solargis	DWD	PVGIS SARAH2	Average
					temperature °C	temperature °C	temperature °C	temperature °C	°C
Month					1996-2015	1994 - 2021	2004 - 2023	2005-2020	average monthly sum
January					0.5	1.0	1.5	0.8	1.0
February					1.6	2.1	2.2	1.4	1.9
March					5.2	5.1	5.3	4.4	5.0
April					10.2	9.5	9.9	9.6	9.8
May					14.9	13.9	13.9	13.5	14.1
June					17.7	17.5	17.7	17.3	17.5
July					19.9	19.4	19.7	19.5	19.6
August					19.7	19.1	19.1	18.6	19.2
September					15.0	14.7	15.2	14.8	14.9
October					10.6	10.2	10.6	10.1	10.4
November					5.6	5.3	5.8	5.3	5.5
December					1.5	1.9	2.9	2.4	2.1
Annual average					**10.2**	**10.0**	**10.3**	**9.8**	**10.1**

Appendix G - Windspeed data (NASA 1984 – 2013)

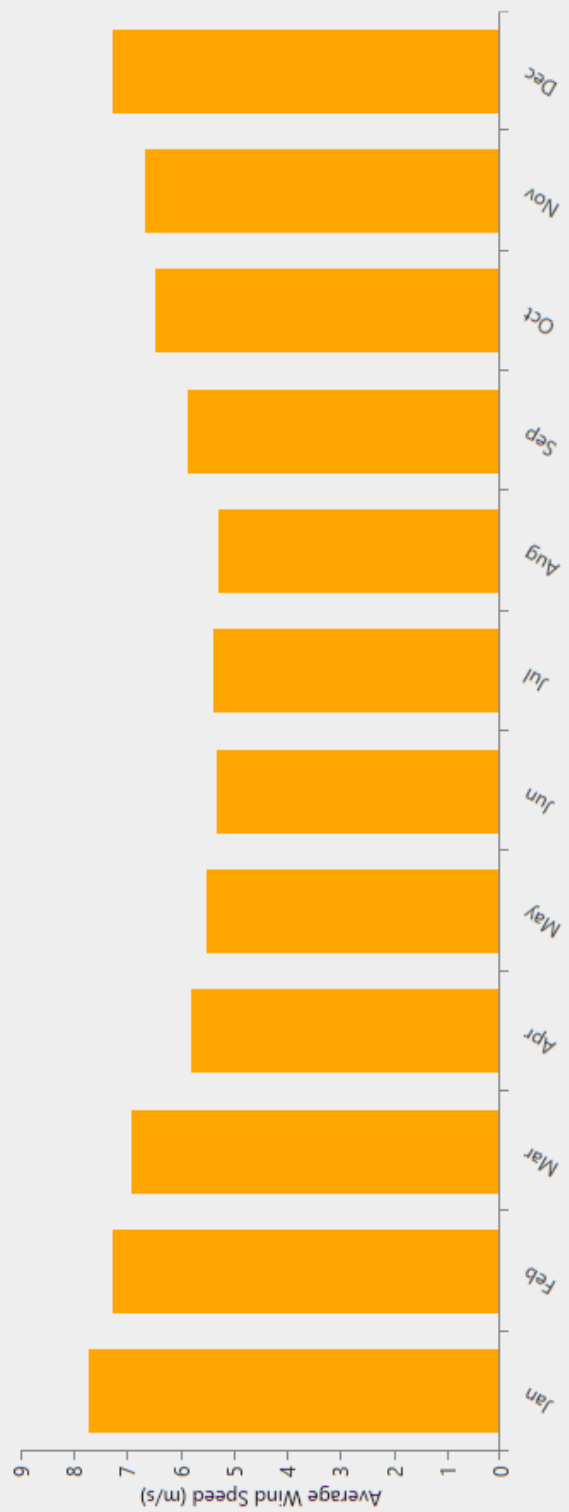

Appendix H - Datasheet Trina module

Mono Multi Solutions

THE

TALLMAX M PLUS

FRAMED 144 HALF-CELL MODULE

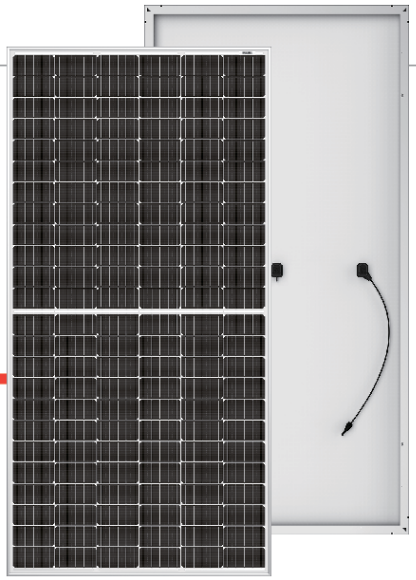

144-Cell
MONOCRYSTALLINE MODULE

345-395W
POWER OUTPUT RANGE

19.9%
MAXIMUM EFFICIENCY

0~+5W
POSITIVE POWER TOLERANCE

PRODUCTS	COLOR OF FRAME	POWER RANGE
TSM-DE14H(II)	Silver	345-395W
TSM-DE14H.08(II)	Black	345-395W

Founded in 1997, Trina Solar is the world's leading comprehensive solutions provider for solar energy. we believe close cooperation with our partners is critical to success. Trina Solar now distributes its PV products to over 60 countries all over the world. Trina is able to provide exceptional service to each customer in each market and supplement our innovative, reliable products with the backing of Trina as a strong, bankable partner. We are committed to building strategic, mutually beneficial collaboration with installers, developers, distributors and other partners.

Comprehensive Products And System Certificates

IEC61215/UL1703/IEC61730/IEC61701/IEC62716
ISO 9001: Quality Management System
ISO 14001: Environmental Management System
ISO14064: Greenhouse gases Emissions Verification
OHSAS 18001: Occupation Health and Safety Management System

Trinasolar

Increased value

- Reduce BOS cost with high power bin and 1500V system voltage
- Low thermal coefficients for greater energy production at higher temperature

Half-cell design brings higher efficiency

- New cell string layout and split J-box location to reduce the energy loss caused by inter-row shading
- Integrated LRF(Light Redirecting Film) to enhance power, specially for ground-mount applications
- Lower cell connection power losses due to half-cell layout (144 monocrystalline)

Highly reliable due to stringent quality control

- Over 30 in-house tests (UV, TC, HF etc)
- Increased module robustness to minimize micro-cracks
- PID resistant and free of snail trails
- Internal test requirement of Trina more stringent than certification authority

Certified to withstand the most challenging environmental conditions

- 2400 Pa negative load
- 5400 Pa positive load

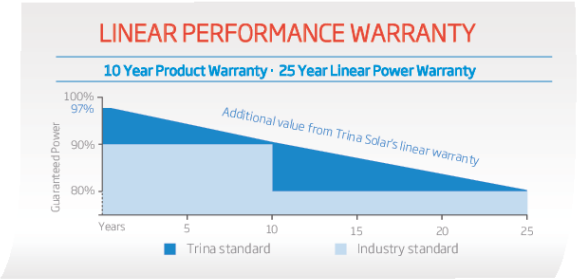

TALLMAX M PLUS

FRAMED 144 HALF-CELL MODULE

DIMENSIONS OF PV MODULE(mm)

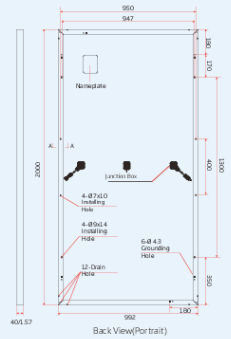

Back View(Portrait)

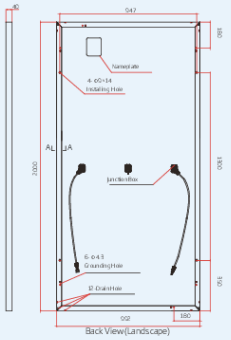

Back View(Landscape)

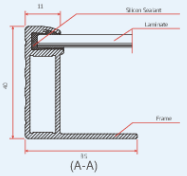

(A-A)

I-V CURVES OF PV MODULE(375W)

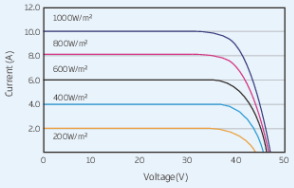

P-V CURVES OF PV MODULE(375W)

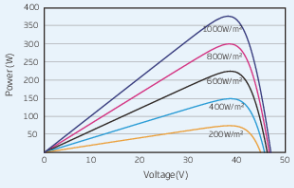

ELECTRICAL DATA (STC)

Peak Power Watts-P_{MAX} (Wp)*	345	350	355	360	365	370	375	380	385	390	395
Power Output Tolerance-P_{MAX} (W)	0 ~ +5										
Maximum Power Voltage-V_{MPP} (V)	38.2	38.4	38.6	38.8	39.0	39.2	39.4	39.6	40.1	40.5	40.8
Maximum Power Current-I_{MPP} (A)	9.04	9.13	9.21	9.28	9.37	9.44	9.52	9.60	9.61	9.64	9.69
Open Circuit Voltage-V_{OC} (V)	46.3	46.5	46.9	47.2	47.4	47.6	47.8	48.0	48.5	49.7	50.1
Short Circuit Current-I_{SC} (A)	9.55	9.60	9.68	9.73	9.83	9.88	9.93	9.99	10.03	10.08	10.13
Module E°ciency η_m (%)	17.4	17.6	17.9	18.1	18.4	18.6	18.9	19.2	19.4	19.7	19.9

STC: Irradiance 1000W/m^2, Cell Temperature 25°C, Air Mass AM1.5.
*Measuring tolerance: ±3%.

ELECTRICAL DATA (NOCT)

Maximum Power-P_{MAX} (Wp)	257	261	265	268	272	276	280	284	287	291	295
Maximum Power Voltage-V_{MPP} (V)	35.4	35.7	35.9	36.2	36.3	36.6	36.9	37.1	37.4	37.9	38.3
Maximum Power Current-I_{MPP} (A)	7.26	7.32	7.38	7.42	7.49	7.54	7.59	7.64	7.67	7.68	7.74
Open Circuit Voltage-V_{OC} (V)	43.2	43.3	43.7	44.0	44.2	44.4	44.5	44.7	45.2	46.3	46.5
Short Circuit Current-I_{SC} (A)	7.71	7.75	7.82	7.86	7.94	7.98	8.02	8.07	8.10	8.14	8.17

NOCT: Irradiance at 800W/m^2, Ambient Temperature 20°C, Wind Speed 1m/s.

MECHANICAL DATA

Solar Cells	Monocrystalline 156.75 × 78.375 mm (6.17× 3.09 inches)
Cell Orientation	144 cells (6 × 24)
Module Dimensions	2000 × 992 × 40 mm (78.74 × 39.06 × 1.57 inches)
Weight	23 kg (50.7 lb)
Glass	3.2 mm (0.13 inches), High Transmission, AR Coated Heat Strengthened Glass
Encapsulant Material	EVA(White/Transparent)
Backsheet	White
Frame	40 mm (1.57 inches) Anodized Aluminium Alloy
J-Box	IP 68 rated
Cables	Photovoltaic Technology Cable 4.0mm² (0.006 inches²), Portrait: N 140mm/P 285mm (5.51/11.22 inches) Landscape: N 1400 mm /P 1400 mm (55.12/55.12 inches)
Connector	TS4

TEMPERATURE RATINGS

NOCT(Nominal Operating Cell Temperature)	44°C (±2°C)
Temperature Coefficient of P_{MAX}	-0.37%/°C
Temperature Coefficient of V_{OC}	-0.29%/°C
Temperature Coefficient of I_{SC}	0.05%/°C

MAXIMUM RATINGS

Operational Temperature	-40~+85°C
Maximum System Voltage	1500V DC (IEC)
	1500V DC (UL)
Max Series Fuse Rating	20A

(DO NOT connect Fuse in Combiner Box with two or more strings in parallel connection)

WARRANTY

10 year Product Workmanship Warranty
25 year Linear Power Warranty

(Please refer to product warranty for details)

PACKAGING CONFIGURATION

Modules per box: 27 pieces
Modules per 40' container: 594 pieces

Trinasolar

CAUTION: READ SAFETY AND INSTALLATION INSTRUCTIONS BEFORE USING THE PRODUCT.

Version number: TSM_DE14H(II)_EN_2019_B

www.trinasolar.com

Appendix I - Datasheet Astronergy module

Warranty

12 12-year Product Warranty

30 30-year Linear Power Warranty

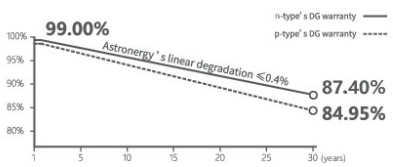

Key Features

- TOPCon / Half-cut
- Low temperature coefficient (Pmpp)
- Non-destructive cutting
- PID resistance
- Low BOS cost & LCOE
- Bifacial gain

ISO 9001:2015:ISO Quality Management System
ISO 14001:2015:ISO Environment Management System
ISO 45001:Occupational Health and Safety
The first solar company which passed the Nord IEC/TS 62941 certification audit

2022 TOP Performance PVEL Tier 1 BloombergNEF Underwritten by International Insurer

605~625W	0~+5W	22.4%	≤ 1.0%	≤ 0.4%
POWER RANGE	POWER SORTING	MAX. MODULE EFFICIENCY	FIRST YEAR POWER DEGRADATION	YEAR 2-30 POWER DEGRADATION

Mechanical Specifications

Outer dimensions (L x W x H)	2465 x 1134 x 30 mm
Cell type	n-type mono-crystalline
No. of cells	156 (6*26)
Frame technology	Aluminum, silver anodized
Front / Back glass	2.0+2.0 mm
Cable length (Including connector)	Portrait: (+)350 mm,(-)250 mm; Customized length
Cable diameter (IEC/UL)	4 mm^2 / 12 AWG
① Maximum mechanical test load	5400 Pa (front) / 2400 Pa (back)
Connector type (IEC/UL)	HCB40 (Standard) / MC4-EVO2A (Optional)
Module weight	34.7 kg
Packing unit	36 pcs / box (Subject to sales contract)
Weight of packing unit (for 40'HQ container)	1304 kg
Modules per 40' HQ container	576 pcs

① Refer to Astronergy crystalline installation manual or contact technical department.
Maximum Mechanical Test Load=1.5× Maximum Mechanical Design Load.

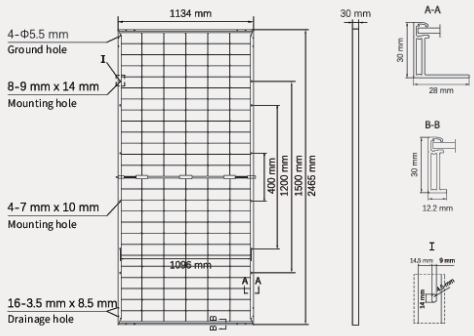

Electrical Specifications

STC: Irradiance 1000W/m^2, Cell Temperature 25° C, AM=1.5

Rated output (Pmpp / Wp)	605	610	615	620	625
Rated voltage (Vmpp / V)	45.63	45.79	45.96	46.12	46.29
Rated current (Impp /A)	13.26	13.32	13.38	13.44	13.50
Open circuit voltage (Voc / V)	55.21	55.41	55.61	55.81	56.01
Short circuit current (Isc /A)	13.78	13.87	13.95	14.03	14.11
Module efficiency	21.6%	21.8%	22.0%	22.2%	22.4%

NMOT: Irradiance 800W/m^2, Ambient Temperature 20° C, AM=1.5, Wind Speed 1m/s

Rated output (Pmpp / Wp)	455.0	458.7	462.5	466.2	470.0
Rated voltage (Vmpp / V)	42.95	43.10	43.26	43.41	43.57
Rated current (Impp /A)	10.59	10.64	10.69	10.74	10.79
Open circuit voltage (Voc / V)	52.44	52.63	52.82	53.01	53.20
Short circuit current (Isc /A)	11.13	11.19	11.26	11.32	11.39

Electrical Specifications (Integrated power)

Pmpp gain	Pmpp / Wp	Vmpp / V	Impp /A	Voc / V	Isc /A
5%	646	45.96	14.05	55.61	14.64
10%	677	45.96	14.72	55.61	15.34
15%	707	45.97	15.39	55.62	16.03
20%	738	45.97	16.05	55.62	16.73
25%	769	45.97	16.72	55.62	17.43

Electrical characteristics with different rear power gain (reference to 615W)

Curve

Current-Voltage (615W)

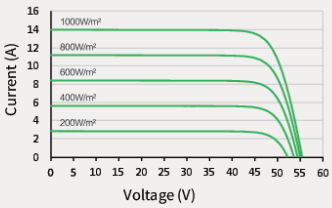

Power-Voltage (615W)

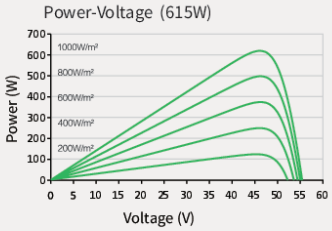

Current-Voltage (615W)

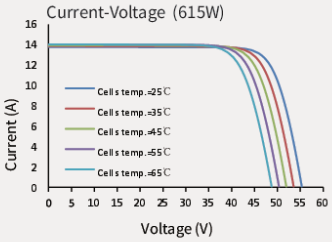

Temperature Ratings (STC)

Temperature coefficient (Pmpp)	-0.29%/°C
Temperature coefficient (Isc)	+0.043%/°C
Temperature coefficient (Voc)	-0.25%/°C
Nominal module operating temperature (NMOT)	41±2°C

Operating Parameters

No. of diodes	3
Junction box IP rating	IP 68
Max. series fuse rating	30 A
Max. system voltage (IEC/UL)	1500V_{DC}

https://www.astro-energy.com

202304

Appendix J - Datasheet SG110CX inverter

SG110CX

Multi-MPPT String Inverter for 1000 Vdc System

HIGH YIELD

- 9 MPPTs with max. efficiency 98.7%
- Compatible with bifacial module
- Built-in PID recovery function

SMART O&M

- Touch free commissioning and remote firmware upgrade
- Smart IV Curve Diagnosis *
- Fuse free design with smart string current monitoring

SAVED INVESTMENT

- Compatible with Al and Cu AC cables
- DC 2 in 1 connection enabled
- Q at night function

PROVEN SAFETY

- IP66 and C5 protection
- Type II SPD for both DC and AC
- Compliant with global safety and grid code

CIRCUIT DIAGRAM

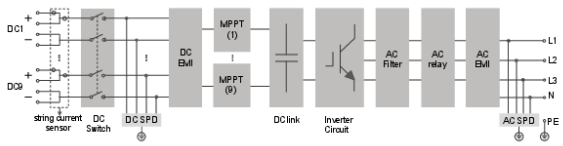

EFFICIENCY CURVE

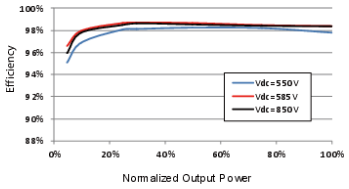

SUNGROW
Clean power for all

Type designation	SG110CX
Input (DC)	
Max. PV input voltage	1100 V **
Min. PV input voltage / Start-up input voltage	200 V / 250 V
Nominal PV input voltage	585 V
MPP voltage range	200 – 1000 V
No. of independent MPP inputs	9
No. of PV strings per MPPT	2
Max. PV input current	26 A * 9
Max. DC short-circuit current	40 A * 9
Output (AC)	
AC output power	110 kVA @ 45 °C / 100 kVA @ 50 °C
Max. AC output current	158.8 A
Nominal AC voltage	3 / N / PE, 400 V
AC voltage range	320 – 460V
Nominal grid frequency / Grid frequency range	50 Hz / 45 – 55 Hz, 60 Hz / 55 – 65 Hz
Harmonic (THD)	< 3 % (at nominal power)
Power factor at nominal power / Adjustable power factor	> 0.99 / 0.8 leading – 0.8 lagging
Feed-in phases / AC connection	3 / 3-PE
Efficiency	
Max. efficiency	98.7 %
European efficiency	98.5 %
Protection and Function	
DC reverse polarity protection	Yes
AC short-circuit protection	Yes
Leakage current protection	Yes
Grid monitoring	Yes
Ground fault monitoring	Yes
DC switch	Yes
AC switch	No
PV string monitoring	Yes
Q at night function	Yes
PID recovery function	Yes
Arc fault circuit interrupter (AFCI)	Optional
Surge protection	DC Type II (optional: Type I + II) / AC Type II
General Data	
Dimensions (W*H*D)	1051*660*362.5 mm
Weight	89 kg
Topology	Transformerless
Degree of protection	IP66
Night power consumption	< 2 W
Operating ambient temperature range	-30 to 60 °C (> 50 °C derating)
Allowable relative humidity range	0 – 100 %
Cooling method	Smart forced air cooling
Max. operating altitude	4000 m (> 3000 m derating)
Display	LED, Bluetooth+APP
Communication	RS485 / Optional: WLAN, Ethernet
DC connection type	MC4 (Max. 6 mm²)
AC connection type	OT / DT terminal (Max. 240 mm²)
Compliance	IEC 62109, IEC 61727, IEC 62116, IEC 60068, IEC 61683, VDE-AR-N 4110:2018, VDE-AR-N 4120:2018, IEC 61000-6-3, EN 50549, AS/NZS 4777.2:2015, CEI 0-21, VDE 0126-1-1/A1 VFR 2014, UTE C15-712-1:2013, DEWA
Grid Support	Q at night function, LVRT, HVRT,active & reactive power control and power ramp rate control

*: Only compatible with Sungrow Logger, EyeM4 and iSolarCloud
**: The inverter enters the standby state when the input voltage ranges between 1,000V and 1,100V. If the maximum DC voltage in the system can exceed 1000V, the MC4 connectors included in the scope of delivery must not be used. In this case MC4 Evo2 connectors must be used.

Appendix K - Datasheet SG350HX inverter

SG350HX

Multi-MPPT String Inverter for 1500 Vdc System

HIGH YIELD

- Up to 16 MPPTs with max. efficiency 99%
- 20A per string, compatible with 500Wp+ module
- Data exchange with tracker system, improving yield

LOW COST

- Q at night function, save investment
- Power line communication (PLC)
- Smart IV Curve diagnosis*,active O&M

GRID SUPPORT

- SCR≥1.15 stable operation in extremely weak grid
- Reactive power response time <30ms
- Compliant with global grid code

PROVEN SAFETY

- 2 strings per MPPT, no fear of string reverse connection
- 24h real-time AC and DC insulation monitoring

CIRCUIT DIAGRAM

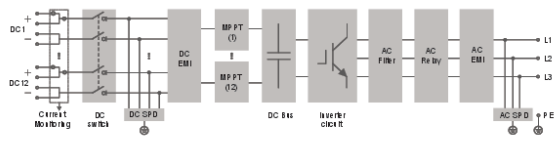

EFFICIENCY CURVE

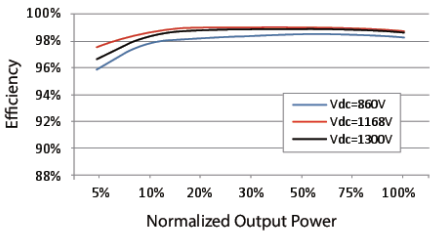

SUNGROW
Clean power for all

Type designation	SG350HX
Input (DC)	
Max. PV input voltage	1500 V
Min. PV input voltage / Startup input voltage	500 V / 550 V
Nominal PV input voltage	1080 V
MPP voltage range	500 V – 1500 V
No. of independent MPP inputs	12 (Optional: 14 / 16)
Max. number of input connector per MPPT	2
Max. PV input current	12 * 40 A (Optional: 14 * 30 A / 16 * 30 A)
Max. DC short-circuit current per MPPT	60 A
Output (AC)	
AC output power	352 kVA @ 30°C / 320 kVA @ 40 °C / 295 kVA @ 50°C
Max. AC output current	254 A
Nominal AC voltage	3 / PE, 800 V
AC voltage range	640 – 920 V
Nominal grid frequency / Grid frequency range	50 Hz / 45 – 55 Hz, 60 Hz / 55 – 65 Hz
THD	< 3 % (at nominal power)
DC current injection	< 0.5 % In
Power factor at nominal power / Adjustable power factor	> 0.99 / 0.8 leading – 0.8 lagging
Feed-in phases / Connection phases	3 / 3
Efficiency	
Max. efficiency / European efficiency	99.02 % / 98.8 %
Protection	
DC reverse connection protection	Yes
AC short circuit protection	Yes
Leakage current protection	Yes
Grid monitoring	Yes
Ground fault monitoring	Yes
DC switch / AC switch	Yes / No
PV string current monitoring	Yes
Q at night function	Yes
Anti-PID and PID recovery function	Optional
Surge protection	DC Type II / AC Type II
General Data	
Dimensions (W*H*D)	1136 * 870 * 361 mm
Weight *	≤ 116 kg
Isolation method	Transformerless
Degree of protection	IP66
Power consumption at night	< 6 W
Operating ambient temperature range	-30 to 60°C
Allowable relative humidity range	0 – 100 %
Cooling method	Smart forced air cooling
Max. operating altitude	4000 m (> 3000 m derating)
Display	LED, Bluetooth+APP
Communication	RS485 / PLC
DC connection type	MC4-Evo2 (Max. 6 mm², optional 10mm²)
AC connection type	Support OT/DT terminal (Max. 400 mm²)
Compliance	IEC 62109, IEC 61727, IEC 62116, IEC 60068, IEC 61683, VDE-AR-N 4110:2018, VDE-AR-N 4120:2018, EN 50549-1/2, UNE 206007-1:2013, P.O.12.3, UTE C15-712-1:2013
Grid Support	Q at night function, LVRT, HVRT, active & reactive power control and power ramp rate control, Q-U control, P-f control

* Due to the multi-supplier for some key components, the actual weight may have a ±10% deviation, please refer to the actually delivered product.

Appendix L - Datasheet McPhy AWE electrolyzer

McPhy

Driving clean energy forward

MCLYZER PRODUCT LINE

Pressurized alkaline electrolysis

30 bar

200 to 3200 Nm^3/h

1 to 16 MW

mcphy.com

MCLYZER PRODUCT LINE

Specifications[1]

	McLyzer 200	McLyzer 400	McLyzer 800	McLyzer 3200
Power class	1 MW	2 MW	4 MW	16 MW
Electrolyzer type	Pressurized alkaline			
Number of stacks	1	4	4	16
System design lifetime (mechanical)	> 20 years			
H_2 OUTPUT				
H² nominal flow rate	200 Nm³/h	400 Nm³/h	800 Nm³/h	3200 Nm³/h
H² purity	> 99.998 % after gas cleaning			
H² delivery pressure	27 to 30 bar (g), depending on configuration			
PERFORMANCES				
Stack DC consumption, BoL	4,65 kWh/Nm³	4,65 kWh/Nm³	4,65 kWh/Nm³	4,65 kWh/Nm³
System AC consumption, BoL	5,1 kWh/Nm³	5,0 kWh/Nm³	5,0 kWh/Nm³	5,0 kWh/Nm³
Operation range	20 - 100 %	20 - 100 %	20 - 100 %	10 - 100 %
Reaction time	< 30s from hot stand-by to 100 % electrical load			
Ramp-up | Ramp-down[2]	>5 %/s | 20 %/s			
DIMENSIONS (L x W x H) & WEIGHTS[3]				
Stack (per unit)	2.7 x 1.5 x 1.7 m / 9.5 tons			
Stacks & process unit	9.0 x 3.0 x 3.5 m	9.1 x 6.2 x 3.5 m	8.9 x 6.4 x 5.8 m	26 x 25 x 8 m
Electrical unit	6.1 x 2.4 x 2.9 m	6.1 x 3.0 x 2.9 m	9.2 x 2.4 x 2.9 m	26 x 14 x 6 m
Auxiliaries unit	6.1 x 3.0 x 3.0 m	6.1 x 3.0 x 3.0 m	12.0 x 3.0 x 3.0 m	Project specific
INSTALLATION AREA REQUIREMENTS				
Installation area requirements	All equipments delivered in containers	Stacks & process units in building		Stacks in building, process unit outdoor
Ambient temperature	-20°C | +35°C	+5°C | +40°C		
UTILITIES				
Demineralized water	ca 1 l/Nm³ H_2			
Electrolyte	30 % KOH aqueous solution			

1 All figures above are "expected values", may vary depending on operating conditions and can be revised by McPhy according to technological evolution.

2 At system level within nominal operational load range, in % of electrical full load per second.

3 Process unit includes, separators, pumps heat exchangers and purification (all products) and drying unit (all except for McLyzer 800/3200). Electrical unit includes transformers and rectifiers. Auxiliaries unit includes water demineralization, instrument air, control unit. Cooling auxiliaries not included.

McPhy

contact@mcphy.com

June 2023 | supermood-design.fr

Appendix M - Datasheet Enapter AEM Nexus electrolyzer

Enapter

AEM Nexus 1000

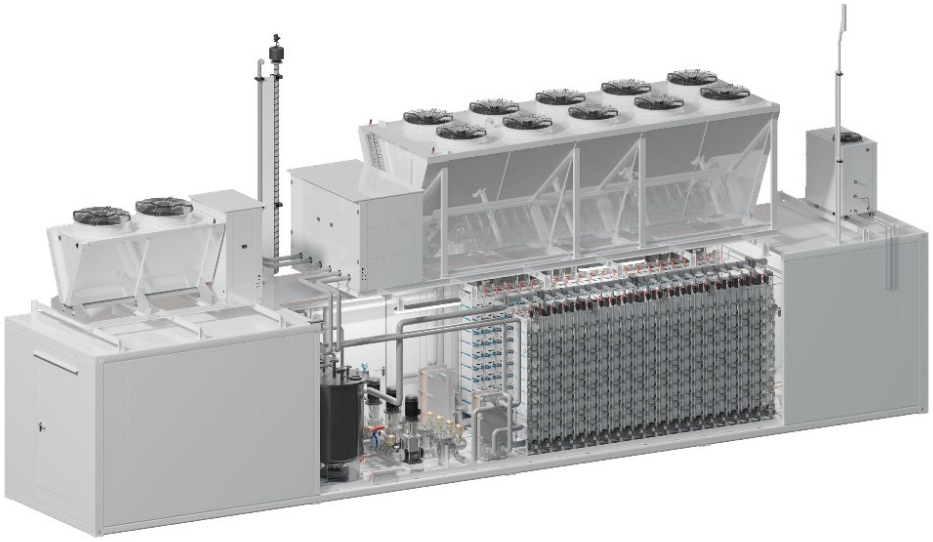

Key features

- H_2 Output: 210 Nm^3/h, up to 35 barg, 99.95% purity (99.999% with optional dryer)
- Cost-efficiency
- High degree of redundancy
- Rapid reaction times to variable renewables

The AEM Nexus 1000 is the first AEM Electrolyser of the megawatt class. A ≈ 1 MW containerised electrolyser largely pre-assembled for fast commissioning featuring 420 AEM stack modules around a common balance of plant (BoP).

AEM Nexus 1000

www.enapter.com/aem-nexus

AEMNexus1000-DTS-COM02_rev04

Specifications

Enapter

AEM Nexus 1000

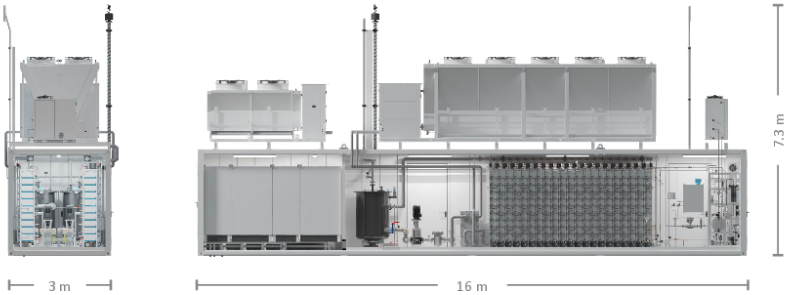

H_2 nominal flow	210 Nm^3/h 453 kg/24h	Net volume flow rate
H_2 outlet pressure	Up to 35 barg	
H_2 purity	99.95% in molar fraction, equals dew point of -30 °C	Impurities: H_2O < 500 ppm, O_2 < 5 ppm
H_2 purity with optional dryer	99.999% in molar fraction, equals dew point of -65 °C	Impurities: H_2O < 5 ppm, O_2 < 5 ppm ≈ 5 kW consumption during regeneration
H_2 outlet temperature	5 – 55 °C	
O_2 nominal flow	105 Nm^3/h	Vented at atmospheric pressure
Nominal power consumption	1,008 kW 1,200 kW	Beginning of life (BOL) Near end of life (EOL)
Voltage	3 × 400 VAC	±10 %
Frequency	50/60 Hz	± 10 %; THD < 5 %
H_2O nominal consumption	190 L/h	Purified water
H_2O inlet quality	Minimum ASTM D1193-06 Type IV or recommended Type II or Type III[1]	
H_2O inlet temperature	5 – 55 °C	1 – 4 barg
Operational flexibility	3% – 100%	Of nominal H2 flow rate
Turndown ratio	33:1	Maximum flow/Minimum flow
Specific power consumption (Efficiency)	4.8 kWh/Nm^3H_2 53.3 kWh/kgH_2 62.5% (LHV)	Including all utilities inside the battery limits of the AEM Nexus 1000 (at BOL)
Hot startup time	0 – 100% in 100 seconds	Electrolyte is at min. 35 °C
Cold startup time	0 – 100% in 30 minutes	Assuming 5 °C ambient temperature
Shut down time	100 – 0 % in 3 minutes	Normal, gradual shut down
Hot standby power consumption	160 kW Max.	Stacks are hydrated and electrolyte circulates at min. temperature (35 °C)
Cold standby power consumption	20 kW Max.	All components in standby; container heating is on (only with < 5 °C ambient)
Ambient operating temperature	-15 – 35 °C	Up to 45 °C with hot-ambient version
Sound Pressure Level	62 db(A) Max.	At 10 m (Including all utilities)
Process heat output	300 kW	BOL; ≈ 50 °C
Dimensions	16 × 3 × 7.3 m	(L × W × H)
Weight	≈ 40 tons	

[1] Please, check the Battery limits and the Owner's Manual for the complete requirements list.

Note: The product is under continuous improvement and the technical specifications might be subject to change. Please make sure to refer to our website for the most recent specifications.

Enapter

AEMNexus1000-DTS-COM02_rev04

Appendix N - Datasheet H-TEC PEM electrolyzer

Hydrogen is now.
H-TEC SYSTEMS

LARGE
SCALE.
MAX
OUTPUT.

H-TEC SYSTEMS
Hochleistungs-
Elektrolyseure

H-TEC SYSTEMS
PEM-Elektrolyseur
Modular Hydrogen Platform (MHP)

DE

PEM-Elektrolyseure für ein nachhaltiges Energiesystem – **H-TEC SYSTEMS Modular Hydrogen Platform (MHP)**

Modular, skid-mounted, ready-to-install: Die H-TEC SYSTEMS Modular Hydrogen Platform (MHP) ist ein skalierbares Baukastensystem zur industriellen Produktion von grünem Wasserstoff mittels der PEM-Technologie. Dazu lassen sich 10 MW Blöcke zu Multi-MW Systemen mit einer Elektrolyseleistung von 10 bis mehr als 100 MW kombinieren. Das System ist für die einfache Installation im Innenbereich auf vormontierten Skids optimiert. Jeder 10 MW Block ist mit integrierter Prozesswasseraufbereitung und elektrischer Leistungsversorgung ausgestattet. Zusätzlich kann das System nach Bedarf um eine Frischwasser- und Wasserstoffaufbereitung sowie eine Prozesswärmerückgewinnung oder Sauerstoffnutzung ergänzt werden. Der H-TEC SYSTEMS MHP Elektrolyseur überzeugt durch seinen herausragenden Systemwirkungsgrad, hohe Verfügbarkeit und ein erprobtes Wartungskonzept. Dies äußert sich in besonders geringen Wasserstoffgestehungskosten und einem stabilen, sicheren Betrieb.

10 MW Block

H_2 Produktion nominal	4600 kg / d | 2130 Nm^3 / h
Energieverbrauch [1]	4,6 kWh/Nm^3 H_2 | 51 kWh/kg
Systemwirkungsgrad [1]	77 %
Leistungsklasse	10 MW
Modulationsbereich H_2 Produktion	213 – 2130 Nm^3/h | 10 – 100 %
H_2 Reinheit inklusive optionaler Wasserstoffaufbereitung	3.0 oder 5.0 (erfüllt ISO 14687:2019 Tabelle 2)
H_2 Reinheit ohne optionaler Wasserstoffaufbereitung	Wassergesättigt bei 65 °C und 30 bar (g)
H_2 Übergabedruck	30 bar (g)
Lastwechsel	30 s (Minimallast bis Nominallast)
Benötigte Wasserqualität mit optionaler Wasseraufbereitung	TrinkwV 2020 | EU Richtlinie 2020/2184-EU
Benötigte Wasserqualität ohne optionaler Wasseraufbereitung	VE-Wasser (vollentsalzt)
VE-Wasserverbrauch nominal	1850 kg/h
Abmessungen L x B x H (indoor)	ca. 10 x 24 x 4,5 m
Temperatur (indoor)	+5 °C bis +40 °C

Technische Änderungen vorbehalten
[1] Batterielimit für die Effizienz: Stacks und Converter; Standardbedingungen: BoL (Begin of Life), 15 °C, 30 bar (g) H_2 Übergabedruck, 2000 Nm^3/h, bezogen auf Higher Heating Value (HHV).

Wir sind der Treibstoff der globalen Energiewende

Als technologischer Vorreiter gestalten wir die Wasserstofftechnologie seit über 25 Jahren entscheidend mit. Wir glauben, dass Mobilität, Produktion und Konsum emissionsfrei möglich sind – und alternativlos. Dazu baut H-TEC SYSTEMS auf Kooperationen mit visionären Kunden und Partnern sowie die Power unseres Mutterkonzerns MAN Energy Solutions. Gemeinsam machen wir die Wasserstofferzeugung grün und die CO_2-neutrale Transformation aller Sektoren real.

Mehr unter **h-tec.com**

Revision 1.0

Appendix O - Datasheet Sunfire AWE electrolyzer

sunfire®

RENEWABLES
EVERYWHERE

SUNFIRE.DE

RENEWABLE HYDROGEN FOR ALL APPLICATIONS

SUNFIRE-HYLINK ALKALINE

PRODUCT

Sunfire-HyLink Alkaline is our established, large-scale electrolysis solution. With several decades of proven system runtime and pressurized hydrogen output, our electrolyzer is the cost effective, reliable and ready-to-use solution for any hydrogen project.

APPLICATIONS

Our electrolyzer provides renewable hydrogen as an essential element for decarbonizing industries, mobility and energy.

+ Steel: Direct reduction of iron, blast furnace injection, protective atmosphere, etc.
+ Refineries: Desulphurization, hydrocracking, hydrogenation, etc.
+ Chemicals: Ammonia production, hydrogenation, isotope separation, etc.
+ Mobility: Fuel cell vehicles for road and rail
+ Energy: Industry and space heat, power balancing, etc.

CORE ADVANTAGES

+ **Robustness**
  Proven technology with demonstrated system runtime of more than 30 years
+ **CAPEX**
  Lowest electrolyzer costs reduce capital requirements
+ **Pressure**
  Renewable hydrogen is delivered at a pressure of up to 30 bar (g)
+ **Scalability**
  10 MW modular design enables effective scaling to large electrolysis capacities
+ **Adaptability**
  Easy integration into any environment – whether industrial or greenfield

sunfire®

SUNFIRE-HYLINK ALKALINE 10 MW – TECHNICAL DATA

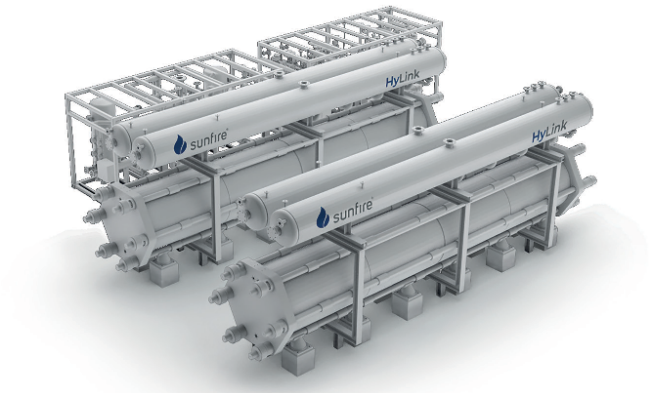

	HYLINK ALKALINE 10 MW
Hydrogen production	
Net production rate	2,174 Nm^3/h
	195 kg/h
Production capacity dynamic range	25 % … 100 %
Delivery pressure	30 bar (g) without additional compression
Hydrogen purity*	99.8 % before gas cleaning
Electrical efficiency	
Specific energy consumption at stack level (DC)	4.18…4.54 kWh/Nm^3
Specific energy consumption at module level (AC)	4.29…4.67 kWh/Nm^3
Feedstock	
Demineralized water consumption	1.85 m^3/h
Electrolyte	26 % KOH aqueous solution
Other specs	
Proven system runtime	> 30 years
Stack lifetime**	90,000 equivalent operating hours
Footprint***	~ 375 m^2
Ambient temperature	5 °C … 40 °C

* Up to 99.998 % after gas cleaning
** Equivalent operating hours are calculated based on the operation profile of the electrolyzer (including e.g. start-stops)
*** Average space requirement for a 10 MW module comprising stacks, balance of stack, module control cabinet, and power supply unit

Sunfire GmbH · Gasanstaltstraße 2 · 01237 Dresden · Germany · +49 351 896797-0 · info@sunfire.de · sunfire.de

Our standardized high performance product and its key features

Output from a 20 MW_{el} module	
Hydrogen production rate	4,000 Nm^3/h^*
Hydrogen pressure at AWE module	0.300 barg
Hydrogen purity, saturated with H_2O at 40 °C	99.9 % (v/v)
Oxygen production rate	2,000 Nm^3/h^*
Oxygen pressure at AWE module	0.200 barg
Oxygen purity, saturated with H_2O at 40 °C	99.5 % (v/v)

Operability	
The turn down ratio of the electrolysis modules	10 %
The turn up ratio of the electrolysis modules	100 %
Ramp-speed (up and down, hot system)	Suitable to renewable energy sources
Start-up times: Cold to 100 % load	40 – 60 min.
Availability	up to 98 %

Power consumption at start of life (DC)	
Electrolyzer, at max. capacity	4.5 kWh/Nm^3 (DC)

50,1 kWh/kg
78,7% efficiency (HHV)

360 kg/h max. 8,6 t/day

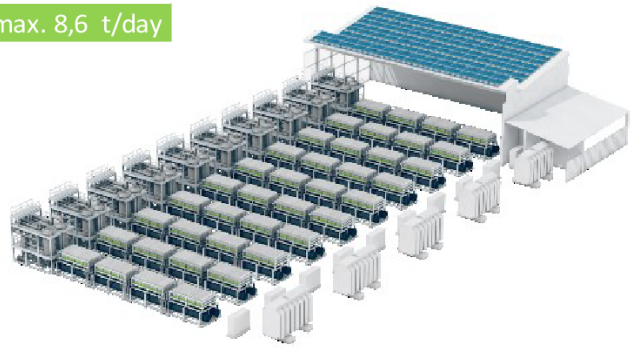

Power consumption at start of life (AC)

System at nominal capacity:

- incl. transformation / rectifying
- incl. hydrogen compression to 30 bar_g
- incl. all other electrical consumers within battery limits (purification of 99,999 %)

4.9 kWh/Nm^3 (AC)

* Nm^3 is defined as 1 m^3 of gas (100%) at 273.15 K and 1.013 bar

thyssenkrupp nucera

Appendix Q - Datasheet Battery energy storage SUNGROW

ST2236UX

Liquid Cooling Energy Storage System

LOW COSTS

- Highly integrated ESS for easy transportation and O&M
- All pre-assembled, no battery module handling on site
- 8 hour installation to commission, drop on a pad and make electrical connections

SAFE AND RELIABLE

- DC electric circuit safety management includes fast breaking and anti-arc protection
- Multi level battery protection layers formed by discreet standalone systems offer impeccable safety

EFFICIENT AND FLEXIBLE

- Intelligent liquid cooling ensures higher efficiency and longer battery cycle life
- Modular design supports parallel connection and easy system expansion
- IP54 outdoor cablinet and optional C5 anti-corrosion

SMART AND ROBUST

- Fast state monitoring and faults record enables pre-alarm and faults location
- Integrated battery performance monitoring and logging

SUNGROW
Clean power for all

Type designation	ST2236UX
Battery Data	
Cell type	LFP
Battery capacity (BOL)	2236 kWh
Battery voltage range	1123 ~ 1500 V
General Data	
Dimensions of battery unit (W * H * D)	9340*2600*1730 mm
Weight of battery unit	24,000 kg
Degree of protection	IP 54
Operating temperature range	-30 to 50 °C (> 45 °C derating)
Relative humidity	0 ~ 95 % (non-condensing)
Max. working altitude	3000 m
Cooling concept of battery chamber	Liquid cooling
Fire safety standard / Optional	Fused sprinkler heads, NFPA 69 explosion prevention and ventillation IDLH gases
Communication interfaces	RS485, Ethernet
Communication protocols	Modbus RTU, Modbus TCP
Compliance	CE, IEC 62477-1, IEC 61000-6-2, IEC 61000-6-4, IEC 62619
1 HOURS APPLICATION-ST2236UX*2-4000UD-MV	
BOL kWh (DC)	4,472 kWh
ST2236UX Quantity	2
PCS Model	SC4000UD-MV
Grid Connection Data	
Max.THD of current	< 3 % (at nominal power)
DC component	< 0.5 % (at nominal power)
Power factor	> 0.99 (at nominal power)
Adjustable power factor	1.0 leading ~ 1.0 lagging
Nominal grid frequency	50 / 60 Hz
Grid frequency range	45 ~ 55 Hz / 55 ~ 65 Hz
Transformer	
Transformer rated power	4,000 kVA
LV / MV voltage	0.8 kV / 33 kV
Transformer cooling type	ONAN (Oil Natural Air Natural)
Oil type	Mineral oil (PCB free) or degradable oil on request

Appendix R - Datasheet Battery energy storage TRICERA

20FT 3.6 MWH UNIT

TRICERA energy

BATTERY ENERGY STORAGE SYSTEM

Based on the innovative FlexRACK
with Automotive Battery Moduls

UP TO 3.6 MWH PER 20FT HC UNIT

FLEXIBLE PROJECT CONFIGURATION

READY FOR AC- AND DC-COUPLING

The **TRICERA 20ft HC storage unit** is a compact 1500 V design, efficiently housing batteries, a battery control and energy management system, HVAC system, and extensive safety features, suited for all environmental conditions.
The batteries can be configured for up to **3.6 MWh** for use in various applications. Several different battery topologies are available depending on power requirements for **up to 2 C**.

TRICERA offers a robust, modular solution based on proven industrial technology that minimizes installation and maintenance time, extends system life and increases safety.

FEATURES

- **Individually customizable** and scalable in capacity; performance and HVAC system according to customer and project requirements.
- Cost effective and flexible battery rack construction **FlexRACK** to incorporate various types of automotive battery modules.
- **AC- and DC-Coupling in hybrid systems** possible e.g. solar PV, wind, EV Charging.
- Includes TRICERAs **in-house developed software** BCC and EMS.
- **On- / Off Grid** ready
- **Battery Cluster Controller (BCC)**
  - Monitoring and control of batteries and HVAC system
  - System BMS integrated in BCC
  - Monitoring of safety functions and alarming when limit values are exceeded
  - Communication to Inverter
- **Energy Management System (EMS)**
  - Available for several services
  - Interface to marketer
  - Interface communication via Modbus TCP / IP

*Pictured enclosure with optional hot climate equipment

www.tricera.energy

20FT 3.6 MWH UNIT

TRICERA energy

TECHNICAL SPECIFICATIONS

Electrical Parameters	Battery Chemistry[1]	NMC, LFP
	DC Voltage[1]	Up to 1,500 V_{DC}
	Nominal DC Energy Capacity[1]	Up to 3.6 MWh
	C-Rate[1]	Up to 2 C
	Aux Load Energy per Enclosure[2]	25 kW_{peak}
System Parameters	Cooling Power[2]	10 to 45 kW_{th}
	Heating and Cooling[2]	HVAC, Air
	Operating Temperature[2]	-20 to +50 °C ambient temp.
	Altitude	1,000 m
Housing	Container	20ft High Cube Open Side
	Corrossion class[2]	Up to C5
	Dimensions	2,896 x 2,438 x 6,058 mm (HxWxL)
	Weight	Up to 31,000 kg
	Other	Static tested, CSC optionally
Fire detection and Suppression	• Smoke Detection, Temperature Sensors, BCC Monitoring and Detection **Optional:** • Sprinkler system as dry riser with external C-coupling and fine spray nozzles • Gas extinguishing system NOVEC 1230	
Software	EMS Key Functions	Frequency Regulation, Ancillary Service, Renewable Integration, Energy Arbitrage, Demand Management, Load Leveling, Peak Shaving, Micro Grid System, Black Start Capability Integration, Grid Stability, Commercial Application
	Communication Interface	via Modbus TCP / IP
Norms	EN 60364, EN 60664, EN 61439-1, ISO 13849, EN 60664, EN 61000-6-2, EN 61000-6-4, IEC 62660, UN 38.3 (Modul/Tray)	

[1] Depending on available battery type
[2] Depending on project location and use case

www.tricera.energy

V1.03/05.23

Energy Storage Station of the Luneng Haixi Complementary Multi-energy Demonstration Project (50MW/100MWh)

Energy Storage Solutions

Since energy storage is a key part of energy transition and power transformation, CATL has always been committed to providing first-class energy storage solutions to the world. CATL has developed a safe, efficient, and economical electrochemical energy storage system that is widely adaptive to the fields of power generation, power transmission and distribution, and power consumption, helping to optimize the energy structure, enhance the safety of the power system, and reduce the cost of energy use.

CATL Cell Solutions

Cell 280Ah

Basic Parameters		
Capacity [Ah]	280	
Charge/discharge rate [P]	0.5	
Cycle life [25℃, @80%SOH, 70%SOH]	6,000	8,000
Dimensions [L*W*H] [mm]	173.9*71.7*207.2	

Testing and certification

IEC 62619 · UL 1973 · UL 9540A · UN 38.3

Cell 280Ah

Basic Parameters		
Capacity [Ah]	280	
Charge/discharge rate [P]	1	
Cycle life [25℃, @80%SOH, 70%SOH]	5,000	7,000
Dimensions [L*W*H] [mm]	173.9*71.7*207.2	

Testing and certification

IEC 62619 · IEC 62133 · UL1642 · UN 38.3

Cell 306Ah

Basic Parameters		
Capacity [Ah]	306	
Charge/discharge rate [P]	0.5	
Cycle life [25℃, @80%SOH, 70%SOH]	8,000	10,000
Dimensions [L*W*H] [mm]	173.9*71.7*207.2	

Testing and certification

IEC 62619 · UL 1973 · UL 9540A · UN 38.3

Cell 285Ah

Basic Parameters		
Capacity [Ah]	285	
Charge/discharge rate [P]	1	
Cycle life [25℃, @80%SOH, 70%SOH]	7,000	9,000
Dimensions [L*W*H] [mm]	173.9*71.7*207.2	

Testing and certification

IEC 62619 · IEC 62133 · UL1642 · UN 38.3

Liquid Cooling Solution

EnerC
Containerized Liquid Cooling Battery System

High level of safety
- LFP batteries with high thermal stability
- Protection level of IP55 to meet the requirements of outdoor applications
- Resistance up to C5 corrosion level, with 20-year reliability
- Prevention-oriented fire protection strategy, with a separate fire protection system

Long service life
- Available for integration with CATL's advanced technologies (e.g. optional cell with super-long cycling up to 12,000 cycles)
- Integrated high-efficiency liquid-cooling system, with the temperature difference in the container limited to 5℃

High integration
- Modular design for the 1,500V system
- Separate arrangement of electrical room and battery room for convenient maintenance
- Non-walk-in/modular design with high integration, saving the floor space by 35%
- Prefabricated installation, reducing on-site installation costs and commissioning time

Basic Parameters	
Configuration	10P416S
Cell capacity [Ah]	280
Rated voltage [V]	1331.2
Rated energy [MWh]	3.72
IP Rating	IP55
Product weight [T]	35
Dimensions [L*W*H] [mm]	6058*2462*2896

Testing and certification

IEC 62619 | UL 1973 | UL 9540A | IEC 62477-1

EnerOne
Outdoor Liquid Cooling Battery System

High level of safety
- LFP batteries with high thermal stability
- Protection level of IP66 to meet the requirements of outdoor applications
- Resistance up to C5 corrosion level, with 20-year reliability
- Separate fire protection system

Long service life
- Available for integration with CATL's advanced technologies (e.g. optional cell with super-long cycling up to 12,000 cycles)
- Integrated frequency conversion liquid-cooling system, with cell temperature difference limited to 3℃, and a 33% increase of life expectancy

High integration
- Modular design, compatible with 600 - 1,500V system
- Separate water cooling system for worry-free cooling
- Modular design with a high energy density, saving the floor space by 50%
- Transportation after assembly, reducing on-site installation costs and commissioning time

Basic Parameters	
Configuration	1P416S
Cell capacity [Ah]	280
Rated voltage [V]	1331.2
Rated energy [kWh]	372.7
IP Rating	IP66
Product weight [kg]	3500
Dimensions [L*W*H] [mm]	1300*1300*2280

Testing and certification

IEC 62619 | UL 1973 | UL 9540A | IEC 62477-1

Appendix T - Wind and PV Power Output from HOMER

Wind turbine power output

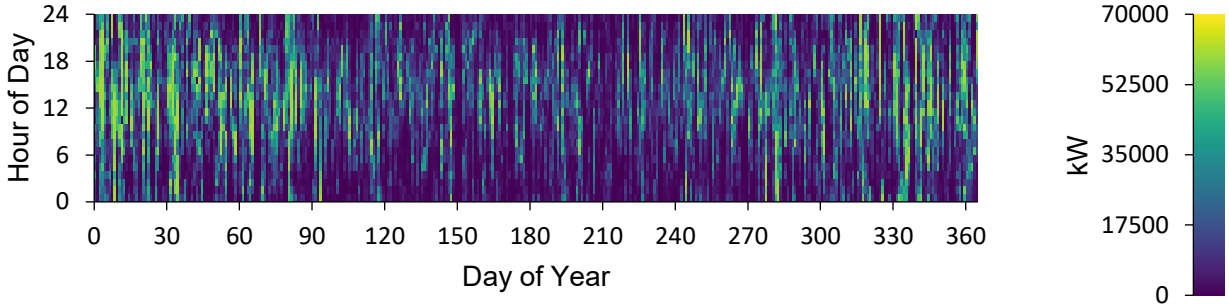

PV power output

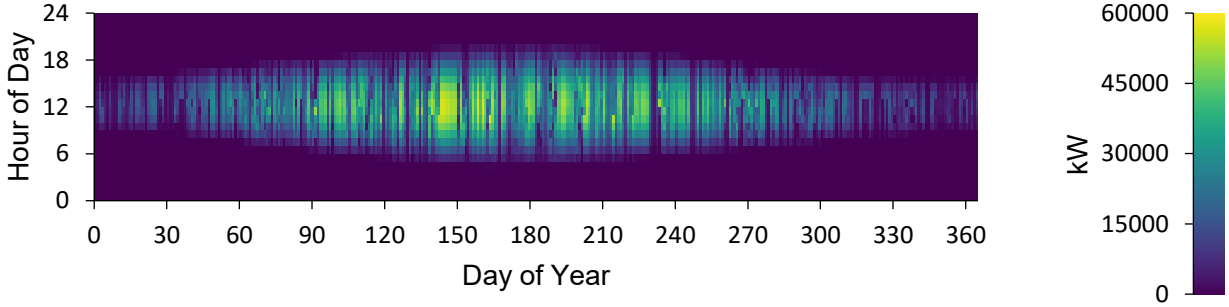

Appendix U - Grid purchase and sale from HOMER